A reappraisal and 3D characterisation of fracture systems within the Devonian Orcadian Basin and its underlying basement: an onshore analogue for the Clair Group

DICHIARANTE, ANNA,MARIA

APPENDIX A

Field Localities

Here the lineament analysis and field data are presented.

Figs A.1-A.4 show an overall lineament analysis, rose diagrams of lineaments at scale 1:100k and 1:10k and a Landsat and Geological Map of the Northern Scotland (with the 16 selected localities presented in this study), respectively. In Figs A.5-A.20 the localities (e.g. Strathy Bay, Portskerra, etc.) and the sub-localities which have not been presented in the main thesis body (e.g. L1, L2, L3, etc.) are reported.

For each locality, the following analysis and plots are provided:

- **A**: 1:1K Lineament Analysis map and relative sub-locality sites
- **B**: Frequency-Azimuth and Length-Azimuth plots of lineaments
- **C:** A complete synthesis of structural data collected during the fieldwork

For each sub-locality (e.g. L1, L2) the following are provided:

- Representative outcrop photographs and sketches
- Equal area stereonet plots and density contours

All the rose diagrams are produced with GeOrient software with 10% sector angle. All the field-work stereonet and contour density plots are equal area projection, lower hemisphere and they have been produced with Stereo32 software.

Lineament and basement geology map of Northern Scotland (1:100k) (*Wilson, 2006 modified)*

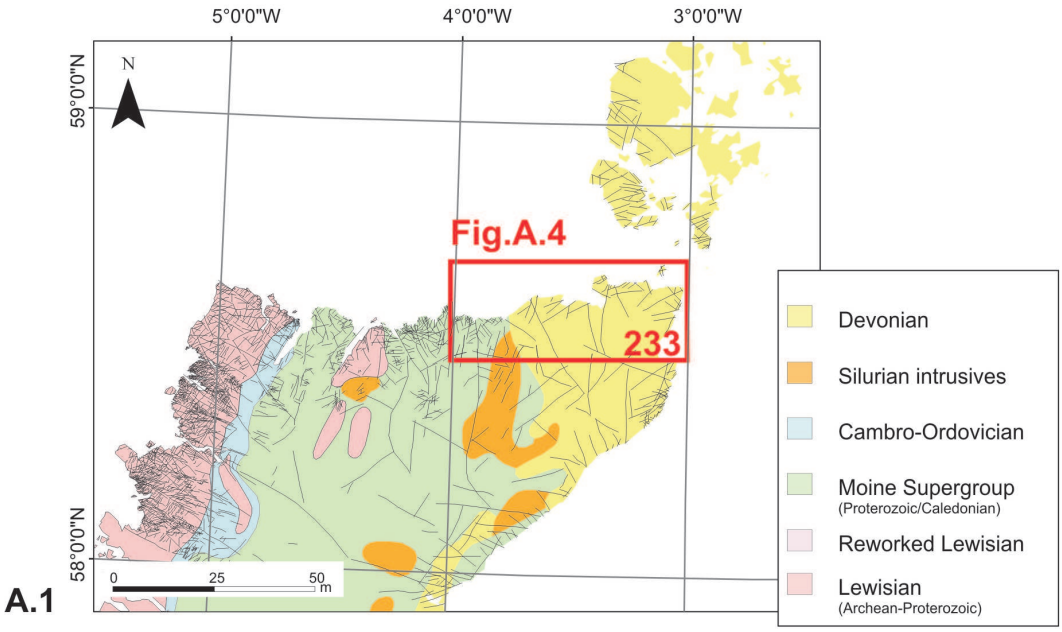

A.1

Lineament analysis plot

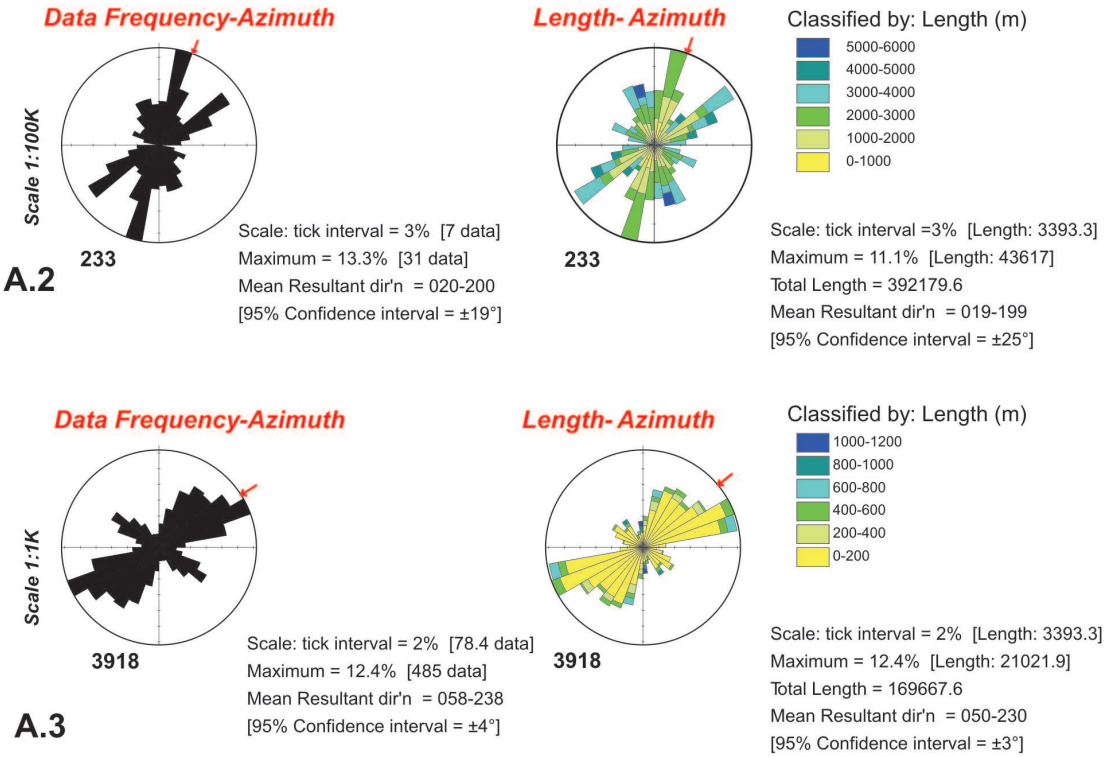

A.2

A.3

Lineament analysis has been conducted at scale 1:100K and 1:1K using existing and new interpretations respectively from Landsat Images.
233 lineaments were recognized at 1:100k scale by Wilson 2006 for the area of interest (red box in **Fig. A.1**). Data Frequency-Azimuth plot (**Fig. A.2 left**) shows that lineaments are mainly oriented NNE-SSW and NE-SW with mean in direction N20-200 (red arrow in the plot). Each straight lineament has been measured in order to produce the Length-Azimuth distribution plot in **Fig. A.2 right**. The latter shows similar distribution pattern of the Frequency-Azimuth plot. However, the longer lineament (length > 5000 m) trends NNW-SSE.
3918 lineaments have been picked and measured at scale 1:1K. Data Frequency plot (**Fig. A.3 left**) shows that lineaments are mainly oriented NE-SW to ENE-WSW and NW-SE with mean in direction N058-238 (red arrow in the plot). Relative Length-Azimuth plot (**Fig. A.3 right**) shows similar distribution. However, the longer lineaments observed (length >5000 m) trend N-S.

Landsat image and geological Map of Northern Scotland with 16 selected fieldwork localities

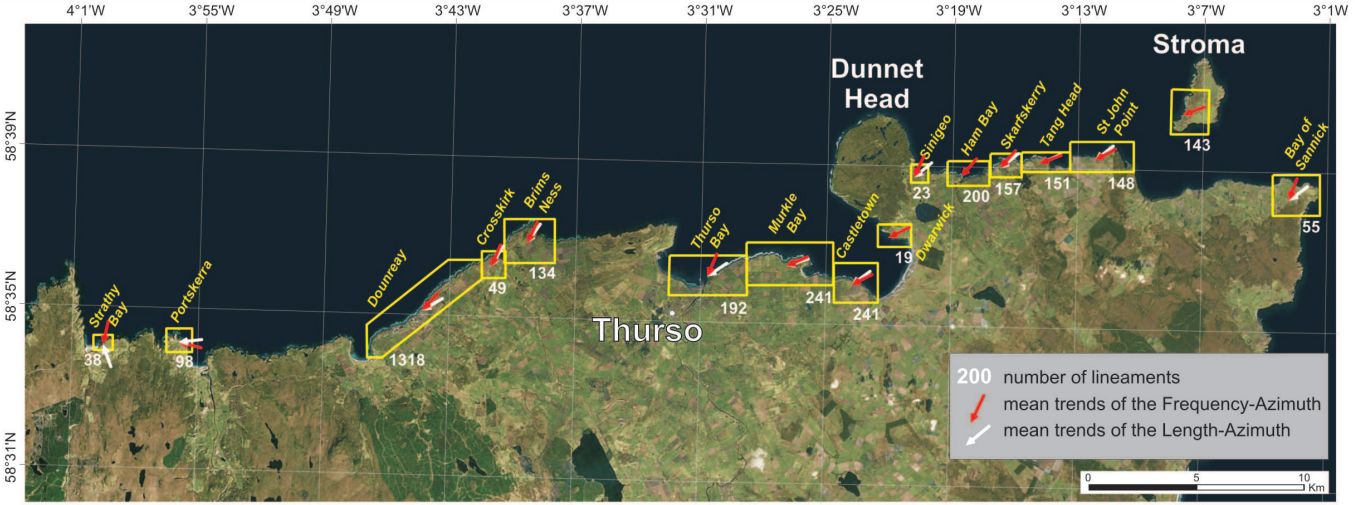

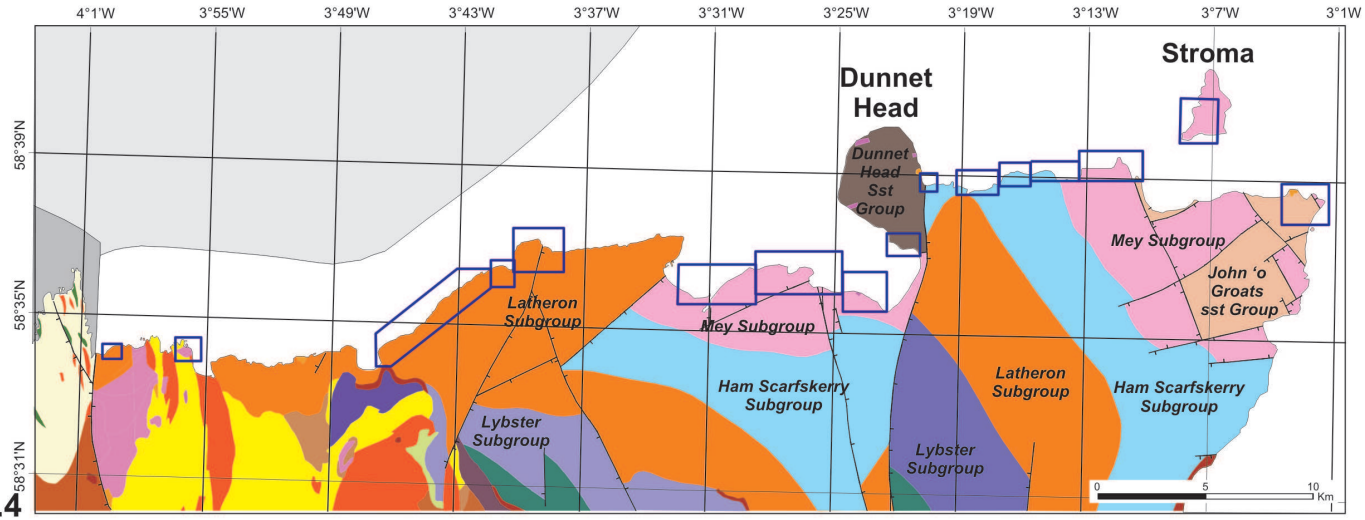

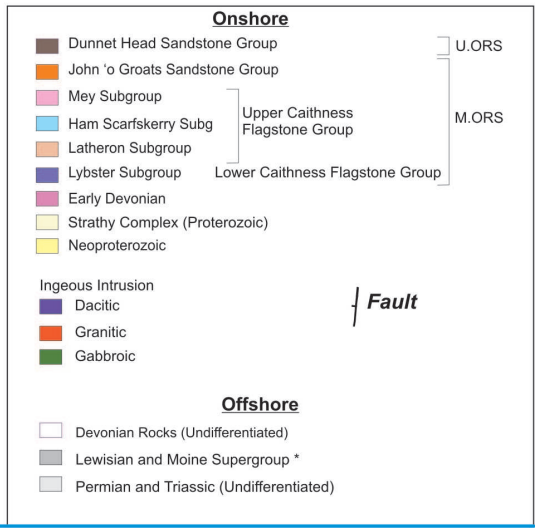

The yellow boxes in **Fig. A.4 top** are areas of interest were detailed lineament analysis and fieldwork have been conducted. The white arrows and red arrows in **Fig. A.4 top** represent mean trends of the Frequency-Azimuth and Length-Azimuth plots. Large majority of them (14 of 16) point between NE-SW and ENE-WSW. More variability is observed for lineaments in the western areas (e.g. Strathy Bay and Portskerra). Major details and interpretations are in the following sections. **Fig. A.4 bottom** shows the onshore and offshore geology.

A.4

A.5.1 Location: Strathy Bay

1:1K Lineament Analysis

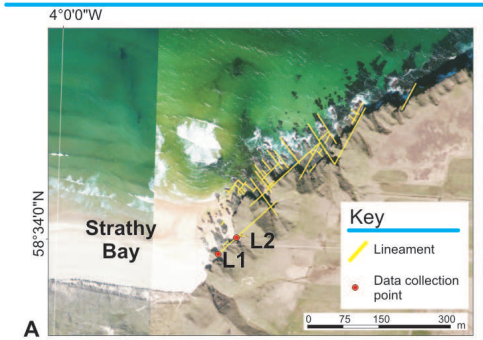

Strathy Bay (NC 837 658) lies at the hangingwall of the Strathy Bay Fault. It is a regional N-S trending fault which juxtaposed Middle ORS and the Strathy Bay complex which is dominated by weakly layered and banded gneiss with less common horneblende gneiss and quartz-megnetite rocks, scarce quartz garnet rocks and calc-silicates. The Fault is not exposed but forms a prominent lineament at large scale in aerial photos.

On the Middle ORS, 38 lineaments have been recognized at scale 1:1K (**Fig. A**). They show 2 major clusters in direction NE-SW and NW-SE. Frequency-Azimuth plot shows a mean in direction 161°-341° (red arrow in **Fig. B left**). Relative length distribution show a similar distribution. However, mean in this case is recorded in direction 003°-193°. The high values of confidence interval underline the little scatter in the 2 population sets.

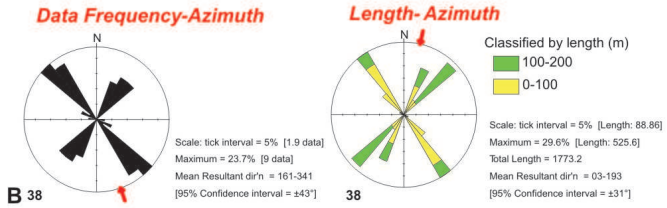

The two trend of lineaments observed by aerial photos correspond to the two main fault plane sets observed in the field. Meter-scale fractures parallel to these two sets occur in the platform.

Overall structural data

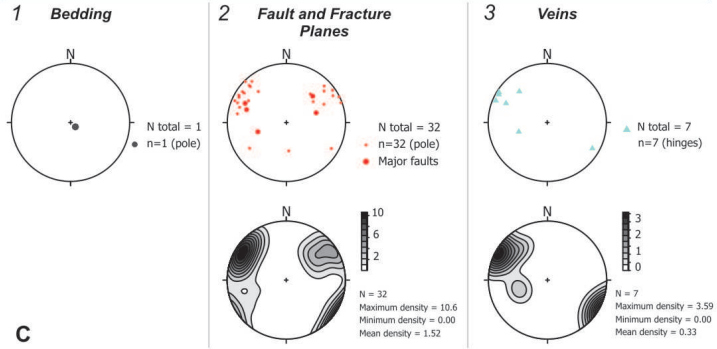

The Middle ORS dips 10° to the NW. Two major sets of fractures have been recorded: NE- and NW-trending. Fault and fracture dips range between 40° to 88°. Shallower fault dip data are recorded for NW-SE faults (**Fig. C2**). 6 measures of kinematics have been recorded: NW-SE faults show dextral oblique kinematics (2 data), pitch values 57° and 65°. NE-SW kinematics show dextral oblique kinematics (3 data) and strike-slip dextral (1 data) kinematic, pitch value 24°, 46° and 65°, respectively.

Veins trend mainly NE-SW with generally high values of dip (between 60° and 86°) (**Fig. C3**) They suggest an extension in direction NW-SE.

A.5.2

L1 (NC 84111 65998) - Strathy Bay

GROUP 3

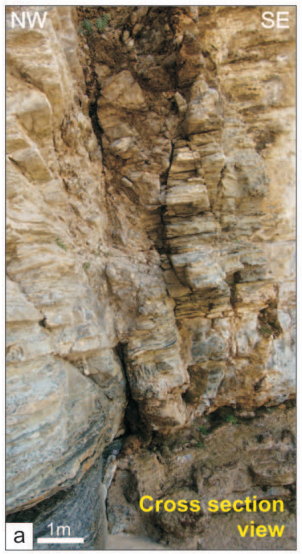

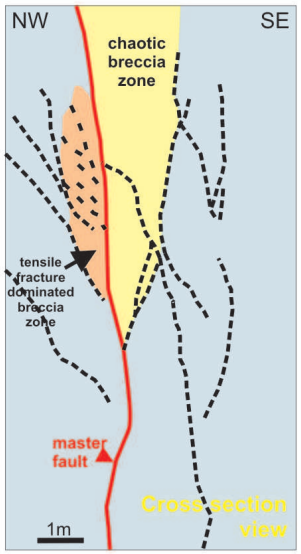

L2 (NC 84144 66024)

Calcite filled tensile veins

Dextral oblique slickelines

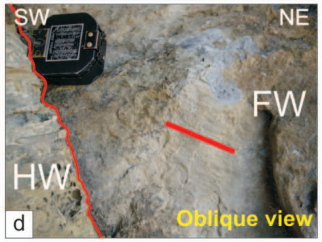

Normal oblique slickelines

NE-SW trending faults are particularly long and easily detectable from aerial photos due to selective erosion (**Fig. L1a** and **L1b**). **Fig. L1a** shows an example of NE-SW trending fault in cross-section view. The fault zone comprises an area dominated by breccia and tensile fractures and an area dominated by chaotic breccia. Large amount of displacement is localized on the master fault. The orientation of tensile fractures is consistent with normal displacement of the master fault. Fault planes are asssociated with carbonate mineralization and veining (**Fig. L1c**) Dextral oblique slickenlines and normal oblique slickenlines have been recorded on smaller fault planes adjacent to the master fault (**Fig. L1 d** and **L1e**).

Stress inversion of the strieated fault planes shows extension direction in direction NW-SE (see **Appendix B**).

A.6.1 Location: Portskerra

1:1K Lineament Analysis

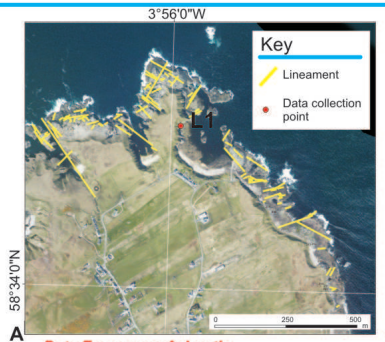

Portskerra is located close to the edge of the Devonian basin at the footwall of the Strath Halladale Fault (a major Devonian growth fault).

98 lineaments have been recognized at scale 1:1K and they show two major clusters in direction NE-SW and NW-SE (**Fig. B left**) with a mean in direction (84°-264°).

Relative lenght-azimuth plot (**Fig. B right**) shows a similar distribution with three major clusters in directions NE-SW, ENE-WSW and NW-SE. The longer lineament is in direction NW-SE. Mean direction is 104°-284°.

The bedding of the ORS at Portskerra is sub-horizontal (**Fig. C1**).

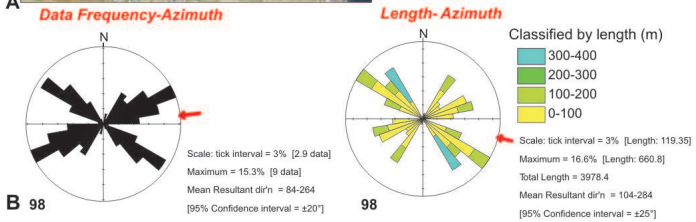

There is not a clear distinction between the orientation of faults and fractures within the Moine basement **(Fig. C2)** and overlying Devonian cover (**Fig. C3**) sequences. Within the Moine there are two distinct fracture trends NW-SE with dip value between 46°and 84° and NE-SW with dip values between 70° and 90°.

Structural data

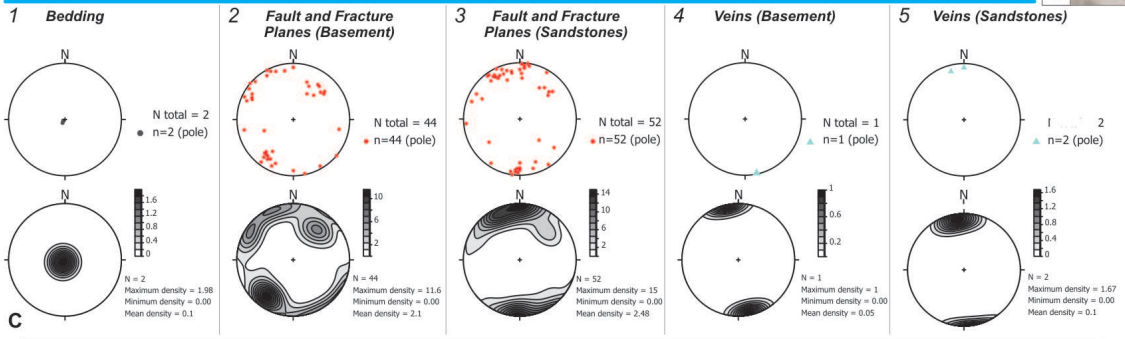

The vast majority of structures in the cover sequence is ENE-WSW to E-W (**Fig. C2** and **C3**); few NW-SE trending faults have been recorded too. Basement-hosted fracture sets are consistent in orientation with those observed elsewhere on the North coast and the dominance of the ENE-WSW structures in the cover sequence in are consistent with those observed east of Thurso Bay. Kinematic variability in fracture orientation may be related to the morphology of the unconformity (?). Veins cutting both basement and cover sequences are oriented ENE-WSW (**Fig. C4-C5**).

A.6.2

L1 (NC 87701 66479) - Portskerra

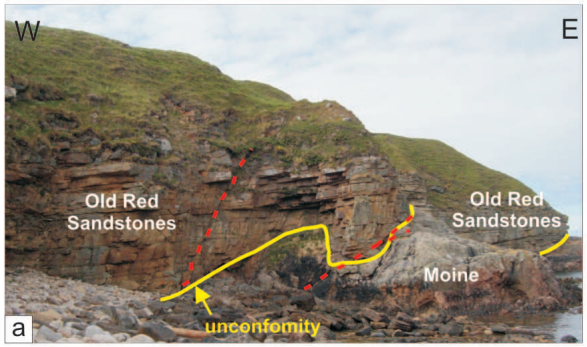

Quartz filled tensile veins

Oblique slickenlines

In location **L1**, the irregular shaped unconformity between the Moine basement rocks and the Middle ORS occurs (**Fig. L1a**). Some faults propagate from the basement up into the covers (**Fig. L1b**).

Figs L1c, L1d and **L1e** show tensile veins and oblique slickenlines occurring in the basement rocks. Another interesting feature of the Moine-hosted fractures is the Devonian aged fracture fill **(Fig. L1f)**, which suggests that these fractures were open and well connected to the surface during the Devonian.

A.7 Location: Dounreay

1:1K Lineament Analysis

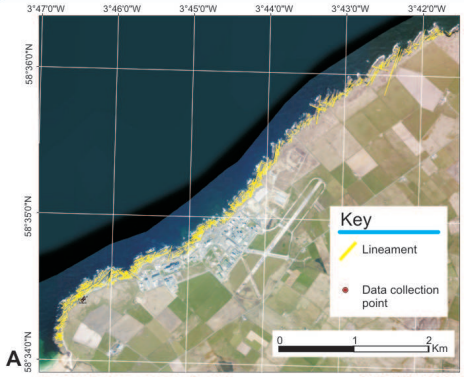

Dounreay district lies in the western part of the onshore outcrop of the Orcadian Basin, west of the Bridge of Forss Fault, a reactivated NNE-SSW trending fault (see **Chapter 2**).

Rocks in outcrop comprise predominantly lacustrine rhythmically-bedded Middle Devonian (Eifelian) sandstones, siltstones and shales. The onshore lineament analysis revealed two dominant sets of structures in NE and SE directions (**Fig. B left**) with a mean in direction 060°-240°. Relative length-azimuth plot (**Fig. B right**) shows a similar distribution. Longer lineaments trend N-S to NNE-SSW. Mean direction is (043°-223°).

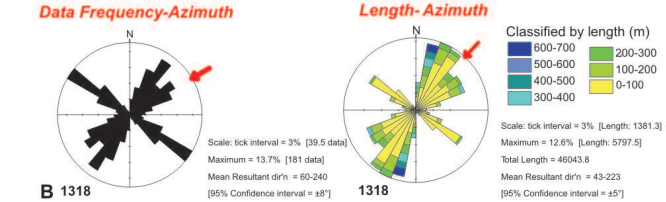

The two trend of lineaments observed by aerial photos correspond to the two main fault plane sets observed in the field. The middle ORS dips between 5° and 12° to the NW (**Fig. C1**).

Overall structural data

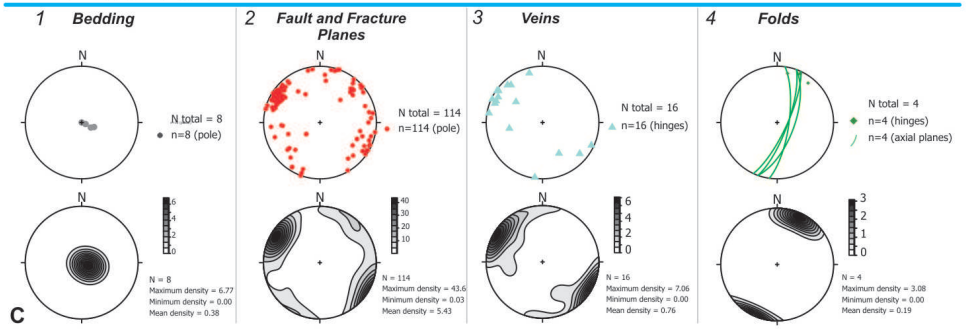

Two major sets of fractures have been recorded in NNE-SSW and NW-SE directions. Faults and fractures are mainly NNE-SSW oriented, although subordinate numbers of NE-SW and NW-SE trends also occur. Fault dips mainly range between 50° and vertical. Shallower fault dips are recorded for NW-SE faults (**Fig. C2**). Veins mainly NNE- to NE- trending and they generally show high values of dip, between 50° and 88° (**Fig. C3**). Fold hinges are NNE-SSW trending and gently plunging to the NNE (4° to 12°)(**Fig. C4**).

A.8.1 Location: Crosskirk

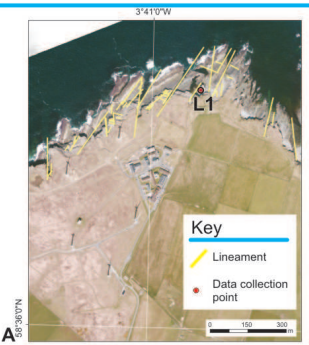

Crosskirk is located north of Dounreay district and rocks in outcrop belong to the Middle Old Red Sandstones, Upper Caithness Sandstones .

49 lineaments have been recorded at scale 1:1K (**Fig. A**) and they show 3 major clusters in direction N-S, NE-SW and ENE-WSW with a mean in direction N29 (**Fig. B left**). Relative Length-Azimuth plot shows that the longer lineaments (up to 300 m) trend NE-SW with a mean in direction 023°-203° (red arrow in **Fig. B right**). N-S lineaments are less than 300 m long and NW-SE lineaments are less than 100 m long.

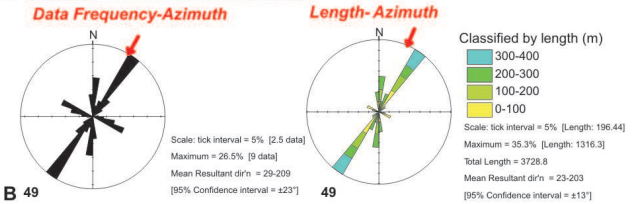

NE-SW and N-S trending lineaments represents regional to subregional faults while NW-SE lineaments represent fractures and joints.

The Middle ORS dip 4 to10° to the NW **(Fig.C1)**.

Overall structural data

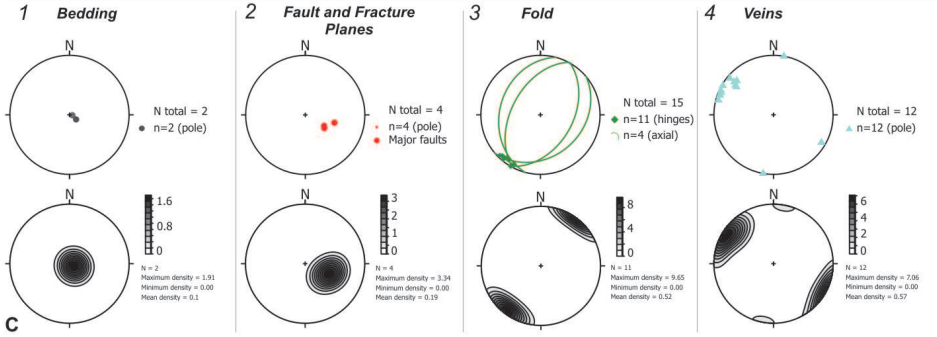

Field data ensured that the picked lineaments corresponded to faults, fractures and joints. One major set of low angle (30° to 40°) faults has been recorded, NE-trending **(Fig.C2)**. The faults show small-scale displacement and are associated to NE-SW trending folds with axial planes dipping towards both NW and SE and hinges plunging to SW **(Fig.C3).** Veins trend NE-SW and dip between 67 and 90°**(Fig.C4).** They suggest an extension in direction NW-SE.

A.8.2

L1: ND 02489 70162 - Crosskirk

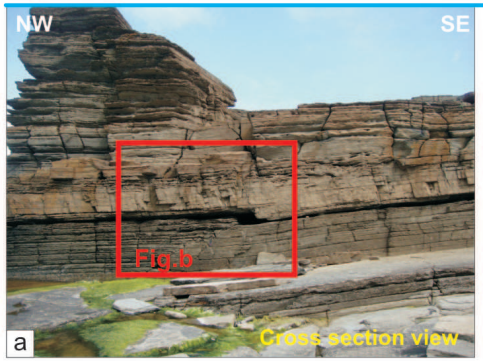

Calcite filled tensile veins

Fibrous carbonate mineralization

Fault breccia

Figs L1a and **L1b** show a deformation zone consisting of a thrust fault and kink folds developed parallel to bedding. Fold hinges trend is NNE-SSW (208°- 233°) and gently (3° to 8°) plunge to SSW.
Thin carbonate veins (**Figs L1c** and **L1d**) occurs on the outcrop cutting it at almost 90°.
The rock fault is a breccia made up of angular clasts an gouge (**Figs L1e**).

A.9.1 Location:Brims Ness

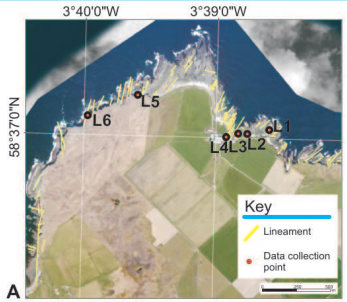

Brims Ness is located in the centre of Caithness area and it sets on Middle ORS (Middle Devonian). The Bridge of Forss Fault zone is one of the largest (regional) faults in the area. It trends generally NNE-SSW but the main fault plane is not exposed.

134 lineaments have been recognized at scale 1:1K (**Fig. A**) and they show 2 major clusters in direction N-S to NE-SW and WNW-ESE with a mean direction 36°-216° (red arrow in **Fig. B left**). Relative Length-Azimuth plot show similar distribution however N-S lineaments are the longer ones (up to 400-500 m) while WNW-ESE are shorter (less than 100 m).

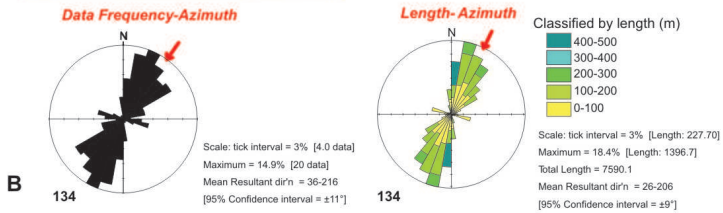

Overall structural data

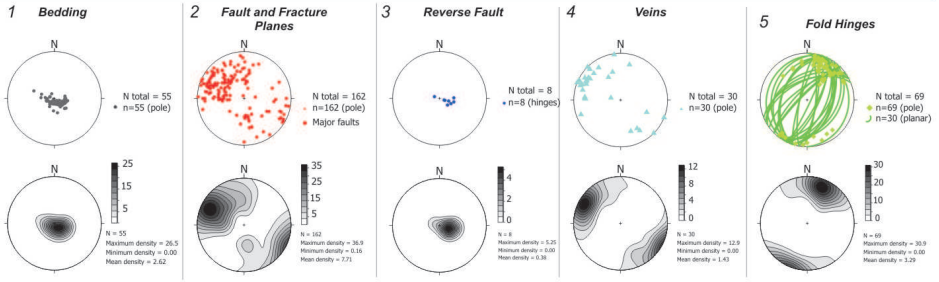

Bedding is sub-horizontal (**Fig. C1**), although some open folds and local variations in the bedding occur (e.g. open fold in locality L1).162 normal faults and fractures have been recorded (**Fig. C2**). They show large variability in trend and dip. NNE to NE trending faults represent the larger cluster of data with, to a less extent, N-S and E-W trending faults. Reverse faults (**Fig. C3**) are mainly N-S trending with dips beteween 12° and 35°.
Veins are mainly NE-SW trending, however few E-W and N-S veins have also been recorded (F**ig. C4**). Fold hinges trend NNE to NE and plunge between 02° and 44° with a major cluster around 20° (**Fig. C5**). Axial planes are NE-SW trending and have variable dip values (between 12° and 84°). Flexural slip is NE-SE trending and about 35° plunging to the NW (**Fig. C5**).

A.9.2

L6 (ND 03628 71346) — Group 3 - Reactivated

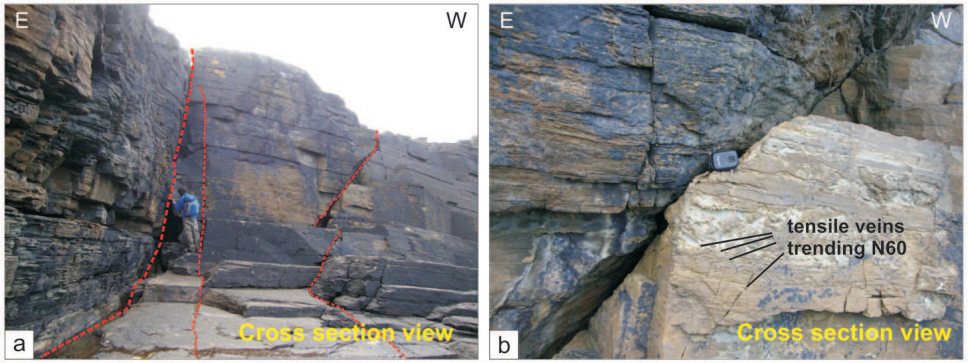

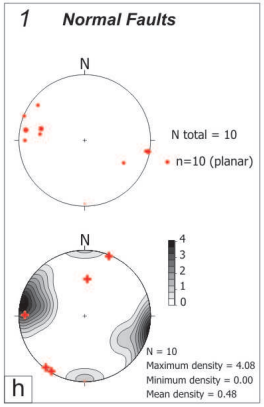

In **Loc6** (ND 03628 71346) 3 major N-S (dip-direction between 100° and 105°) trending faults occur. Fault dips vary between 58° and 80°. Faulting is localized in discrete fault planes not associated with damage zones. Lineations on minor fault planes show strike-slip sinistral kinematic (2° pitch).

The main fault (left in **Fig. L6a**) is associated with 3 cm thick calcite breccia (**Figs L6d** and **L6e**). The calcite is oil stained which gives a black appearence to it (Figs L6f-g).

A.9.3

L7 (ND 03355 71210) - Brims Ness

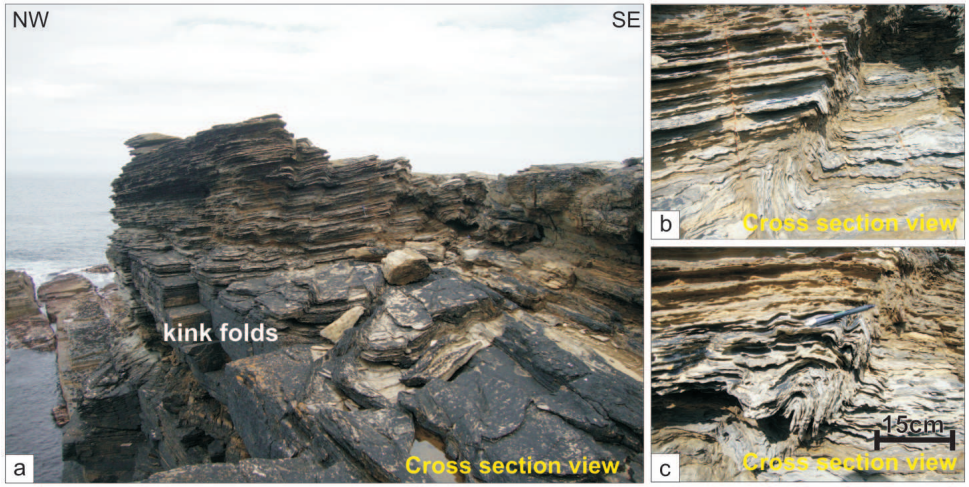

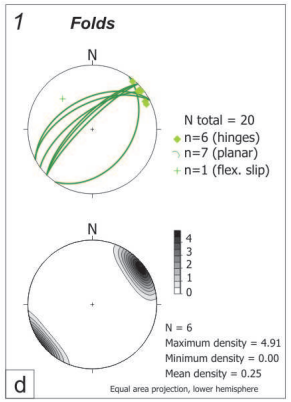

In Loc7 (**ND 03355 71210**) kink shape folds verging to SE occur (**Figs L7a-c**). Hinges trend between 40° and 65° and they plunge between 3° and 8° to the north. Folds are NE-SW trending Axial planes dip mainly to the NW (between 315° and 333°) and SE (125°)

No carbonate mineralization is associated with folding.

A.10.1 Location:Thurso Bay

1:1K Lineament Analysis

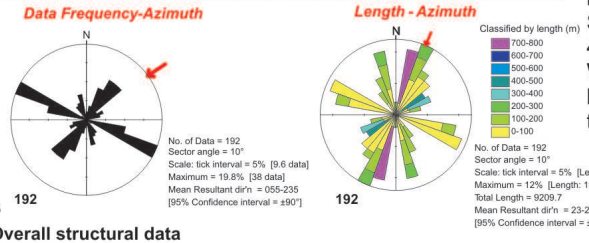

Thurso Bay is located in the central part of Caithness area. It sets on Middle Old Red Sandstones, Mey Supergroup.

192 lineaments have been recognized at scale 1:1K. They show 2 main clusters in NE-SW and WNW-ESE directions (**Fig. B left**) with mean in direction 055°-235°. Relative length-azimuth distribution shows a more complex pattern with longer lineaments in direction NNE-SSW and NE-SW (up to 700m and 400m) (**Fig. B right**).

WNW-ESE and NNW-SSE lineaments also occur, however their length is less than 300m.

Overall structural data

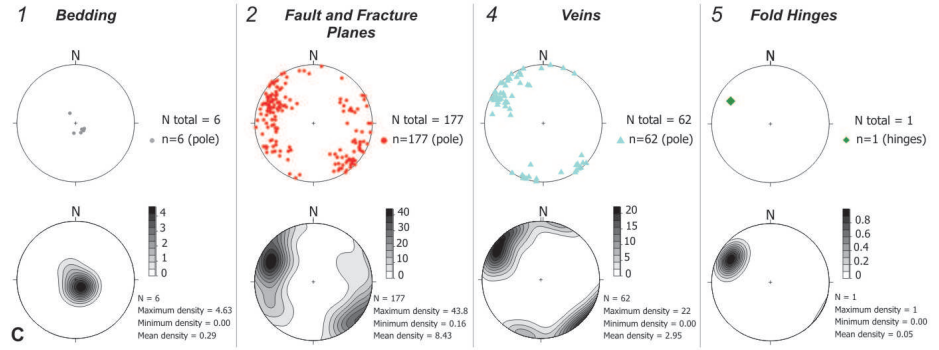

Bedding is mainly NE-SW trending and dipping between 12° and 16°(**Fig. C1**).

177 faults and fractures have been recorded. They show 2 major clusters in direction NE-SW and NW-SE. E-W and N-S trending faults also occur (**Fig. C2**). 62 veins have been recorded, they trend mainly NE-SW (51 data), few E-W to WNW-ESE veins have been also recorded (11 data) (**Fig. C3**). A fold hinge trending NW-SE and plunging (23° to NW) has been recorded (**Fig. C4**).

A.10.2

L1 (ND 10683 69160) - Thurso Bay

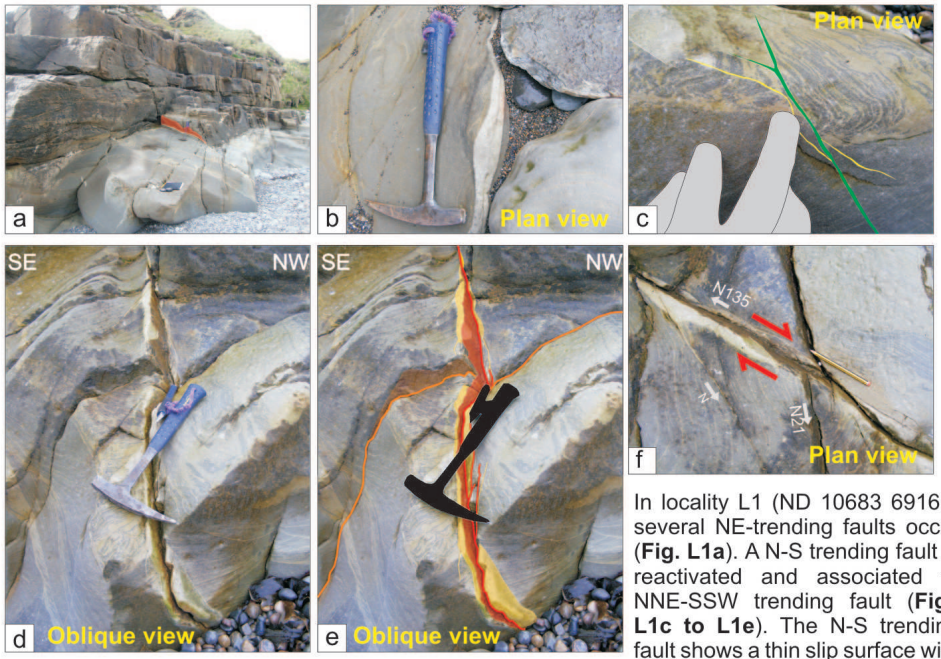

In locality L1 (ND 10683 69160) several NE-trending faults occur (**Fig. L1a**). A N-S trending fault is reactivated and associated to NNE-SSW trending fault (**Figs L1c to L1e**). The N-S trending fault shows a thin slip surface with 2 cm alteration zone, possibly cemented. The same alteration is also observed in a NW-SE trending fault showing dextral shear sense (**Fig. L1b**).

No direct measurement of kinematics have been possible in this area.

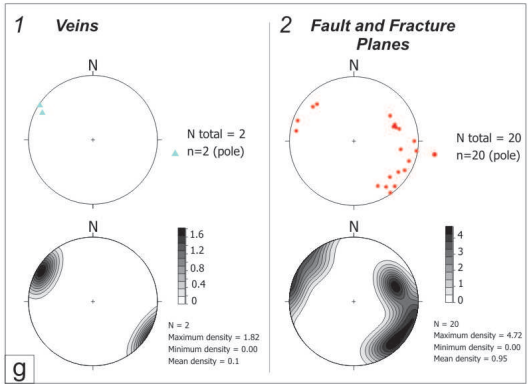

A.11.1 Location: Murkle Bay

1:1K Lineament Analysis

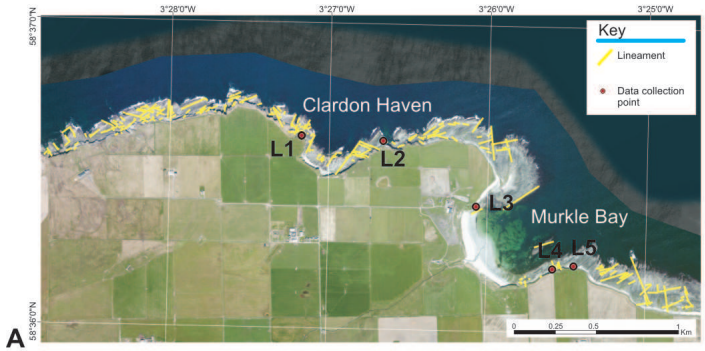

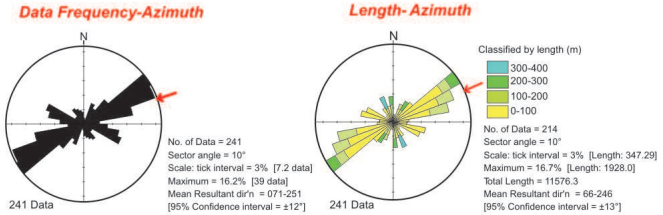

At Murkle Bay and in the nearby area of Clardon Haven, 21 lineaments have been picked. They show mostly ENE-WSW and WNW-ESE trends with a mean in direction 071°-251° (**Fig. B left**). Lenght-Azimuth plot shows a similar distribution (**Fig. B right**). Longer lineaments trend NNW-SSW (up to 400 m), N-S (up to 300 m) and ENE-WSW (up to 300 m).

Bedding is generally sub-horizontal with some dip variations (03° to 26°) next to major faults.
One area with steeper dip (44°) occurs (**Fig. C1**).

Overall structural data

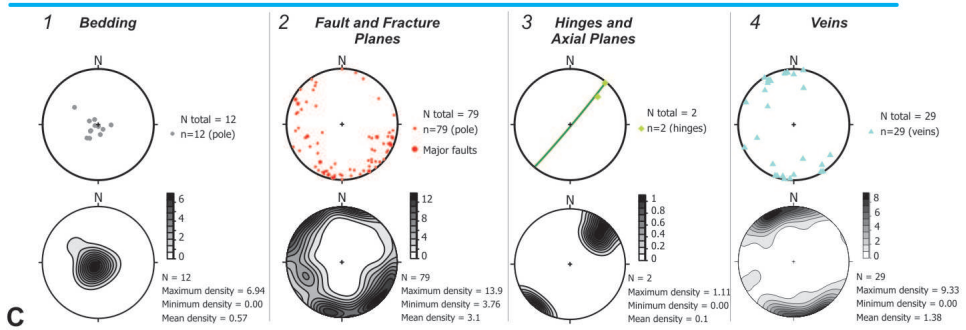

Large variability in fracture and fault trends have been recorded; however main faults trend N-S to NNE -SSW and E-W. The two hinges data recorded trend in NE-SW direction and gently (02° and 30°) plunge to the NE. The axial plane trends NE-SW and it is near vertical (**Fig. C3**). Veins are mainly E-W with dip values between 54° and 90° (mean around 88°) (**Fig. C4**).

A.11.2

L1 (ND 15691 70086) - Murkle Bay

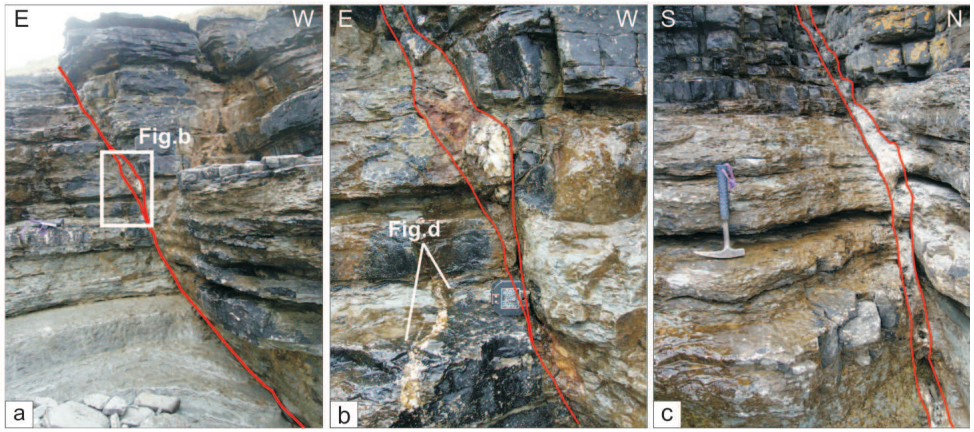

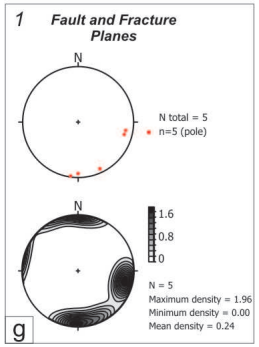

In locality L1 (ND 15691 70086), N-S and E-W trending faults occur (**Figs L1a**, **L1b** and **L1c**). They show large amount of carbonate mineralization and in the more developed instances pyrite and bitumen. Carbonate mineralization is generally pale with occasionally hematite and bitumen staining (**Fig. L1e**)

A.11.3

L2 (ND 16184 70034) - Murkle Bay

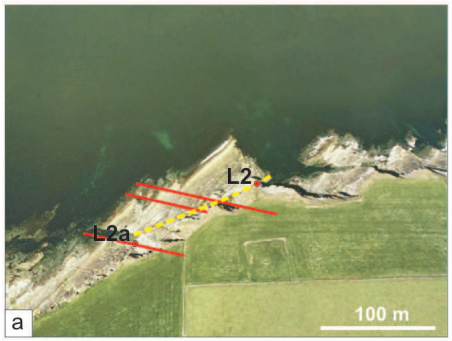

L2: ND 16184 70034

L2a: ND 16052 69953

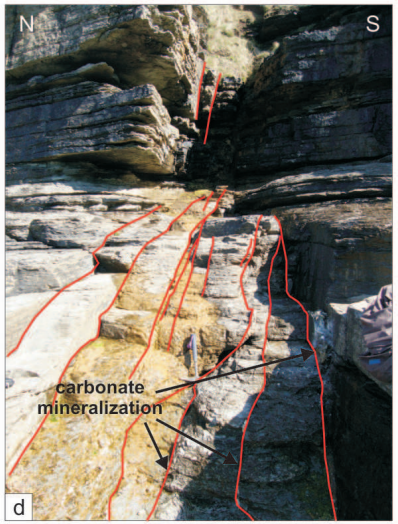

In locality L2 (ND 16184 70034) a lineament observed form aerial photo has been investigated during fieldwork (dashed yellow line in **Fig. L1a**). A small-scale fold is developed in relay zone oblique (?) movement of ENE-WSW trending fault.
N-S trending faults occur in locality L2a (ND 16052 69953) forming a “fracture corridor”. Carbonate mineralization occurs on both bounding faults and on smaller fractures (**Fig. L1d**)

A.11.4

L3 (ND 16739 69655) - Murkle Bay

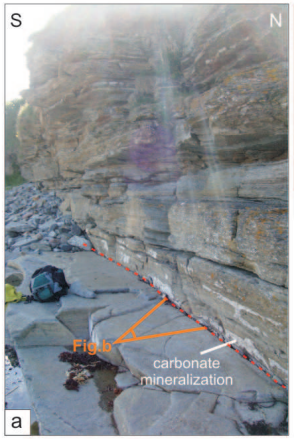

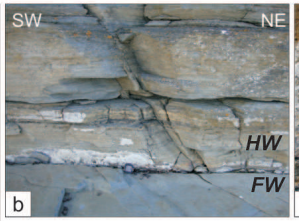

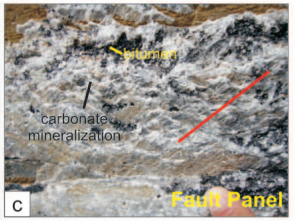

In locality L3 (ND 16739 69655) a NE-SW (045°) trending fault parallel to the cliff occurs (**Figs L3a and L3b**). The dip of the structure is 80° to northwest. The displacement of this structure is difficult to assess.
Well developed slickenlines and steeps in the calcite show sinistral oblique kinematic (45° pitch) **(Fig. L3c)**. Large carbonate mineralization and bitumen occur in the fault rocks (**Fig. L3d**). In some instances, calcite and clasts of wall rock are brecciated in the fault zone (**Fig. L3e**). The vein in **Fig. L3f** is up to 20cm thick and associated joints suggest oblique sinistral sense of shear.

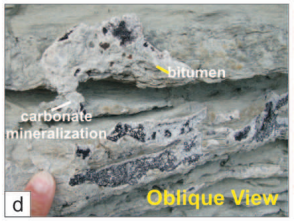

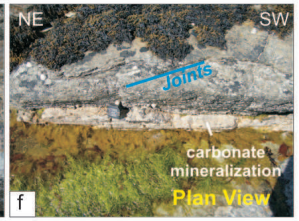

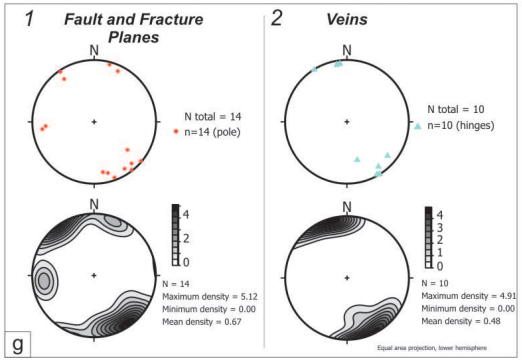

A.12 Location: Castletown

1:1K Lineament Analysis

Castletown lies west of Dunnet Head, 8 km East of Thurso.
126 lineaments have been recognized at scale 1:1K **(Fig. A)**. They show a major cluster in direction NE to ENE. NW-SE and N-S trending lineaments also occur **(Fig. B left)**. Frequeny-szimuth plot shows a mean in direction 054°-234° (red arrow). Length-azimuth plot **(Fig. B right)** shows a similar distribution. Longer lineaments (300-400 m) trend ENE-WSW. The mean is recorded in direction 042°-242° (red arrow).

A

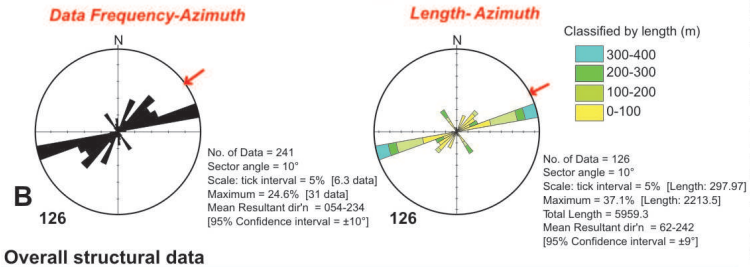

On the coastal platform north of Castletown village, Mey Subgroup rocks dip sub-horizontally to gently (06°) to the NW **(Fig. C1)**.
Faults trend mainly ENE-WSW and N-S. Dip values are between 62° and 90° **(Fig. C2)**.
Veins are mainly ENE-WSW and N-S trending. E-W trending veins have also been recorded. Their dip values are beween 48° (1data) and vertical **(Fig. C3)**.

Overall structural data

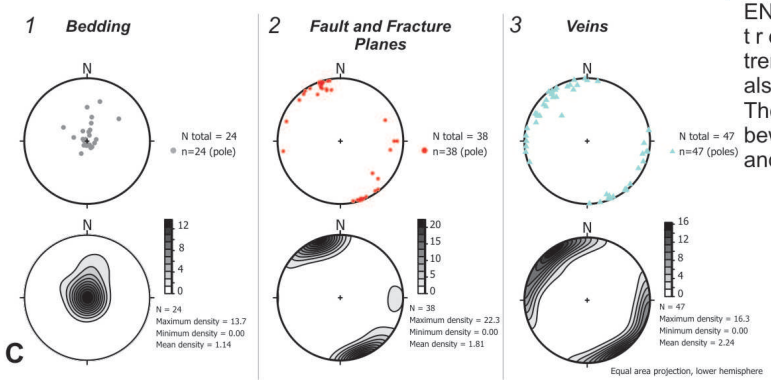

A.13.1 Location: Dwarwick

1:1K Lineament Analysis

Dwarwick is located on the southern side of the Dunnet Head peninsula, at the footwall of the Brough Fault and the rocks in outcrop belong to the Upper ORS.
At Dwarwick, the contractional structures observed in the northern area of Dunnet Head, are not exposed but may lie below an area of beach to the east.
19 lineaments have been recognized at scale 1:1K **(Fig. A).**

A

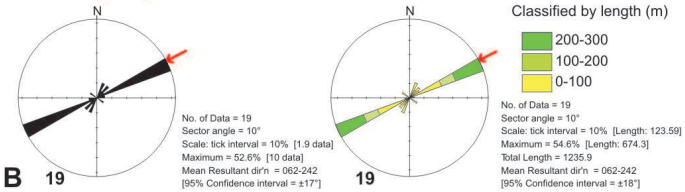

The main set of structures is ENE-WSW trending **(Fig. B left)**. Few NE-SW and SW-SE trending faults occur. Mean distribution plot value is in direction 062°-242° (red arrow). Relative Length-Azimuth distribution (Fig. B right) shows the same pattern with longer lineaments in direction ENE and mean in direction 062°-242° (red arrow in **Fig. B right**)

Overall structural data

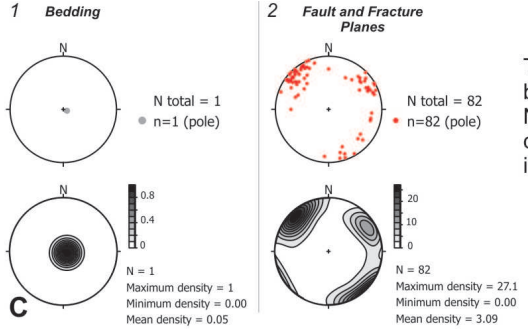

Two main sets of fractures and faults have been recognized at Dwarwick; they are mainly NE-SW and NW-SEtrending **(Fig. C)**. Little carbonate mineralisation has been observed in association with both fracture trends.

A.13.2

L1: ND 20993 71060 - Dwarwick

In locality L1 (ND 20993 71060) at Dwarwick faults and fractures occur mainly as “fracture corridor” (**Figs L1a-L1b**) or as discrete fault and narrow damage zone (**Fig. L1c**). Carbonate mineralization is associated with both NE-SW and NW-SE trending faults (**Figs L1d and L1e**)

A.13.3

STRUCTURAL LOG - Dwarwick

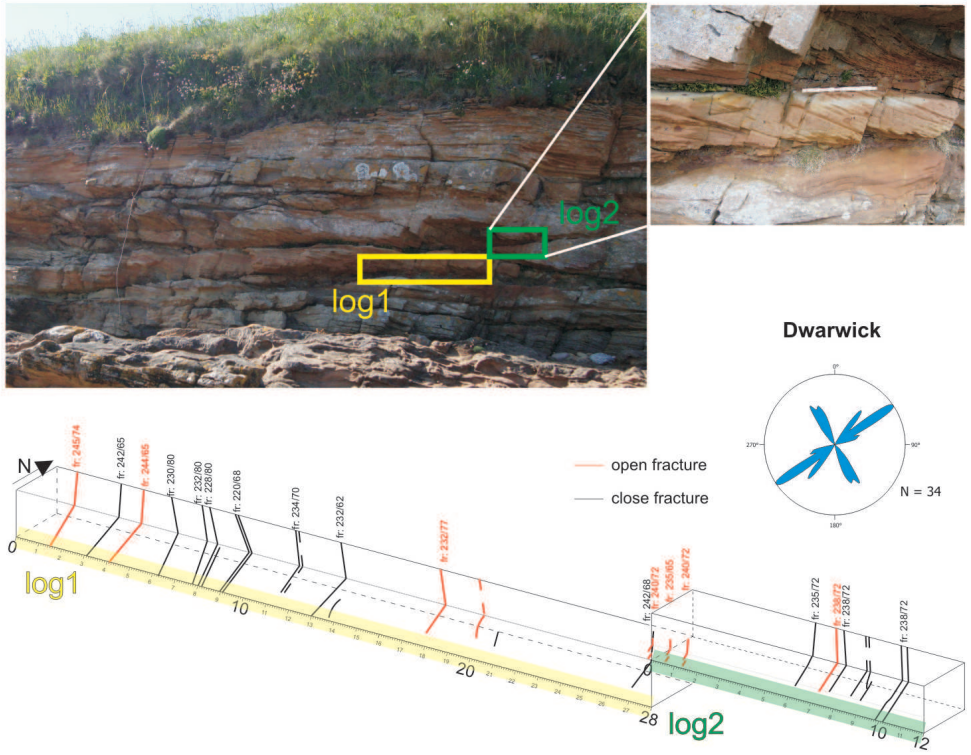

A.14.1 Location: Dunnet Head (Sinigeo)

1:1K Lineament Analysis

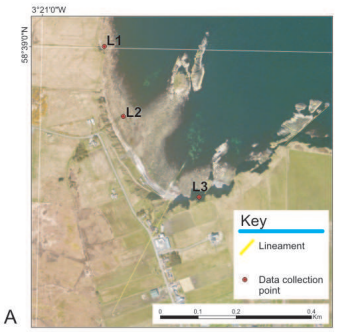

A

Dunnet Head (Sinigeo) is located at the footwall of the inverted Brims-Risa Fault, one of the major regional fault in Caithness. The Brims-Risa fault juxtapposes rock of the Middle Devonian Upper Caithness Flagstones to the east against the Upper Middle Devonian Head Sandstones (*Chapter 4*).
23 lineaments have been recognized at scale 1:1K (**Fig. A**). They show 2 main clusters NNE to NE-and NW-trending (**Fig. B left**). Frequency-Azimuth plot shows a mean in direction 050°-230° (red arrow). Length-Azimuth distribution (**Fig. B right**) shows that the longer lineament is NNE-trending and that NE-trending lineaments are 2 to 3 times longer (200-300 m) than NW-SE trending lineaments (0-100 m). The mean is recorded in direction 020°-208°.

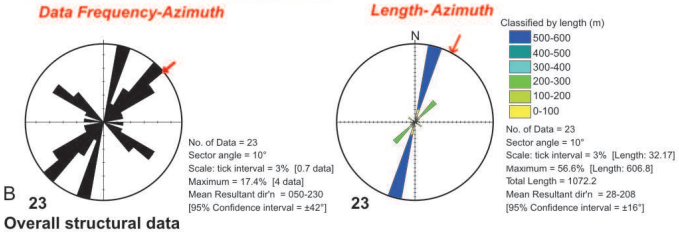

B

Bedding is mainly sub-horizontal to gently (6° to 32°) dipping to West (**Fig. C1**).

Overall structural data

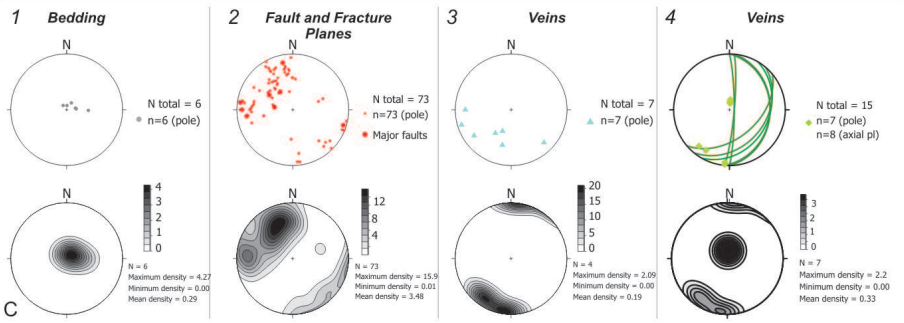

C

Two main trends of faults and fractures have been recorded trending in N-S and NE-SW to E-W directions (**Fig. C2**). Faults and fractures dip between 27° and vertical. 19 measures of kinematics have been recorded and they mainly show dextral oblique kinematics (pitch between 7° and 45°) for NNE-SSW trending faults. Veins are N-S and E-W trending (**Fig. C3**). Fold hinges trend NNE-SSW and they gently (2° to 17°) plunge to SSW. Axial planes trend N-S to NNE-SSW and they dip between 28° and 48° to East (**Fig. C4**).

A.14.2

L1 (ND 21918 74351) - Dunnet Head

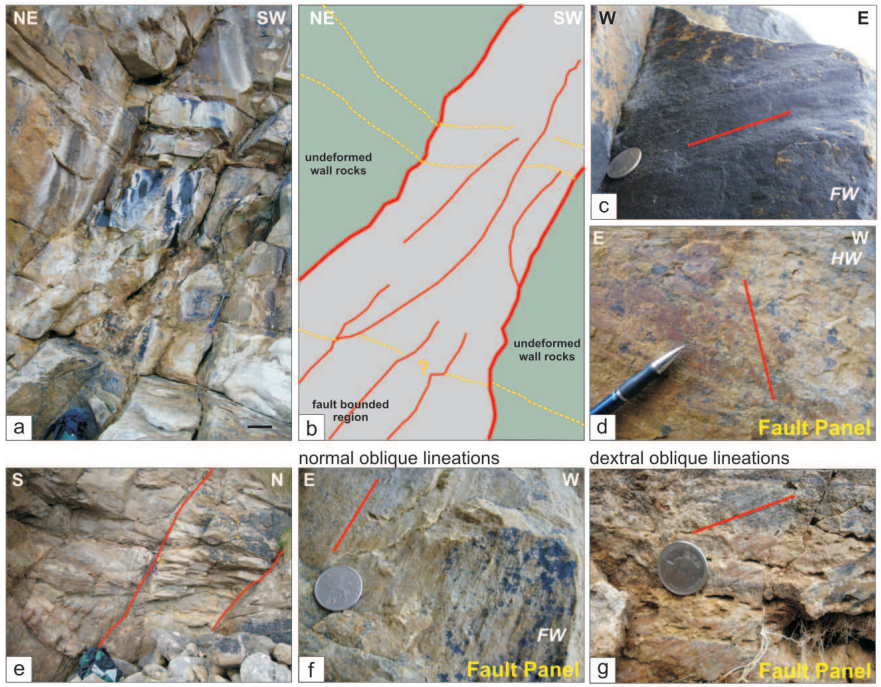

a b c d e f g

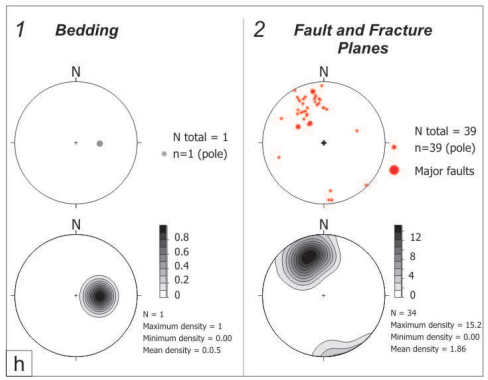

h

In locality L1 (ND 21918 74351) corridors of fractures occur (**Fig. L1a** and **L1e**). The confining faults are E-W trending.
Slickenlines have been recorded on minor E- and NE-trending fault planes. They dip between 45° and 88°. E-W trending faults are strike-slip dextral (pitch of 39°) **(Fig. L1c)** or more normal dextral oblique (pitch 75°) **(Fig. L1d).**
NE-SW trending faults are normal oblique dextral (pitch of 62°) (Fig. **L1f**) or oblique dextral (pitch of 33°). Planes are not associated with carbonate mineralization, however red staining (hematite?) has been observed in some of them **(Fig. L1d).**

A.15.1 Location:Ham Bay

1:1K Lineament Analysis

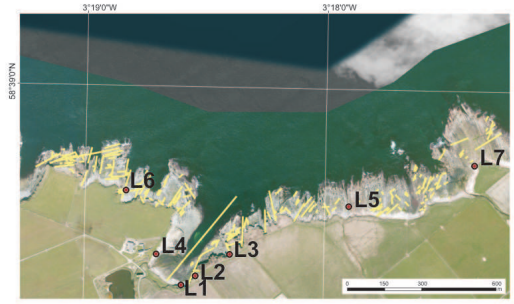

A

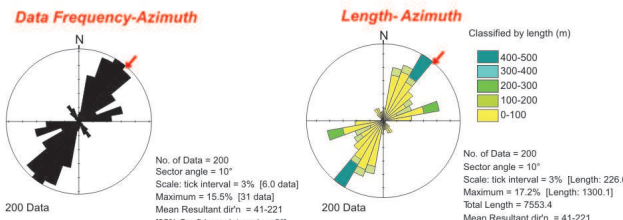

B 200 Data 200 Data

Ham Bay is located east of the Brough Fault and lies in the Middle Old Red Sandstones, Ham-Skarfskerri Subgroup.
200 lineaments have been picked at scale 1:1K (Fig. **A**).
They show 3 major clusters in direction NE-SW, ENE-WSW and NW-SE (**Fig. B left**). NE-SW data show larger scatter of about 20°. Distribution mean is in direction 41°-221° (red arrow).

The Length-Azimuth distribution plot (**Fig. B right**) shows a similar pattern with longer lineaments in direction NE-SW (400-500 m) and ENE-WSW (300 m). NW-SE trending lineament are long less than 100m. Distribution mean is in direction 41°-221°(red arrow).

Overall structural data

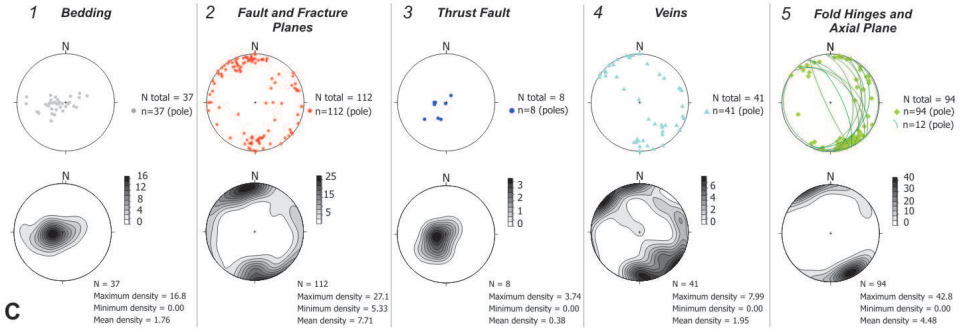

C

A.15.2

L2: ND 24126 73549 - Ham Bay

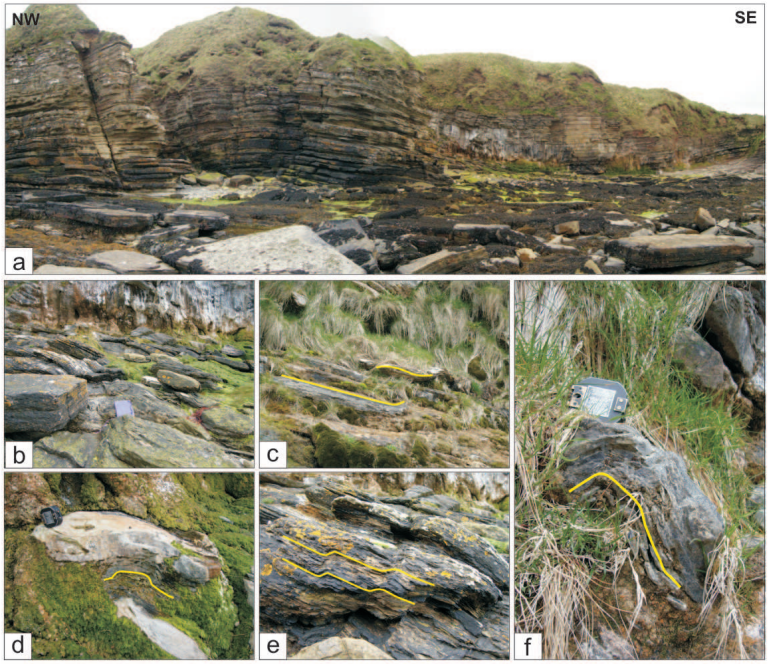

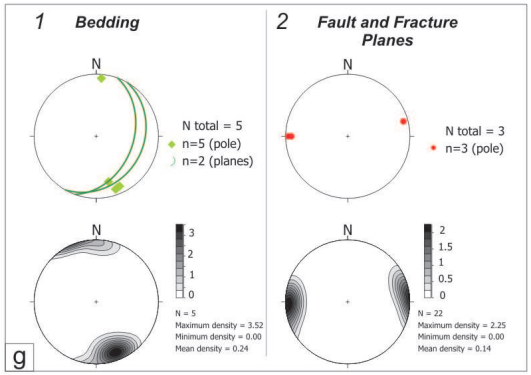

In locality L2 (ND 24126 73549) kink- to box-shaped folds occur (L2d, L2e and L2f).Fold hinges are NNW-SSE trending (158°-160°) and gently plunging to SSW (between 10°and 25°). One hinge data is N-S trending and N-plunging.

Axial planes are NNE-SSW (20° and 30°) and East dipping (25° and 45°).

Faults are N-S trending and 80° to vertical dipping (to both East and West).

A.16.1 Location: Skarfskerry

1:1K Lineament Analysis

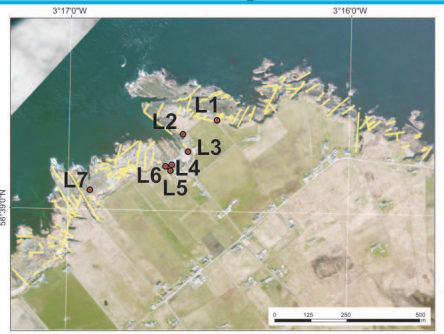

A

Skarfskerry sets within the Ham-Skarfskerry Subgroup, Middle Old Red Sandstones.
157 lineaments have been recognized at scale 1:1K (**Fig. A**)
They show 4 main clusters in NE-SW, E-W, NW-SE and WNW-ESE directions.
NE-SE trending lineaments appear to be the more abundant and the ones with larger scatter (about 30°). Distribution mean is in 51°-231° direction(red arrow in **Fig. B left**).
Relative Length-Azimuth plot show the same distribution **(Fig. B right)**. However the longest lineament recognized is in NW-SE direction. Distribution mean is in 40°-223° direction (red arrow).

B

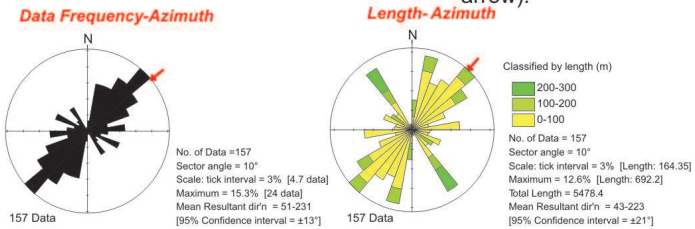

Overall structural data

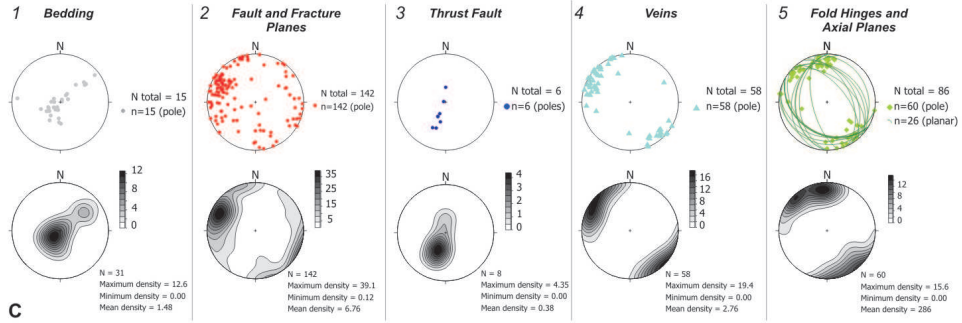

C

A.16.2

L5 (ND 25980 74414) . Skarfskerry

GROUP 2

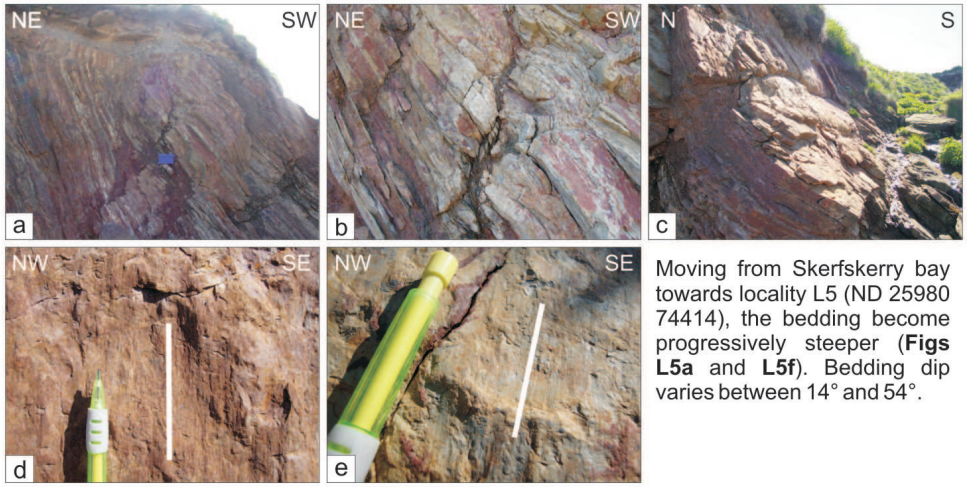

Moving from Skerfskerry bay towards locality L5 (ND 25980 74414), the bedding become progressively steeper (**Figs L5a** and **L5f**). Bedding dip varies between 14° and 54°.

Faults and fractures are NW-SE and E-W trending and dip values are between 20° and 50° (**Fig. L5f**). No kinematics and mineralization occur on fault planes.

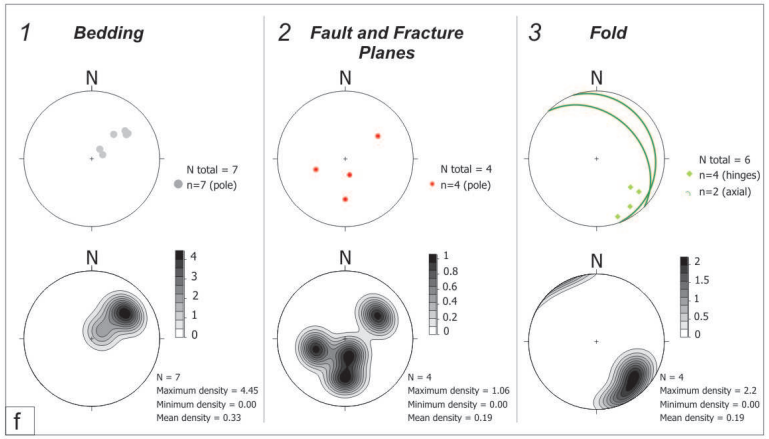

f

Folds occur on the cliff (**Fig. L5b**). Fold hinges are NNW-SSE trending and they gently (15° to 45°) plunge to NE. Axial planes are NNW- to NW-trending and they dip (15° and 35°) to the NE.
Flexural slip data trend on NE-SW (between 232° and 265°) and they plunge between 40° and 76° to NE.

A.16.3 Location: Skarfskerry

L6 (25963 74428) - Skarfskerry — GROUP 3

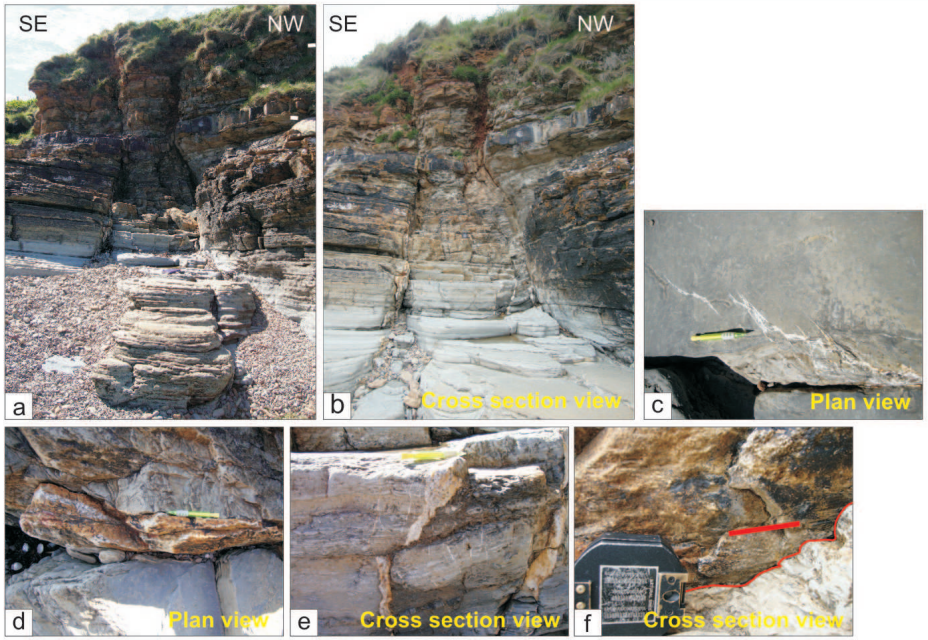

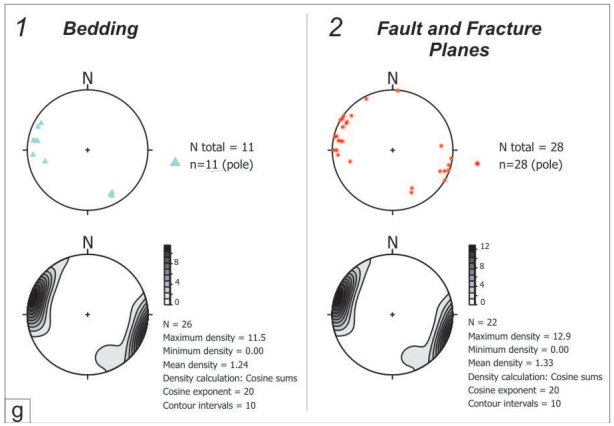

In locality L6 (ND 25963 74428), NE-SW trending faults occur (**Figs L6a -L6b)**.
Kinematic indicators on the fault planes are mainly strike-slip to dextral oblique **(Fig. L6b).** Carbonate veins on the platform are also consistent with dextral shear of the major structures **(Fig. L6c).** Fault planes are associated with carbonate mineralization and hematite staining **(Figs L6d-f)**.

A.16.4

L7 (ND 25713 74322) - Skarfskerry — GROUP 2 - 3

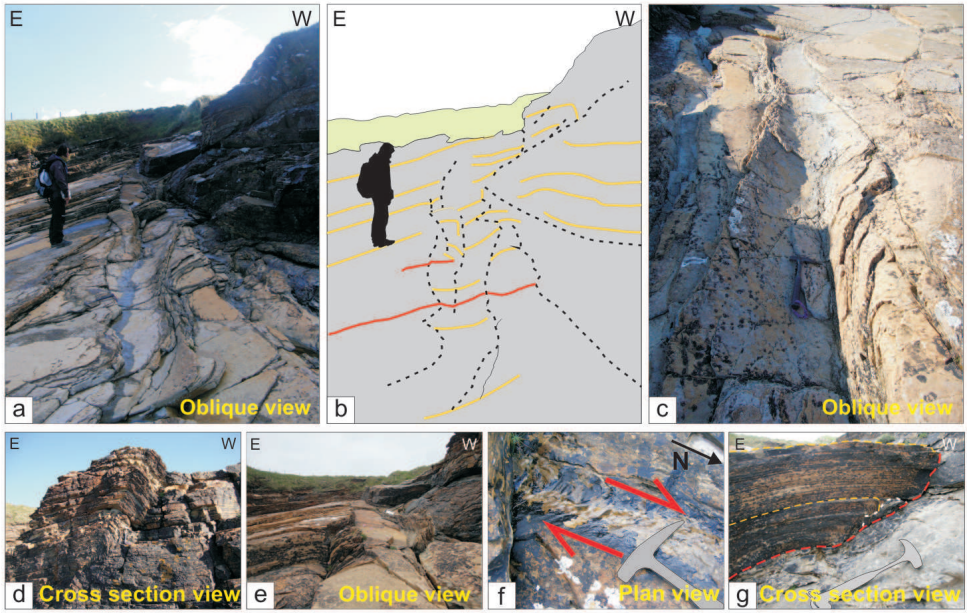

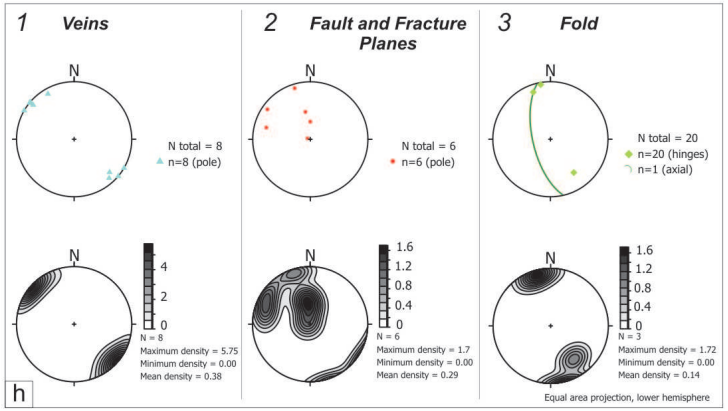

In locality L7 (ND 25713 74322), N-S trending folds occur (**Figs L7a -L7e)**. Fold hinges are N-trending plunging and gently plunging to both N and S. Minor fault planes are mainly NE-SW and E-W trending **(Fig. L7h)** Carbonate veins on the platform are NE-SW **(Fig. L7h)**. Deformation in N-S direction suggests dextral shear (**Fig. L7f**)

A.17.1 Location:Tang Head

1:1K Lineament Analysis

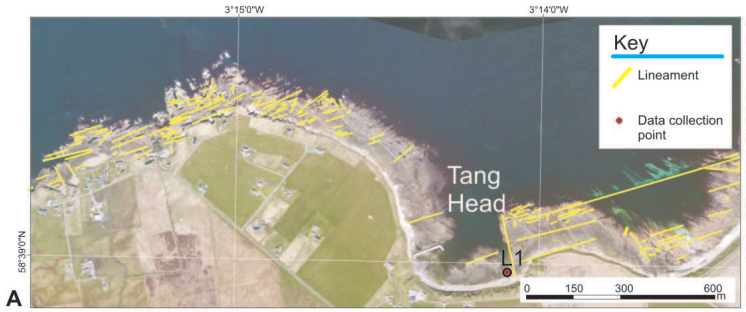

Overall structural data

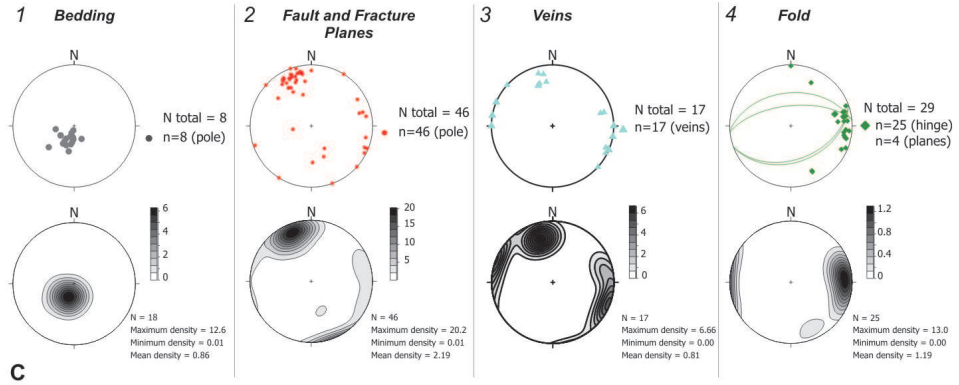

Tang Head is a bay located 18 km ENE of Thurso and 3 km WSW of St. John's Point.151 lineaments have been recognized at scale 1:1K (**Fig. A**).
3 main sets of structures occur: ENE-, NE- and NW- trending (**Fig. B left**). Distribution mean trends in direction 066°-246° (red arrow).
The Length-Azimuth plot shows a similar distribution (**Fig. B right**) with longer lineaments in direction ENE-WSW. NE and NW are 7-8 times shorter than ENE-WSW trending (700 to 800 m). Mean distribution trends in 070°-250° direction (red arrow).

A.17.2

L1 (ND 28387 74190) - Tang Head

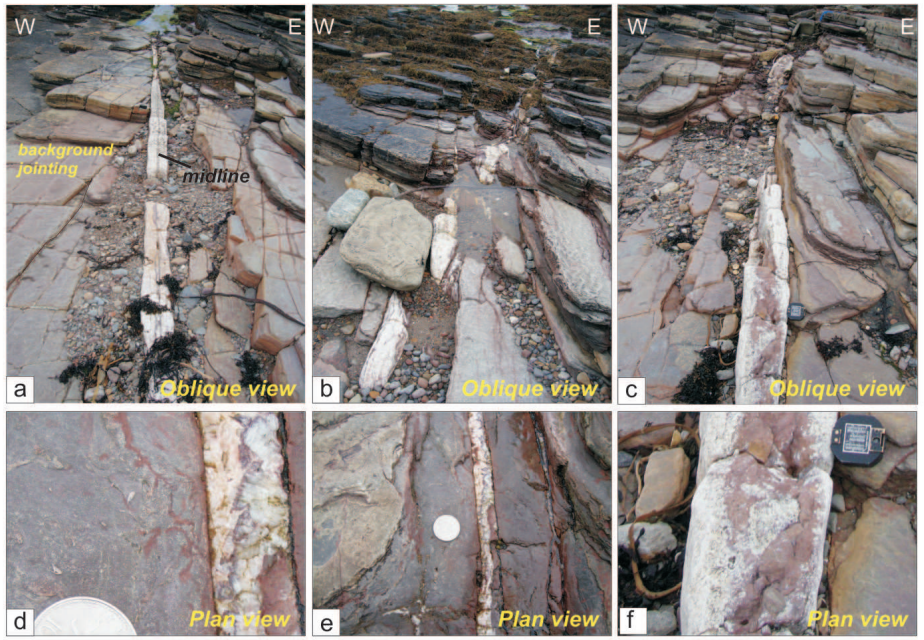

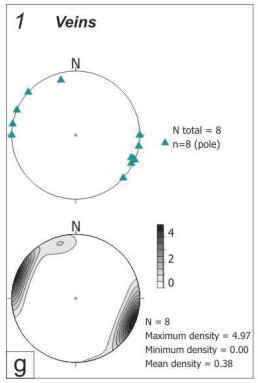

In locality L1 **(ND 28387 74190)** at Tang Head, a series of thick (<20 cm) veins occur (**Figs L1a-e**). They are mainly N-S to NNE-SSW trending and they dip between 83° and 90°. They cut across "background jointing" observed in the platform (**Fig. L1a**) or, in some instances, reactivate N-S fractures (**Figs L1b-c**). Kinematic indicators show both tensile and dextral strike-slip opening.

A.18.1 Location: St. John's Point

1:1K Lineament Analysis

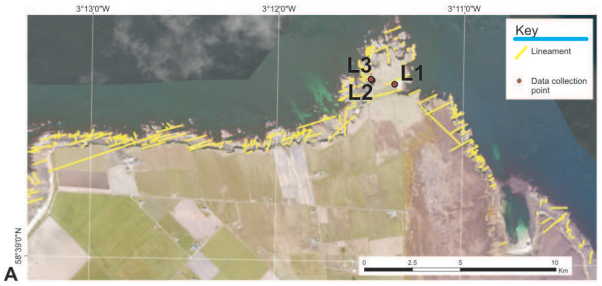

At St. John's Point 211 lineaments have been recognized at scale 1:1K (**Fig. A**).Three main set of structures occur: ENE-WSW, N-S to NNE-SSW and NW-SE trending (**Fig. B left**). Distribution mean trends in direction 052°-232° (red arrow).

Lenght-Azimuth plot shows a similar distribution (**Fig. B right**) with longer lineaments in direction ENE-WSW. N-S and NW-SE lineaments are 6 times, or more, shorter that the ENE-WSW set (600 to 700 m). Mean distribution trends in direction 062°-242° (red arrow).

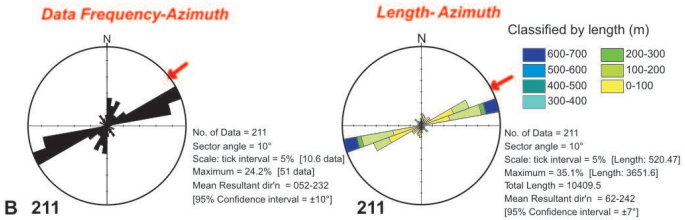

Overall structural data

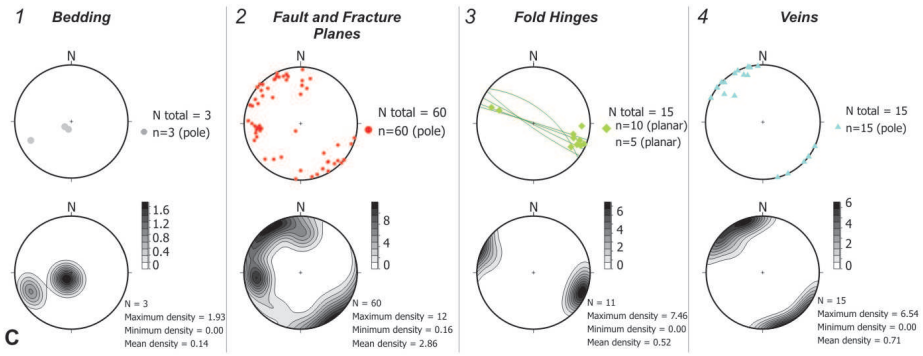

Bedding is sub-horizontal (**Fig. C1**), although some open folds and variations in the bedding occur. 60 normal faults and fractures have been recorded (**Fig. C2**). They show large variability in trend and dip. ENE- and N-trending represent the larger clusters of data. Fold hinges trend WNW-ESE and plunge between 02° and 44° with a major cluster around 20° (**Fig. C3**). Axial planes are WNW-ESE trending. Veins are mainly NE-SW trending (**Fig. C4**).

A.18.2

L2 (ND 30958 75066) - St. John's Point

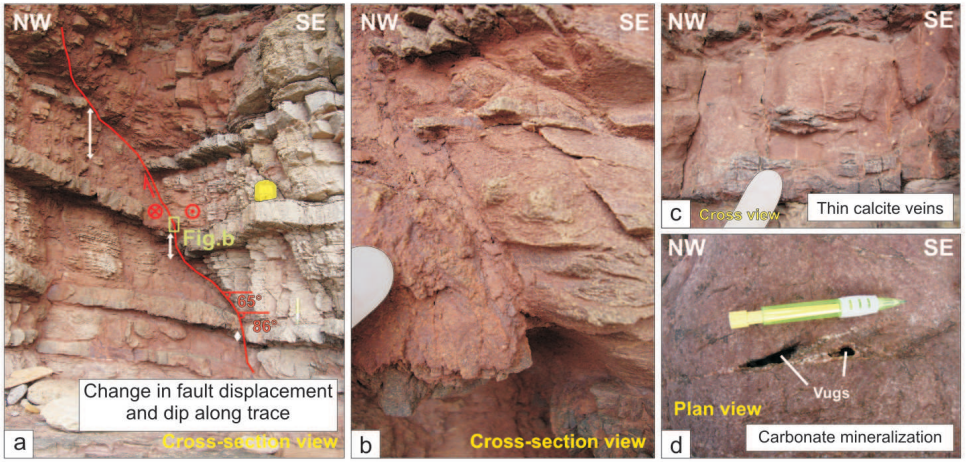

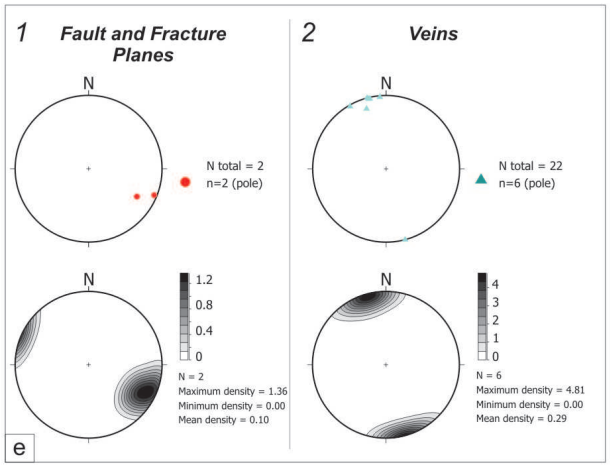

In locality L2 (ND 30958 75066), a NE-SW trending fault occurs. The fault has variable dip values and chances in displacement along dip have been observed (**Fig. L1a**). The fault rock consists of a thin gouge. No mineralization is associated with the fault plane Fig. L2b).

In the nearby cliff and plaform a series of mm-scale veins occur (**Figs L2c-d**) They are ENE-WSW trending and not very continuous in length (<10 cm). In some instances they present cm-scale voids (**Fig. L2d**).

A.18.3

L3 (ND 30959 75069) - St. John's Point

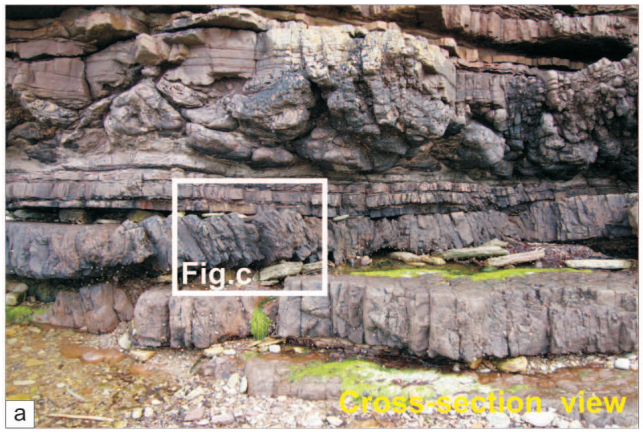

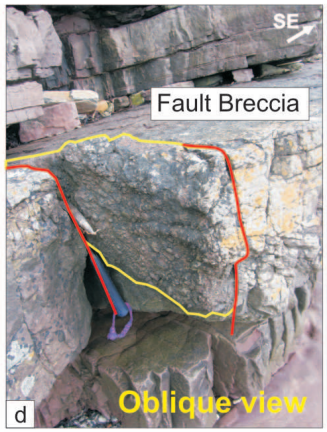

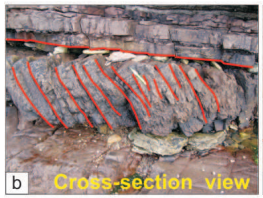

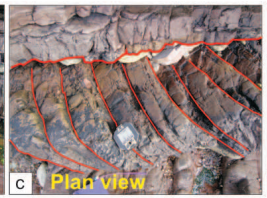

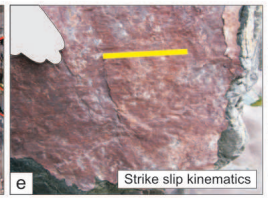

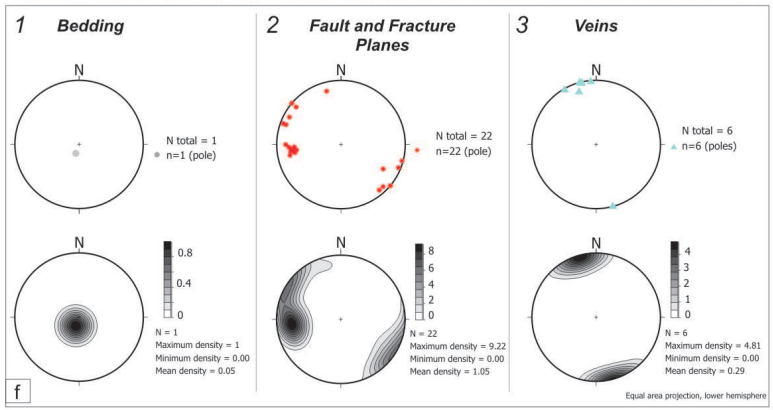

In locality L3 (**ND 30959 75069)** a bedding-confined domino structures occurs (**Fig. L3a**). The faults are N-S trending. The observations in cross-section view and in plan view suggest an oblique sinistral movement along the faults (**Figs L3b-c**).
Also a larger NW-SE trending fault occurs (**Fig. L3d**). Fault rocks consist of cemented breccia and dextral strike-slip slickenlines occur on the fault plane.

A.19.1 Location: Stroma Island

1:1K Lineament Analysis

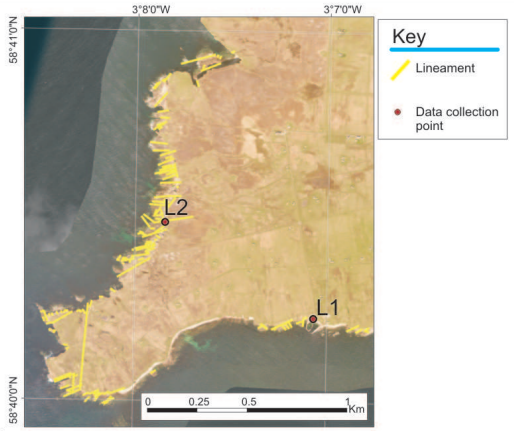

Stoma Island is located north east of St. John's Point. 143 lineaments have been recorded at scale 1:1k (**Fig. A**). and they show 3 major clusters in ENE-, NE- and NNW-directions (**Fig. B left**), with a mean in 067°-247° direction (red arrow). Length-Azimuth plot shows similar distribution with the longer lineament in direction N-S (**Fig. B right**) and mean in 069°-249° direction (red arrow).

A

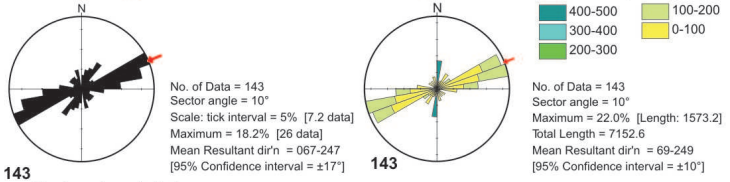

B 143 143

Overall structural data

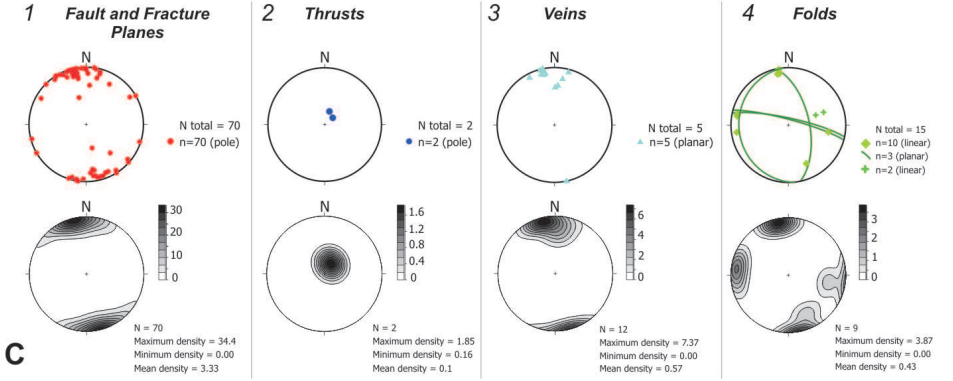

C

A.19.2

L1 (ND 35284 76381) - Stroma Island — GROUP 2

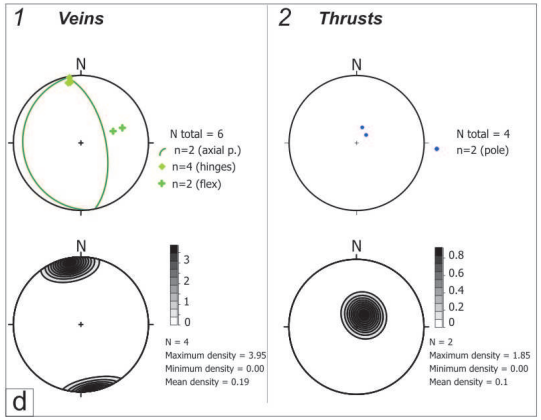

In location L1 (**ND 35284 76381)** a series of N-S trending folds occur (**Figs L1a-c**). Fold hinges trend between 348° and 350° and they gently plunge (between 02°-10°) to the north. Axial planes trend N-S and they dip 15° to the W and 60° to the E (**Fig. D1)**. Associated thrust faults are N-S trending with dip values of 15° and 20° (**Fig. D2**).

A.19.3

L2 (ND 34539 76870) - Stroma Island — GROUP 3

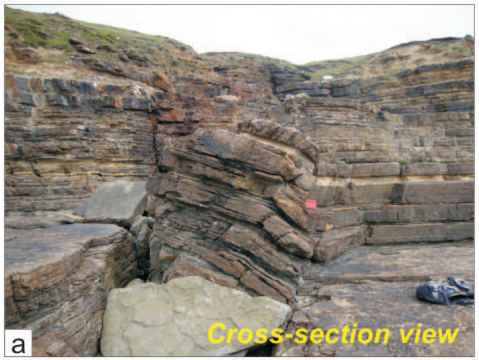

In location L2 (**34539 76870)** WNW-ESE trending folds occur (**Figs L2a**). Fold hinge trend between 262° and 282° and they gently plunge (10°) to the west. Axial planes trend WNW-ESE (102°-105°) and they steeply (80°-82°) dip to the N (**Fig. E3)**. In the area ENE-WSW trending faults occur and they are associated with carbonate mineralization and breaccciation (**Figs L2b-d**). Veins are E-W trending (**Fig. E2**)

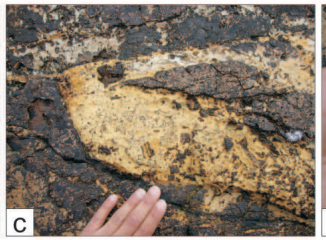

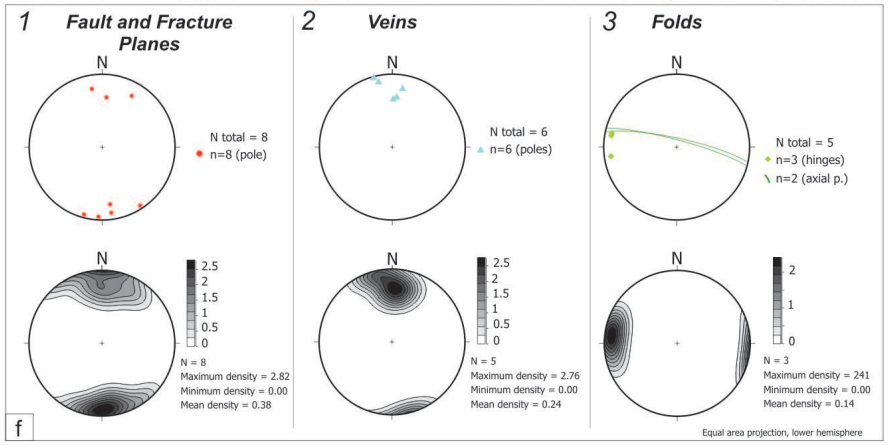

A.20 Location: Bay of Sannick - Thirle Door

1:1K Lineament Analysis

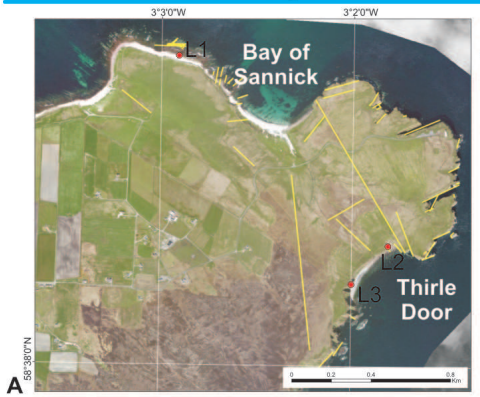

A

Key

Lineament

Data collection point

55 lineaments have been recognized in the area between Bay of Sannick and Thirle Door (**Fig. A**). They show three major clusters in NE to ENE, NNE and NW-SE directions. Mean is in 052°-232° direction (**Fig. B left**). Length- Azimuth plot shows that the longer lineaments (800 to 1000 m) are N-S and NW-SE direction (**Fig. B right**).

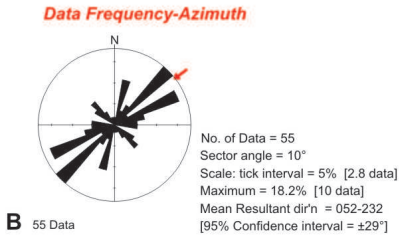

No. of Data = 55
Sector angle = 10°
Scale: tick interval = 5% [2.8 data]
Maximum = 18.2% [10 data]
Mean Resultant dir'n = 052-232
[95% Confidence interval = ±29°]

B 55 Data

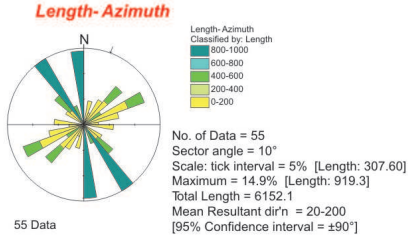

55 Data

No. of Data = 55
Sector angle = 10°
Scale: tick interval = 5% [Length: 307.60]
Maximum = 14.9% [Length: 919.3]
Total Length = 6152.1
Mean Resultant dir'n = 20-200
[95% Confidence interval = ±90°]

Overall structural data

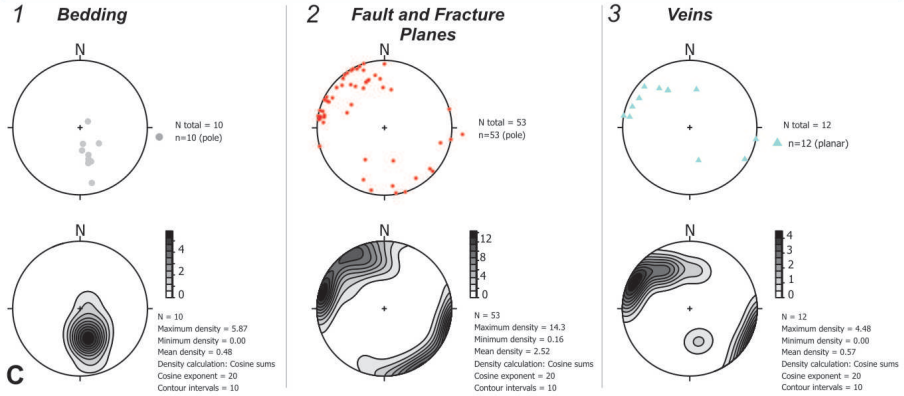

C

APPENDIX B

Stress Inversion - Plots

B.1 Faraid Head — Event 3

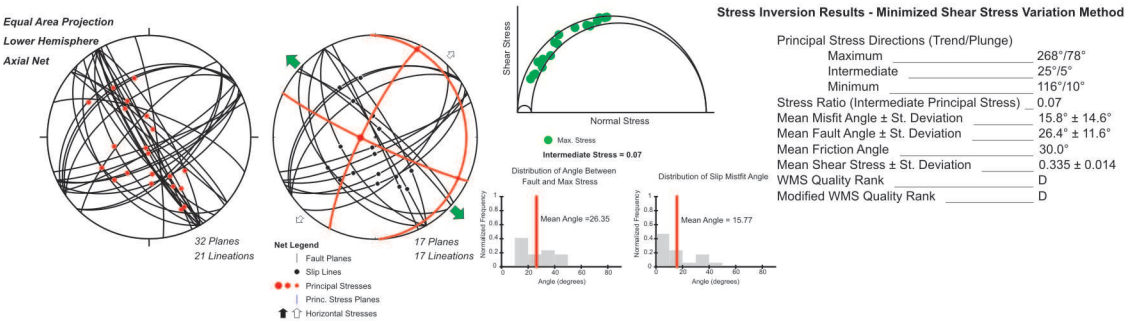

Stress Inversion Results - Minimized Shear Stress Variation Method

Principal Stress Directions (Trend/Plunge)

Maximum	268°/78°
Intermediate	25°/5°
Minimum	116°/10°
Stress Ratio (Intermediate Principal Stress)	0.07
Mean Misfit Angle ± St. Deviation	15.8° ± 14.6°
Mean Fault Angle ± St. Deviation	26.4° ± 11.6°
Mean Friction Angle	30.0°
Mean Shear Stress ± St. Deviation	0.335 ± 0.014
WMS Quality Rank	D
Modified WMS Quality Rank	D

B.2 Kirtomy — Event 3

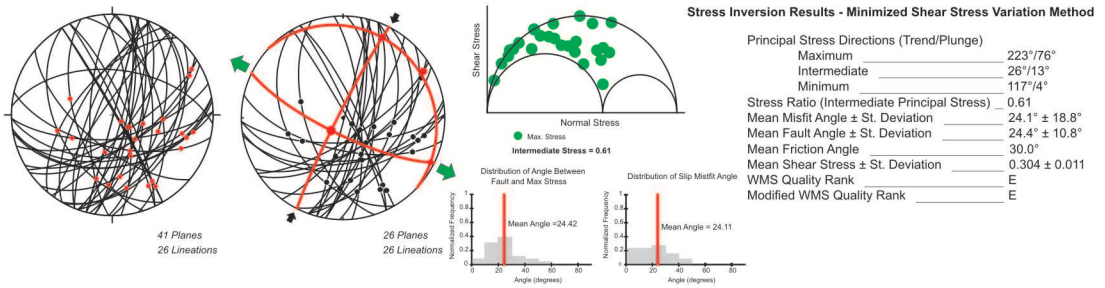

Stress Inversion Results - Minimized Shear Stress Variation Method

Principal Stress Directions (Trend/Plunge)

Maximum	223°/76°
Intermediate	26°/13°
Minimum	117°/4°
Stress Ratio (Intermediate Principal Stress)	0.61
Mean Misfit Angle ± St. Deviation	24.1° ± 18.8°
Mean Fault Angle ± St. Deviation	24.4° ± 10.8°
Mean Friction Angle	30.0°
Mean Shear Stress ± St. Deviation	0.304 ± 0.011
WMS Quality Rank	E
Modified WMS Quality Rank	E

B.3 Strathy Bay — Event 3

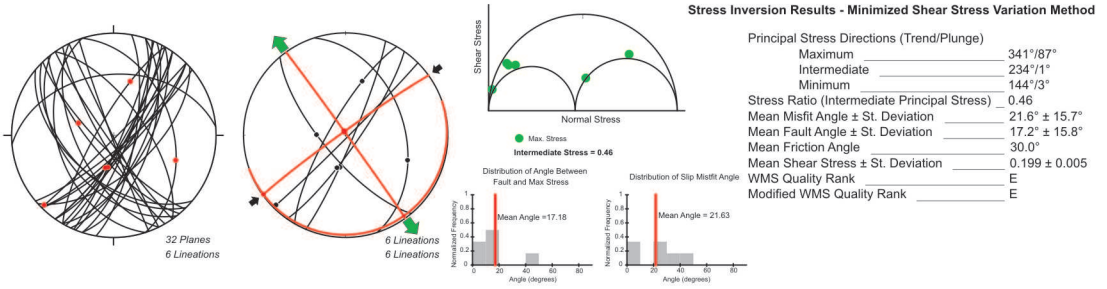

Stress Inversion Results - Minimized Shear Stress Variation Method

Principal Stress Directions (Trend/Plunge)

Maximum	341°/87°
Intermediate	234°/1°
Minimum	144°/3°
Stress Ratio (Intermediate Principal Stress)	0.46
Mean Misfit Angle ± St. Deviation	21.6° ± 15.7°
Mean Fault Angle ± St. Deviation	17.2° ± 15.8°
Mean Friction Angle	30.0°
Mean Shear Stress ± St. Deviation	0.199 ± 0.005
WMS Quality Rank	E
Modified WMS Quality Rank	E

B.4 Portskerra - Bas. — Event 1

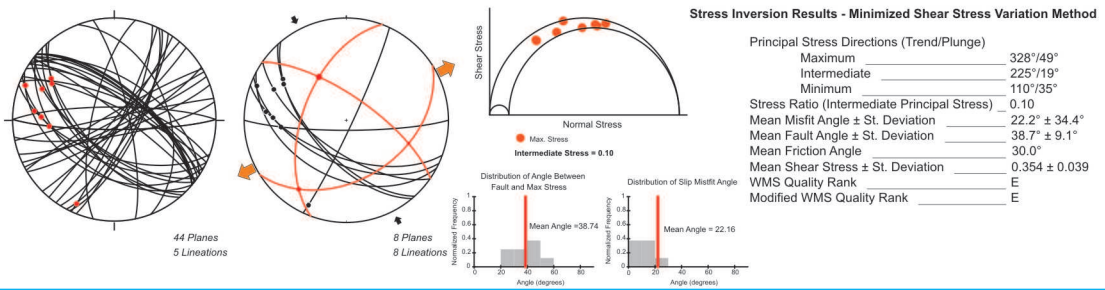

Stress Inversion Results - Minimized Shear Stress Variation Method

Principal Stress Directions (Trend/Plunge)

Maximum	328°/49°
Intermediate	225°/19°
Minimum	110°/35°
Stress Ratio (Intermediate Principal Stress)	0.10
Mean Misfit Angle ± St. Deviation	22.2° ± 34.4°
Mean Fault Angle ± St. Deviation	38.7° ± 9.1°
Mean Friction Angle	30.0°
Mean Shear Stress ± St. Deviation	0.354 ± 0.039
WMS Quality Rank	E
Modified WMS Quality Rank	E

B.4 Portskerra - ORS Event 1

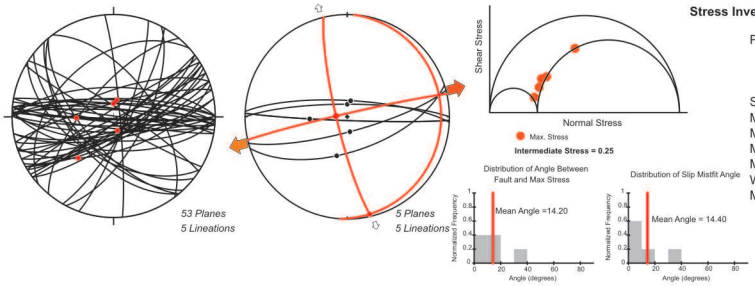

Stress Inversion Results - Minimized Shear Stress Variation Method

Principal Stress Directions (Trend/Plunge)

Maximum	374°/81°
Intermediate	167°/3°
Minimum	77°/9°
Stress Ratio (Intermediate Principal Stress)	0.25
Mean Misfit Angle ± St. Deviation	14.4° ± 11.2°
Mean Fault Angle ± St. Deviation	14.2° ± 9.8°
Mean Friction Angle	30.0°
Mean Shear Stress ± St. Deviation	0.175 ± 0.008
WMS Quality Rank	C
Modified WMS Quality Rank	E

B.5 Dounreay Event 3

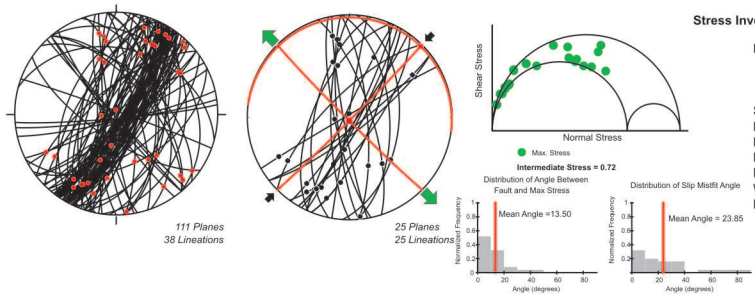

Stress Inversion Results - Minimized Shear Stress Variation Method

Principal Stress Directions (Trend/Plunge)

Maximum	187°/87°
Intermediate	45°/2°
Minimum	315°/2°
Stress Ratio (Intermediate Principal Stress)	0.72
Mean Misfit Angle ± St. Deviation	23.9° ± 22.5°
Mean Fault Angle ± St. Deviation	13.5° ± 10.3°
Mean Friction Angle	30.0°
Mean Shear Stress ± St. Deviation	0.256 ± 0.012
WMS Quality Rank	E
Modified WMS Quality Rank	E

B.6 Brims Ness Event1

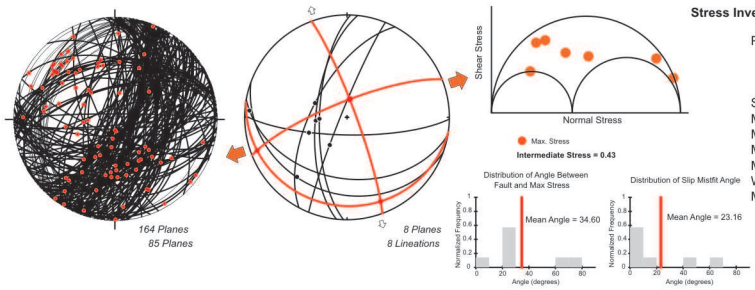

Stress Inversion Results - Minimized Shear Stress Variation Method

Principal Stress Directions (Trend/Plunge)

Maximum	8°/76°
Intermediate	158°/13°
Minimum	250°/7°
Stress Ratio (Intermediate Principal Stress)	0.43
Mean Misfit Angle ± St. Deviation	23.2° ± 22.6°
Mean Fault Angle ± St. Deviation	34.6° ± 26.7°
Mean Friction Angle	30.0°
Mean Shear Stress ± St. Deviation	0.253 ± 0.010
WMS Quality Rank	E
Modified WMS Quality Rank	E

Event 2

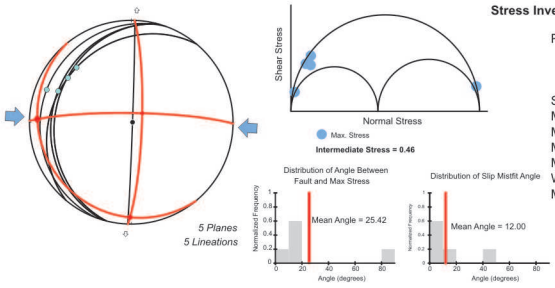

Stress Inversion Results - Minimized Shear Stress Variation Method

Principal Stress Directions (Trend/Plunge)

Maximum	272°/9°
Intermediate	181°/7°
Minimum	51°/79°
Stress Ratio (Intermediate Principal Stress)	0.46
Mean Misfit Angle ± St. Deviation	12° ± 16.2°
Mean Fault Angle ± St. Deviation	25.4° ± 30.5°
Mean Friction Angle	10.0°
Mean Shear Stress ± St. Deviation	0.194 ± 0.007
WMS Quality Rank	C
Modified WMS Quality Rank	C

Event 3

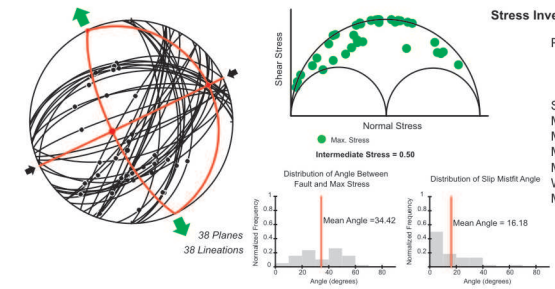

Stress Inversion Results - Minimized Shear Stress Variation Method

Principal Stress Directions (Trend/Plunge)

Maximum	243°/73°
Intermediate	65°/17°
Minimum	334°/0°
Stress Ratio (Intermediate Principal Stress)	0.50
Mean Misfit Angle ± St. Deviation	16.2° ± 14.3°
Mean Fault Angle ± St. Deviation	34.4° ± 16.4°
Mean Friction Angle	30.0°
Mean Shear Stress ± St. Deviation	0.364± 0.012
WMS Quality Rank	D
Modified WMS Quality Rank	D

B.7 Thurso Bay

Event1

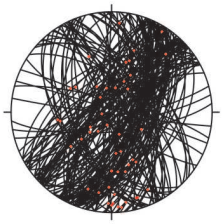

227 Planes
50 Lineations

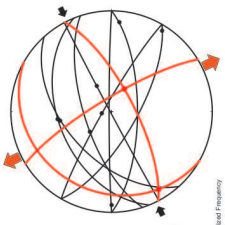

8 Planes
8 Lineations

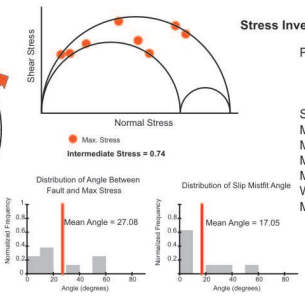

Stress Inversion Results - Minimized Shear Stress Variation Method

Principal Stress Directions (Trend/Plunge)
- Maximum: 29°/69°
- Intermediate: 149°/11°
- Minimum: 242°/18°

Stress Ratio (Intermediate Principal Stress): 0.74
Mean Misfit Angle ± St. Deviation: 17.0° ± 19.9°
Mean Fault Angle ± St. Deviation: 27.1° ± 21.1°
Mean Friction Angle: 30.0°
Mean Shear Stress ± St. Deviation: 0.345 ± 0.010
WMS Quality Rank: D
Modified WMS Quality Rank: D

Event3

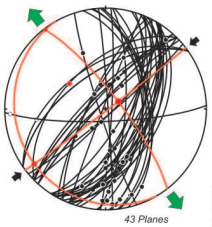

43 Planes
43 Lineations

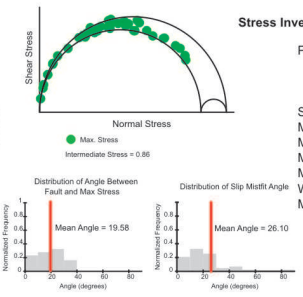

Stress Inversion Results - Minimized Shear Stress Variation Method

Principal Stress Directions (Trend/Plunge)
- Maximum: 60°/78°
- Intermediate: 232°/12°
- Minimum: 323°/2°

Stress Ratio (Intermediate Principal Stress): 0.86
Mean Misfit Angle ± St. Deviation: 26.1° ± 26.1°
Mean Fault Angle ± St. Deviation: 19.6° ± 9.8°
Mean Friction Angle: 30.0°
Mean Shear Stress ± St. Deviation: 0.312 ± 0.026
WMS Quality Rank: E
Modified WMS Quality Rank: E

B.8 Murkle Bay

Event3

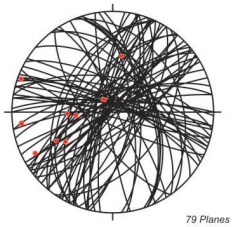

79 Planes
10 Lineations

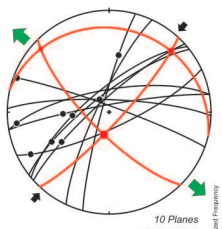

10 Planes
10 Lineations

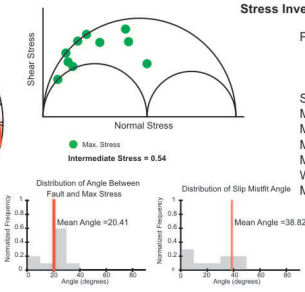

Stress Inversion Results - Minimized Shear Stress Variation Method

Principal Stress Directions (Trend/Plunge)
- Maximum: 193°/72°
- Intermediate: 45°/16°
- Minimum: 313°/9°

Stress Ratio (Intermediate Principal Stress): 0.54
Mean Misfit Angle ± St. Deviation: 38.8° ± 46.3°
Mean Fault Angle ± St. Deviation: 20.4° ± 10.3°
Mean Friction Angle: 30.0°
Mean Shear Stress ± St. Deviation: 0.254 ± 0.027
WMS Quality Rank: E
Modified WMS Quality Rank: E

B.9 Castletown

Event3

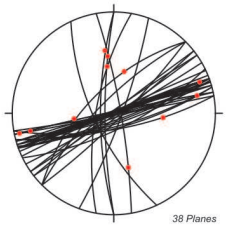

38 Planes
11 Lineations

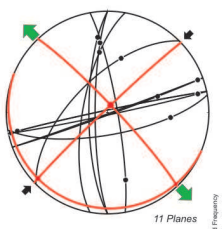

11 Planes
11 Lineations

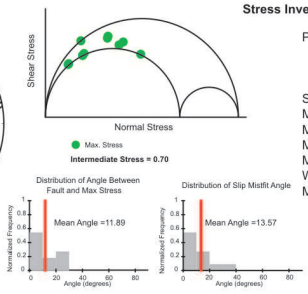

Stress Inversion Results - Minimized Shear Stress Variation Method

Principal Stress Directions (Trend/Plunge)
- Maximum: 22°/84°
- Intermediate: 227°/6°
- Minimum: 136°/3°

Stress Ratio (Intermediate Principal Stress): 0.70
Mean Misfit Angle ± St. Deviation: 13.6° ± 10.4°
Mean Fault Angle ± St. Deviation: 11.9° ± 8.5°
Mean Friction Angle: 30.0°
Mean Shear Stress ± St. Deviation: 0.327 ± 0.003
WMS Quality Rank: C
Modified WMS Quality Rank: C

B.10 Dunnet Head

Event 3

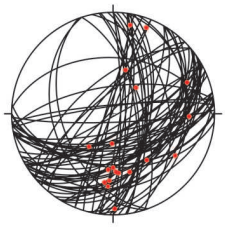

73 Planes
19 Lineations

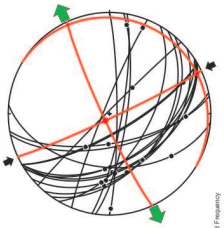

18 Planes
18 Lineations

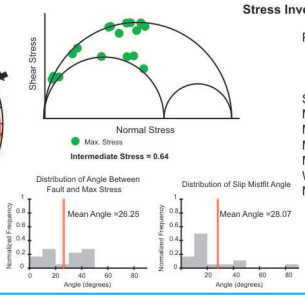

Stress Inversion Results - Minimized Shear Stress Variation Method

Principal Stress Directions (Trend/Plunge)
- Maximum: 211°/83°
- Intermediate: 65°/5°
- Minimum: 335°/4°

Stress Ratio (Intermediate Principal Stress): 0.64
Mean Misfit Angle ± St. Deviation: 28.1° ± 35.1°
Mean Fault Angle ± St. Deviation: 26.3° ± 15.3°
Mean Friction Angle: 30.0°
Mean Shear Stress ± St. Deviation: 0.319 ± 0.039
WMS Quality Rank: E
Modified WMS Quality Rank: E

B.11 Ham Bay Event3

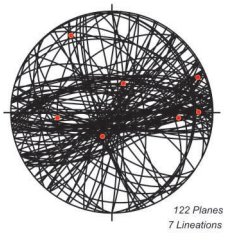

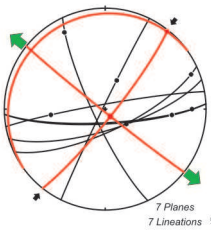

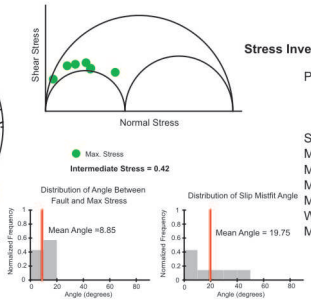

Stress Inversion Results - Minimized Shear Stress Variation Method

Principal Stress Directions (Trend/Plunge)

Maximum	144°/83°
Intermediate	39°/2°
Minimum	308°/7°
Stress Ratio (Intermediate Principal Stress)	0.42
Mean Misfit Angle ± St. Deviation	19.7° ±16.0°
Mean Fault Angle ± St. Deviation	8.8° ± 2.5°
Mean Friction Angle	30.0°
Mean Shear Stress ± St. Deviation	0.200 ± 0.001
WMS Quality Rank	E
Modified WMS Quality Rank	E

B.12 Skarfskerry Event3

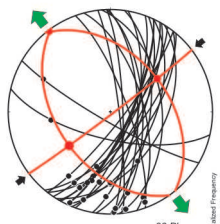

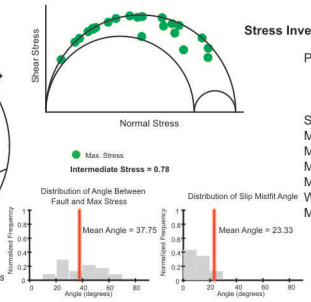

Stress Inversion Results - Minimized Shear Stress Variation Method

Principal Stress Directions (Trend/Plunge)

Maximum	227°/8°
Intermediate	13°/80°
Minimum	136°/5°
Stress Ratio (Intermediate Principal Stress)	0.60
Mean Misfit Angle ± St. Deviation	35.0° ± 46.2°
Mean Fault Angle ± St. Deviation	33.4° ± 17.0°
Mean Friction Angle	30.0°
Mean Shear Stress ± St. Deviation	0.261 ± 0.051
WMS Quality Rank	E
Modified WMS Quality Rank	E

B.13 St.John's Point Event3

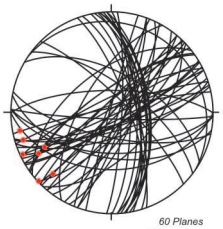

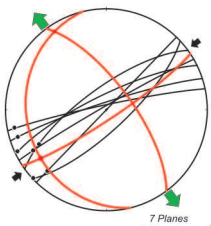

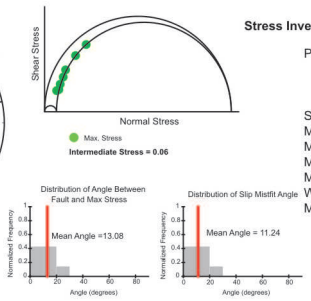

Stress Inversion Results - Minimized Shear Stress Variation Method

Principal Stress Directions (Trend/Plunge)

Maximum	234°/20°
Intermediate	326°/8°
Minimum	76°/68°
Stress Ratio (Intermediate Principal Stress)	0.06
Mean Misfit Angle ± St. Deviation	11.2° ± 5.7°
Mean Fault Angle ± St. Deviation	13.1° ± 6.7°
Mean Friction Angle	30.0°
Mean Shear Stress ± St. Deviation	0.198 ± 0.008
WMS Quality Rank	D
Modified WMS Quality Rank	E

B.14 Duncansby Event1

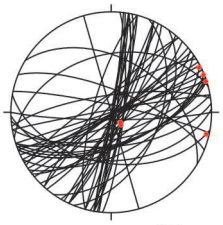

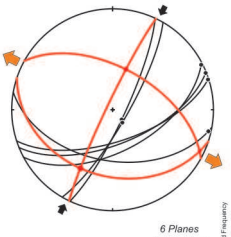

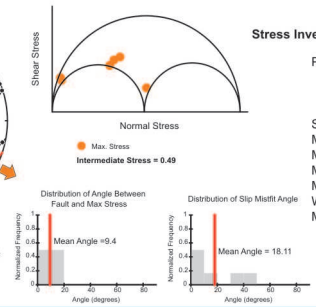

Stress Inversion Results - Minimized Shear Stress Variation Method

Principal Stress Directions (Trend/Plunge)

Maximum	209°/34°
Intermediate	18°/55°
Minimum	115°/5°
Stress Ratio (Intermediate Principal Stress)	0.49
Mean Misfit Angle ± St. Deviation	18.1° ± 17.5°
Mean Fault Angle ± St. Deviation	9.4° ± 4.3°
Mean Friction Angle	30.0°
Mean Shear Stress ± St. Deviation	0.196 ± 0.005
WMS Quality Rank	E
Modified WMS Quality Rank	E

APPENDIX C

Stress Inversion - Data

Tab. C.1: Faraid Head

Group3

#	Dip Azim	Dip	Trend	Plunge	Slip Sense	Norm. Stress	Shear Stress	Max. Shear	Misfit Angle	Fault Angle
1	40	78	354	73	Left Normal	.175	.294	.295	5.5	19.7
2	42	83	26	83	Normal	.131	.234	.234	2.4	15.
3	327	40	324	40	Normal	.473	.48	.495	13.8	43.2
4	240	44	237	44	Normal	.367	.442	.453	12.2	35.5
5	225	45	219	45	Normal	.384	.429	.448	16.6	36.
6	154	70	211	56	Right-Normal	.196	.338	.364	21.5	24.3
7	155	78	182	77	Normal	.108	.262	.262	2.4	16.2
8	152	55	177	52	Right-Normal	.422	.472	.474	4.8	39.3
9	135	55	152	54	Normal	.461	.491	.491	.9	42.3
10	160	83	196	81	Normal	.068	.173	.174	5.6	10.4
11	325	56	329	56	Normal	.219	.387	.403	16.3	27.2
12	65	89	154	45	Right-Normal Diag.	.084	.15	.193	39.2	11.7
13	148	63	175	60	Right-Normal	.304	.438	.44	4.9	32.2
14	60	88	148	40	Right-Normal Diag.	.093	.139	.2	46.1	12.3
15	240	62	255	61	Normal	.134	.275	.277	5.5	17.6
16	60	76	133	50	Right-Normal	.211	.276	.356	39.1	24.2
17	325	42	346	40	Right-Normal	.434	.421	.491	31.	40.9

Tab. C.2: Kirtomy

Group3

#	Dip Azim	Dip	Trend	Plunge	Slip Sense	Norm. Stress	Shear Stress	Max. Shear	Misfit Angle	Fault Angle
1	85	76	156	53	Right-Normal	.28	.39	.397	10.8	24.1
2	135	45	173	38	Right-Normal	.555	.374	.46	35.6	42.9
3	118	39	169	27	Right-Normal Diag.	.655	.377	.465	35.9	52.6
4	100	78	183	31	Normal-Right SS	.137	.302	.328	22.8	19.3
5	145	63	63	15	Normal-Left SS	.325	.273	.392	45.9	23.4
6	193	64	116	25	Normal-Left SS	.61	.138	.147	20.	13.8
7	170	53	105	29	Normal-Left SS	.578	.305	.322	18.7	28.
8	178	55	102	19	Normal-Left SS	.6	.236	.272	29.5	24.7
9	172	47	107	24	Normal-Left SS	.644	.273	.311	28.3	33.5
10	240	44	254	43	Normal	.611	.298	.335	27.3	32.6
11	178	70	240	52	Right-Normal	.508	-.013	.251	92.9	10.
12	105	82	126	81	Normal	.075	.217	.253	30.8	14.3

13	110	65	154	57	Right-Normal	.246	.427	.431	7.6	29.7
14	127	75	191	59	Right-Normal	.111	.215	.292	42.4	16.
15	110	75	129	74	Normal	.118	.314	.322	12.8	20.
16	103	67	137	63	Right-Normal	.248	.424	.428	7.9	29.4
17	110	50	110	50	Normal	.488	.486	.499	13.1	44.1
18	252	60	291	53	Right-Normal	.391	.31	.348	27.2	17.7
19	100	75	125	73	Normal	.167	.327	.36	24.8	22.2
20	105	89	194	35	Normal-Right SS	.037	.167	.167	1.9	7.5
21	150	63	95	48	Left Normal	.355	.382	.382	1.1	22.3
22	92	65	106	64	Normal	.348	.413	.459	25.8	33.6
23	60	87	149	18	Normal-Right SS	.462	.311	.314	7.9	16.3
24	65	78	149	24	Normal-Right SS	.468	.36	.367	11.5	24.8
25	65	84	153	22	Normal-Right SS	.427	.341	.344	7.2	18.8
26	147	73	60	10	Left SS	.234	.262	.329	37.1	13.2

Tab. C.3: Strathy Bay

Group3

#	Dip Azim	Dip	Trend	Plunge	Slip Sense	Norm. Stress	Shear Stress	Max. Shear	Misfit Angle	Fault Angle
1	230	72	271	67	Right-Normal	0.551	0.17	0.175	13.7	21.2
2	135	88	224	24	Normal-Right SS	0.021	0.099	0.124	36.7	6
3	113	84	190	64	Right-Normal	0.143	0.214	0.244	28.7	8.4
4	300	77	17	44	Right-Normal Diag.	0.096	0.228	0.229	6.2	10
5	125	80	195	63	Right-Normal	0.101	0.256	0.257	4.3	13.3
6	72	42	112	35	Right-Normal	0.741	0.262	0.282	23.8	46.3

Tab. C.4: Portskerra Basement

#	Dip Azim	Dip	Trend	Plunge	Slip Sense	Norm. Stress	Shear Stress	Max. Shear	Misfit Angle	Fault Angle
1	180	82	264	36	Normal-Right SS	0.488	0.396	0.45	28.1	41.2
2	208	43	291	7	Normal-Right SS	0.612	0.467	0.472	11.5	50.5
3	200	60	276	22	Normal-Right SS	0.567	0.445	0.458	11.3	46.5
4	205	55	272	29	Normal-Right SS	0.557	0.463	0.466	4.2	46.3
5	215	65	293	24	Normal-Right SS	0.353	0.418	0.426	11.3	33.3
6	115	85	204	10	Normal-Right SS	0.388	-0.126	0.484	105	38.3
7	230	60	303	27	Normal-Right SS	0.244	0.385	0.386	4.3	26.9
8	228	62	300	30	Normal-Right SS	0.247	0.382	0.383	1.7	26.8

Tab. C.5: Portskerra Old Red Sandstones

#	Dip Azim	Dip	Trend	Plunge	Slip Sense	Norm. Stress	Shear Stress	Max. Shear	Misfit Angle	Fault Angle
1	182	87	267	60	Right-Normal	0.235	0.064	0.078	35.3	3.3
2	162	62	195	58	Right-Normal	0.45	0.328	0.331	7.3	31
3		80		80	Normal	0.261	0.127	0.13	13.1	9.3
4	3	77	12	77	Normal	0.273	0.173	0.174	8.3	12.7
5	165	78	170	78	Normal	0.3	0.183	0.184	8.1	14.7

Tab. C.6: Dounreay

Group3

#	Dip Azim	Dip	Trend	Plunge	Slip Sense	Norm. Stress	Shear Stress	Max. Shear	Misfit Angle	Fault Angle
1	115	85	199	50	Right-Normal	0.087	0.191	0.238	36.6	4.1
2	94	50	136	42	Right-Normal	0.579	0.437	0.445	10.8	40.1

3	126	70	210	17	Normal-Right SS	0.115	0.194	0.313	51.6	18.6
4	115	85	202	27	Normal-Right SS	0.087	0.231	0.238	13.6	4.1
5	315	72	235	27	Normal-Left SS	0.114	0.158	0.318	60.2	19.7
6	265	80	351	24	Normal-Right SS	0.443	0.358	0.36	6.4	9.3
7	258	78	263	78	Normal	0.53	0.112	0.333	70.3	11
8	280	89	352	87	Normal	0.237	0.049	0.338	81.6	1.1
9	142	78	58	26	Normal-Left SS	0.042	0.153	0.191	36.8	10
10	295	86	22	37	Normal-Right SS	0.092	0.235	0.245	15.9	4.8
11	125	85	213	24	Normal-Right SS	0.025	0.136	0.136	0.9	3.7
12	330	88	241	22	Normal-Left SS	0.053	0.192	0.192	2.1	4.3
13	112	72	196	19	Normal-Right SS	0.181	0.32	0.349	23.8	17.3
14	270	75	352	29	Normal-Right SS	0.409	0.38	0.38	3.2	14.6
15	120	80	206	23	Normal-Right SS	0.068	0.219	0.226	14.5	8.9
16	142	82	56	27	Normal-Left SS	0.022	0.125	0.136	23.8	6
17	112	72	188	36	Normal-Right SS	0.181	0.348	0.349	5.8	17.3
18	120	80	189	64	Right-Normal	0.068	0.199	0.226	28.5	8.9
19	72	73	145	44	Right-Normal Diag.	0.605	0.282	0.311	25	18.3
20	282	62	343	43	Right-Normal	0.402	0.436	0.436	0.5	28.2
21	118	83	205	24	Normal-Right SS	0.069	0.22	0.22	0.3	6
22	85	76	159	48	Right-Normal	0.45	0.322	0.373	30.3	14.6
23	260	85	348	20	Normal-Right SS	0.488	0.332	0.338	11	4.1
24	86	58	174	3	Right SS	0.564	0.331	0.411	36.3	32.6
25	294	61	347	47	Right-Normal	0.326	0.442	0.444	6.4	29.8

Tab. C.7: Brims Ness

Group1

#	Dip Azim	Dip	Trend	Plunge	Slip Sense	Norm. Stress	Shear Stress	Max. Shear	Misfit Angle	Fault Angle
1	181	76	248	57	Right-Normal	0.608	0.2783	0.2814	4.6232	30.418
2	200	26	220	25	Right-Normal	0.9645	0.175	0.1805	20.813	78.575
3	190	40	274	5	Right SS	0.8962	0.1552	0.2573	52.861	66.188
4	292	85	212	64	Left Normal	0.2586	0.1736	0.2734	50.76	0.6534
5	300	58	211	2	Left SS	0.4908	0.1687	0.3147	57.978	23.378
6	298	62	294	62	Normal	0.4434	0.2664	0.3147	32.332	20
7	276	65	264	65	Normal	0.2973	0.3667	0.3779	15.431	22.879
8	272	68	267	68	Normal	0.2445	0.3485	0.3646	17.236	21.139

Group 2

#	Dip Azim	Dip	Trend	Plunge	Slip Sense	Norm. Stress	Shear Stress	Max. Shear	Misfit Angle	Fault Angle
1	290	12	111	-12	Reverse	0.0196	0.0746	0.1	41.744	2.8616
2	286	23	113	-23	Reverse	0.0787	0.2456	0.2461	2.7675	13.757
3	284	26	125	-25	Left-Reverse	0.1053	0.2806	0.2878	11.961	16.867
4	310	25	135	-25	Reverse	0.1045	0.2397	0.2399	0.5987	11.186
5	92	89	92	89	Normal	0.9829	0.1292	0.1294	2.9489	82.446

Group 3

#	Dip Azim	Dip	Trend	Plunge	Slip Sense	Norm. Stress	Shear Stress	Max. Shear	Misfit Angle	Fault Angle
1	348	45	347	45	Normal	.531	.466	.498	20.8	46.7
2	355	40	346	40	Normal	.643	.455	.479	19.7	53.3
3	348	42	324	40	Left Normal	.58	.497	.492	3.7	49.4
4	335	41	319	40	Left Normal	.552	.486	.485	.7	46.6

5	359	43	343	42	Left Normal	.618	.466	.485	16.8	51.8
6	358	46	341	45	Left Normal	.567	.478	.494	16.	48.7
7	345	64	317	61	Left Normal	.223	.412	.416	7.7	28.1
8	158	45	158	45	Normal	.466	.478	.483	8.8	41.3
9	85	40	125	33	Right-Normal	.886	.268	.265	3.8	65.2
10	90	47	134	38	Right-Normal	.806	.335	.331	4.	57.6
11	98	47	175	14	Normal-Right SS	.761	.327	.381	32.	56.
12	300	82	9	69	Right-Normal	.169	.114	.239	61.7	1.6
13	87	50	155	24	Normal-Right SS	.794	.297	.323	22.7	55.1
14	87	52	156	25	Normal-Right SS	.775	.306	.328	22.7	53.2
15	142	48	178	42	Right-Normal	.467	.497	.499	5.1	43.1
16	153	53	165	52	Normal	.345	.466	.469	4.3	35.3
17	90	67	148	51	Right-Normal	.612	.344	.349	7.1	38.
18	127	47	136	47	Normal	.567	.451	.492	24.3	48.4
19	108	75	184	42	Right-Normal Diag.	.381	.383	.384	2.9	26.7
20	118	70	180	52	Right-Normal	.333	.411	.418	10.	29.1
21	138	52	151	51	Normal	.423	.473	.494	15.7	40.6
22	132	58	145	57	Normal	.369	.439	.476	22.2	36.7
23	112	74	185	46	Right-Normal Diag.	.35	.392	.393	6.2	26.8
24	160	80	177	80	Normal	.028	.144	.148	14.	7.7
25	137	50	215	14	Normal-Right SS	.461	.339	.498	47.2	42.7
26	348	50	311	44	Left Normal	.45	.499	.497	4.2	42.1
27	158	76	188	74	Normal	.052	.21	.212	7.9	12.1
28	140	55	179	48	Right-Normal	.366	.481	.481	2.2	37.2
29	130	80	212	38	Normal-Right SS	.138	.299	.299	2.5	16.3
30	130	84	217	25	Normal-Right SS	.114	.257	.26	7.8	12.5
31	350	65	285	42	Left-Normal Diag.	.236	.404	.421	16.4	28.7
32	342	82	261	49	Left-Normal Diag.	.034	.175	.178	9.9	10.1
33	165	62	218	48	Right-Normal	.2	.301	.373	36.	23.4
34	110	76	199	5	Right SS	.352	.312	.38	35.	25.3
35	110	80	190	43	Right-Normal Diag.	.321	.348	.353	8.3	21.4
36	110	80	195	28	Normal-Right SS	.321	.352	.353	7.2	21.4
37	115	89	203	58	Right-Normal	.224	.225	.287	38.3	11.5
38	110	85	188	67	Right-Normal	.289	.248	.32	39.2	16.5

Tab. C.8: Thurso

Group1

#	Dip Azim	Dip	Trend	Plunge	Slip Sense	Norm. Stress	Shear Stress	Max. Shear	Misfit Angle	Fault Angle
1	252	68	227	66	Left Normal	0.409	0.475	0.476	3.9	36.4
2	228	52	260	47	Right-Normal	0.71	0.447	0.453	5.9	57.4
3	248	46	262	45	Normal	0.765	0.405	0.41	7.3	58.2
4	242	89	330	66	Right-Normal	0.104	0.285	0.304	20	18.5
5	300	84	260	82	Normal	0.572	0.17	0.31	56.3	5.3
6	90	69	5	12	Normal-Left SS	0.151	0.309	0.31	3.2	9.8
7	270	88	180	8	Left SS	0.237	0.287	0.36	37.4	12
8	120	70	32	6	Left SS	0.512	0.378	0.377	2.4	18.9

Group3

1	252	85	338	40	Right-Normal Diag.	0.769	0.164	0.24	47.6	13.7
2	107	67	170	46	Right-Normal	0.441	0.444	0.473	18.7	33.7
3	93	85	182	10	Normal-Right SS	0.535	0.422	0.423	0.6	20.1
4	120	50	167	39	Right-Normal	0.511	0.498	0.499	0.5	45.3

5	295	76	228	57	Left Normal	0.244	-0.034	0.38	95	3.9
6	120	55	174	40	Right-Normal	0.44	0.494	0.494	1.8	40.7
7	315	78	9	70	Right-Normal	0.064	0.218	0.229	17.9	8.3
8	315	78	27	56	Right-Normal	0.064	0.229	0.229	1.8	8.3
9	123	65	167	57	Right-Normal	0.283	0.424	0.446	17.9	30.5
10	117	70	174	56	Right-Normal	0.291	0.402	0.44	23.9	27.8
11	298	77	348	70	Right-Normal	0.205	0.237	0.359	48.5	3.9
12	110	54	154	44	Right-Normal	0.546	0.466	0.49	15.6	44.9
13	291	88	20	35	Normal-Right SS	0.262	0.321	0.391	35.2	8.7
14	140	85	215	71	Right-Normal	0.013	0.104	0.113	23	6.1
15	115	53	189	20	Normal-Right SS	0.511	0.452	0.496	24.1	44.2
16	77	55	155	16	Normal-Right SS	0.857	0.284	0.291	7.6	52.6
17	83	55	164	12	Normal-Right SS	0.808	0.335	0.349	13.4	51.4
18	82	52	163	12	Normal-Right SS	0.834	0.328	0.332	14	54.5
19	105	60	156	47	Right-Normal	0.533	0.446	0.481	21	40.9
20	312	80	22	63	Right-Normal	0.067	0.212	0.23	22.9	5.4
21	94	74	178	19	Normal-Right SS	0.567	0.437	0.44	1.1	30.5
22	120	60	197	21	Normal-Right SS	0.373	0.43	0.479	25.9	36.1
23	325	60	91	-45	Right-Reverse	0.249	-0.367	0.428	149	28.4
24	325	60	89	-44	Right-Reverse	0.249	-0.359	0.428	147	28.4
25	178	80	269	-6	Right SS	0.267	-0.385	0.388	172.1	1.3
26	315	54	305	54	Normal	0.35	0.445	0.461	16.3	30.7
27	135	85	199	79	Normal	0.033	0.112	0.171	49.1	7.8
28	315	75	323	75	Normal	0.086	0.239	0.265	25.7	11.1
29	112	70	180	46	Right-Normal	0.351	0.44	0.457	16.1	29.4
30	115	55	162	44	Right-Normal	0.485	0.486	0.495	9.8	42.4
31	122	58	180	41	Right-Normal	0.382	0.486	0.483	3.8	37.3
32	122	75	161	71	Right-Normal	0.193	0.286	0.382	41.5	21.5
33	317	85	35	67	Right-Normal	0.022	0.116	0.135	30.9	2.3
34	112	62	120	62	Normal	0.431	0.342	0.483	45.2	36.9
35	121	45	182	26	Normal-Right SS	0.577	0.464	0.494	20.4	49.4
36	87	60	174	5	Right SS	0.739	0.364	0.394	21.8	45.7
37	88	57	171	10	Normal-Right SS	0.748	0.374	0.396	17.1	48.4
38	95	60	179	10	Normal-Right SS	0.65	0.419	0.446	19.3	43.7
39	86	88	176	6	Right SS	0.626	0.384	0.382	2.4	18.6
40	112	48	173	29	Right-Normal Diag.	0.602	0.486	0.486	8.9	49.7
41	312	85	55	-69	Right-Reverse	0.047	-0.009	0.193	92.6	0.7
42	325	54	81	-31	Reverse-Right SS	0.343	-0.327	0.469	134.2	33.9
43	312	85	41	10	Normal-Right SS	0.047	0.188	0.193	12.5	0.7

Tab. C.9: Mukle Bay

Group3

#	Dip Azim	Dip	Trend	Plunge	Slip Sense	Norm. Stress	Shear Stress	Max. Shear	Misfit Angle	Fault Angle
1	155	77	242	14	Normal-Right SS	.077	-.181	.189	163.3	1.7
2	322	76	243	37	Normal-Left SS	.18	.322	.384	33.	25.
3	285	84	9	43	Right-Normal Diag.	.154	.255	.255	2.8	6.3
4	295	80	326	78	Normal	.13	.265	.279	17.9	13.3
5	350	84	268	53	Left Normal	.294	.373	.377	8.3	22.9
6	2	80	323	77	Normal	.444	.314	.381	34.5	28.1
7	350	72	263	10	Left SS	.428	.316	.445	44.8	34.8
8	320	72	265	60	Left Normal	.226	.414	.418	8.1	28.3
9	20	85	290	4	Left SS	.539	.186	.269	46.1	23.4

10	318	80	238	44	Left-Normal Diag.	.118	.281	.323	29.5	20.1

Tab. C.10: Castletown

Permo-Triassic

#	Dip Azim	Dip	Trend	Plunge	Slip Sense	Norm. Stress	Shear Stress	Max. Shear	Misfit Angle	Fault Angle
1	160	88	72	47	Left-Normal Diag.	0.12	0.238	0.271	28.8	6.7
2	348	88	258	3	Left SS	0.193	0.31	0.313	7.9	3.3
3	348	88	258	10	Left SS	0.193	0.303	0.313	14.9	3.3
4	270	75	352	26	Normal-Right SS	0.403	0.38	0.381	3.9	17.4
5	315	62	14	44	Right-Normal	0.184	0.322	0.387	33.8	25.4
6	170	72	95	38	Normal-Left SS	0.324	0.41	0.411	1.7	23.4
7	160	89	70	6	Left SS	0.118	0.263	0.267	9.1	5.7
8	280	70	352	40	Right-Normal Diag.	0.321	0.396	0.401	8.5	21.3
9	80	82	165	32	Normal-Right SS	0.494	0.301	0.319	19.4	4.5
10	270	80	354	31	Normal-Right SS	0.382	0.351	0.366	16.3	12.4
11	168	88	78	10	Left SS	0.2	0.322	0.323	4.8	7.3

Tab. C.11: Dunnet Head

Permo-Triassic

#	Dip Azim	Dip	Trend	Plunge	Slip Sense	Norm. Stress	Shear Stress	Max. Shear	Misfit Angle	Fault Angle
1	150	74	67	22	Normal-Left SS	0.051	0.026	0.219	83.1	12.8
2	150	45	177	42	Right-Normal	0.441	0.485	0.496	12.6	41.6
3	315	88	41	62	Right-Normal	0.081	0.165	0.216	40.3	3.6
4	150	50	180	46	Right-Normal	0.356	0.468	0.479	12.2	36.6
5	170	66	182	66	Normal	0.153	0.291	0.336	30.1	19
6	148	44	175	41	Right-Normal	0.461	0.49	0.498	10.7	42.8
7	147	51	185	44	Right-Normal	0.346	0.459	0.475	14.8	35.9
8	185	46	124	27	Normal-Left SS	0.494	0.415	0.457	24.8	38.1
9	168	63	92	26	Normal-Left SS	0.179	0.272	0.366	42	22.2
10	150	75	216	57	Right-Normal	0.044	0.198	0.203	12.8	11.8
11	140	42	164	40	Right-Normal	0.516	0.497	0.497	1.5	45.5
12	100	80	183	34	Normal-Right SS	0.443	0.304	0.322	19.1	12.3
13	98	76	11	12	Normal-Left SS	0.479	-0.27	0.326	146	16.5
14	130	44	184	29	Right-Normal Diag.	0.526	0.459	0.487	19.5	44.6
15	120	58	187	32	Normal-Right SS	0.401	0.435	0.443	10.6	31.9
16	90	84	179	7	Right SS	0.532	0.258	0.258	4.6	9.3
17	292	85	21	10	Normal-Right SS	0.307	0.321	0.322	5	3.9
18	125	45	144	43	Right-Normal	0.539	0.461	0.479	15.7	44.2

Tab. C.12: Ham Bay

Permo-Triassic

#	Dip Azim	Dip	Trend	Plunge	Slip Sense	Norm. Stress	Shear Stress	Max. Shear	Misfit Angle	Fault Angle
1	163	73	125	69	Left Normal	0.159	0.183	0.245	41.7	10.2
2	177	79	90	15	Normal-Left SS	0.24	0.22	0.22	1.9	4.9
3	350	86	264	45	Left-Normal Diag.	0.216	0.251	0.253	6.9	10.5
4	155	72	68	9	Left SS	0.115	0.194	0.237	35.1	10.9
5	177	78	95	34	Normal-Left SS	0.242	0.214	0.224	18.2	5.9
6	245	80	332	15	Normal-Right SS	0.372	0.174	0.203	29.9	11.2
7	296	88	22	65	Right-Normal	0.041	0.167	0.167	4.4	8.3

Tab. C.13: Skarfskerry

#	Dip Azim	Dip	Trend	Plunge	Slip Sense	Norm. Stress	Shear Stress	Max. Shear	Misfit Angle	Fault Angle
1	130	66	194	44	Right-Normal	.178	.377	.38	5.4	24.3
2	122	47	180	30	Right-Normal Diag.	.483	.482	.488	10.8	41.
3	83	83	172	4	Right SS	.679	.393	.407	10.8	41.5
4	128	60	195	35	Right-Normal Diag.	.263	.423	.435	15.	29.5
5	98	58	151	44	Right-Normal	.613	.435	.486	26.6	51.2
6	115	55	180	31	Normal-Right SS	.442	.493	.495	4.2	41.3
7	115	74	195	31	Normal-Right SS	.255	.43	.431	4.	29.
8	120	68	198	28	Normal-Right SS	.246	.427	.431	9.3	29.7
9	124	74	207	23	Normal-Right SS	.154	.35	.36	13.	22.9
10	128	80	213	26	Normal-Right SS	.081	.269	.27	4.7	15.8
11	119	72	202	21	Normal-Right SS	.222	.405	.414	12.1	27.7
12	193	68	262	41	Right-Normal Diag.	.505	-.236	.389	127.	13.4
13	210	82	296	28	Normal-Right SS	.726	-.31	.321	167.9	32.3
14	110	73	189	31	Normal-Right SS	.329	.458	.463	6.5	33.1
15	85	48	171	4	Right SS	.823	.363	.382	15.9	65.1
16	89	68	178	2	Right SS	.665	.429	.455	18.6	50.4
17	88	64	168	20	Normal-Right SS	.701	.448	.446	.6	53.9
18	75	63	159	11	Normal-Right SS	.856	.322	.329	6.8	62.4
19	88	80	177	6	Right SS	.62	.437	.443	9.5	41.5
20	70	76	159	6	Right SS	.854	.277	.281	15.9	53.5
21	112	65	197	11	Normal-Right SS	.369	.446	.482	22.4	37.2
22	100	68	183	18	Normal-Right SS	.508	.493	.492	5.6	43.3
23	115	75	204	3	Right SS	.248	.388	.426	24.1	28.3

Tab. C.14: St. John's Point

Permo-Triassic

#	Dip Azim	Dip	Trend	Plunge	Slip Sense	Norm. Stress	Shear Stress	Max. Shear	Misfit Angle	Fault Angle
1	342	84	253	9	Left SS	0.166	0.29	0.294	8.7	19.4
2	324	72	243	26	Normal-Left SS	0.064	0.103	0.11	21	6.6
3	334	78	245	3	Left SS	0.112	0.215	0.219	10.7	13.8
4	330	87	241	18	Normal-Left SS	0.076	0.116	0.116	2.8	7.1
5	348	86	259	8	Left SS	0.222	0.343	0.352	11.8	24.3
6	137	74	227	1	Right SS	0.1	0.175	0.181	15.4	11.4
7	134	90	224	17	Normal-Right SS	0.084	0.143	0.144	8.4	8.9

Tab. C.15: Duncansby

Group 1

#	Dip Azim	Dip	Trend	Plunge	Slip Sense	Norm. Stress	Shear Stress	Max. Shear	Misfit Angle	Fault Angle
1	190	48	103	3	Left SS	.59	.104	.159	48.9	19.2
2	115	80	137	79	Normal	.06	.191	.201	18.8	9.1
3	120	78	143	77	Normal	.066	.189	.19	2.5	5.5
4	12	84	285	24	Normal-Left SS	.871	.281	.282	2.7	63.3
5	152	56	63	2	Left SS	.361	.244	.279	29.	8.3
6	162	64	72	1	Left SS	.424	.325	.326	4.3	20.
7	158	62	68	1	Left SS	.388	.305	.312	12.2	16.1

APPENDIX D

Transect Plots - Extracontents

Each dataset is here plotted on lin/lin, lin/log, log/lin and log/log axes to enable a visual comparison between distribution types and to investigate which distribution type best fits the data.

R^2 and relative number of values used in determining slopes are reported in Tab. D.1.

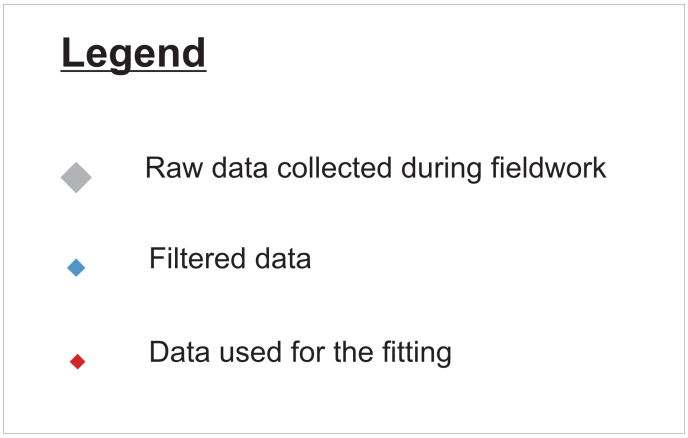

Figure D.1: Colour legend used in the Lin-Lin, Lin-Log, Log-Lin, Log-Log cumulative distribution plots

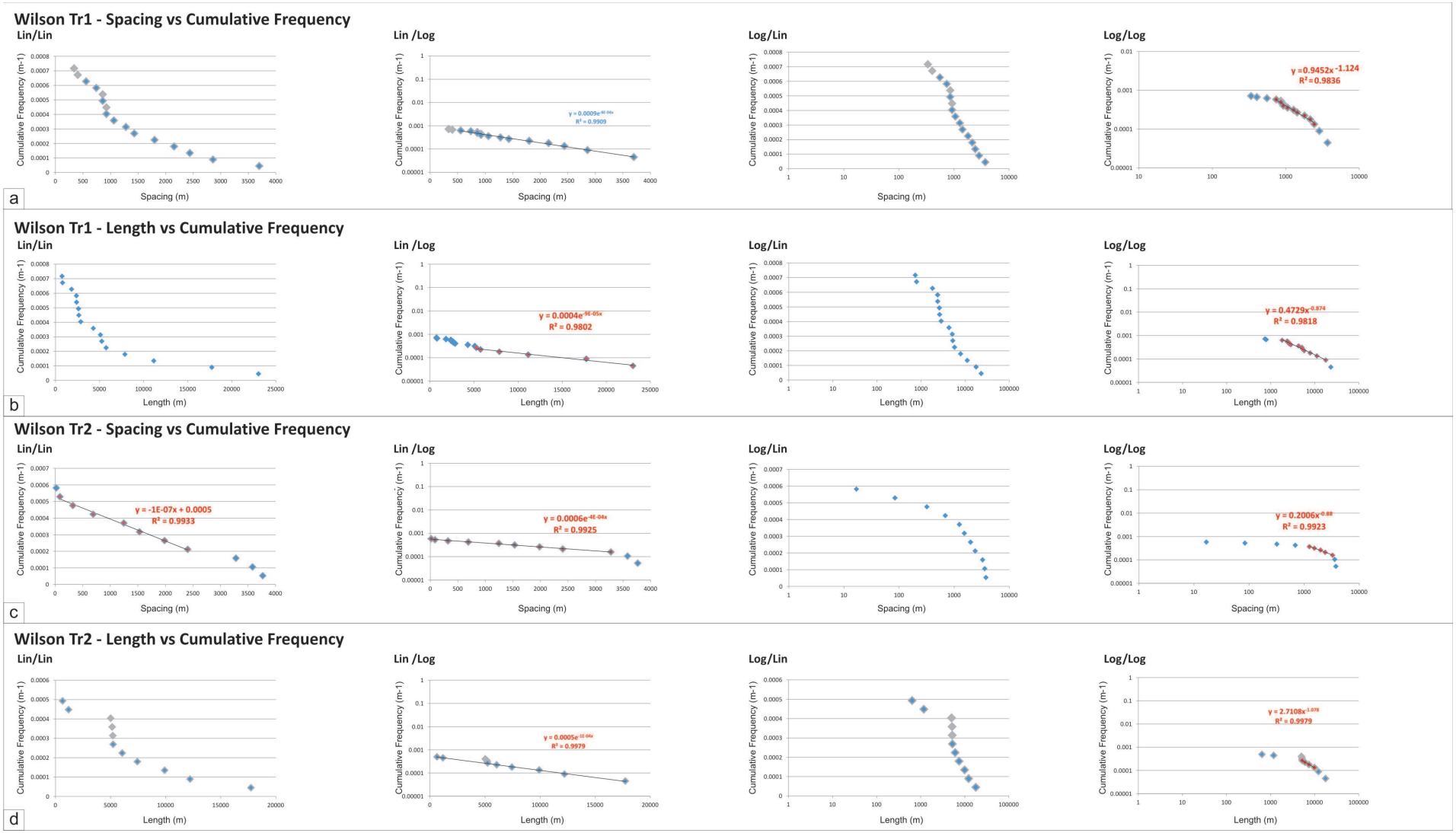

Figure D.2: Lin-Lin, Lin-Log, Log-Lin, Log-Log cumulative distribution plots for the transects Wison Tr1 (a) spacing and (b) length and Wilson Tr2 (c) spacing and (d) length

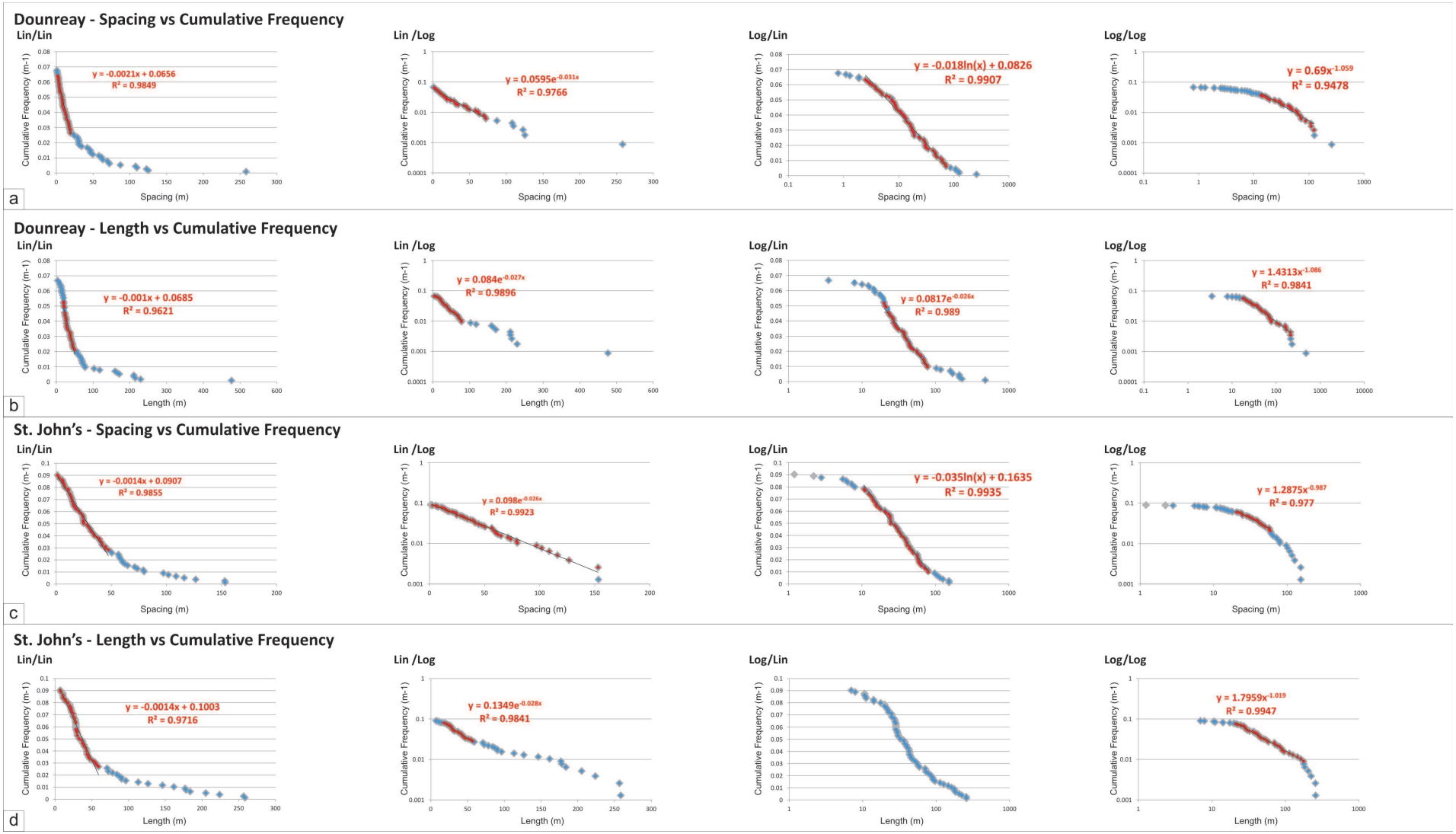

Figure D.3: Lin-Lin, Lin-Log, Log-Lin, Log-Log cumulative distribution plots for the transects Dounreay (a) spacing and (b) length and St. John's (c) spacing and (d) length

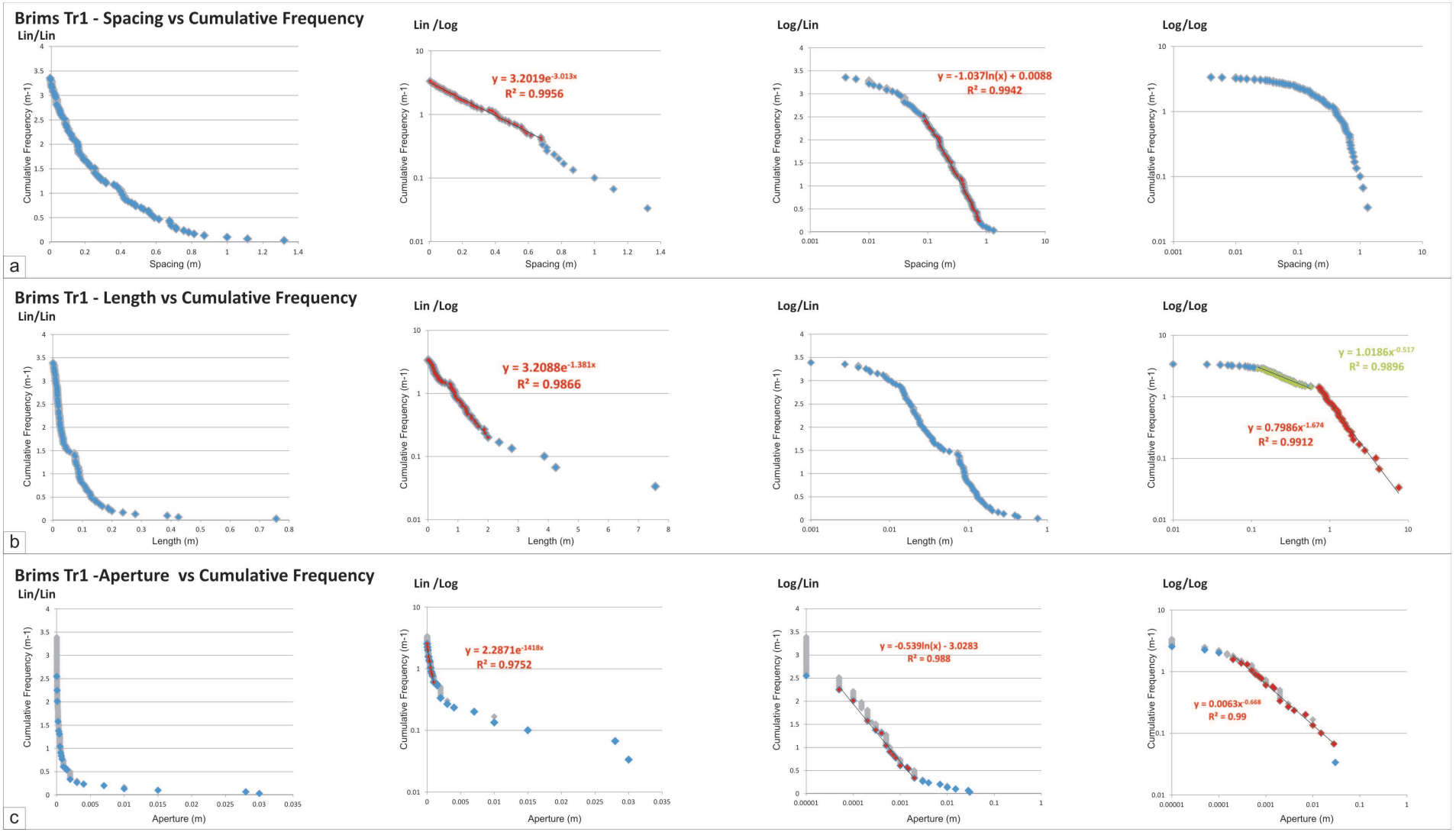

Figure D.4: Lin-Lin, Lin-Log, Log-Lin, Log-Log cumulative distribution plots for the transect Brims Tr1 (a) spacing and (b) length and (c) aperture

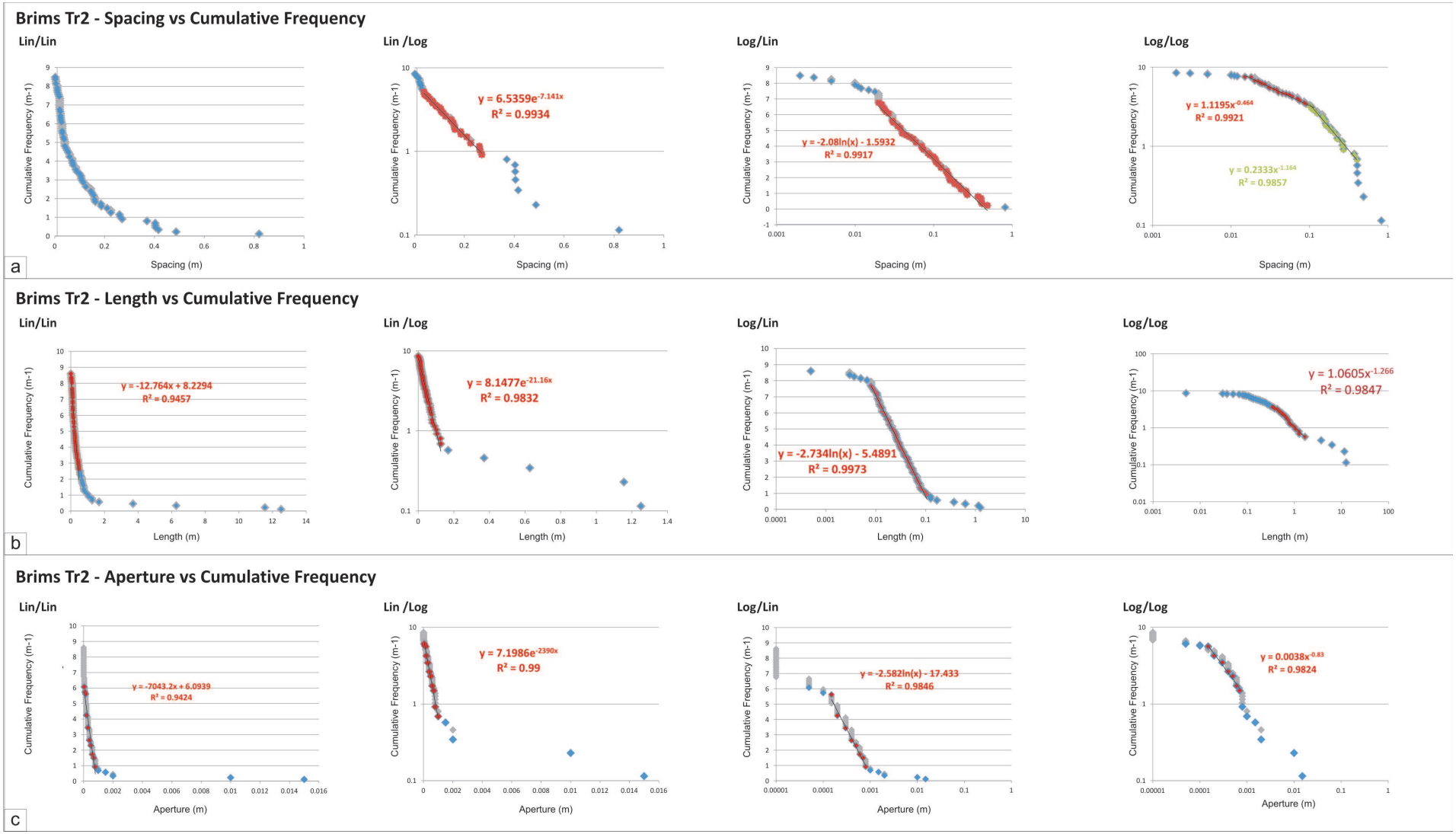

Figure D.5: Lin-Lin, Lin-Log, Log-Lin, Log-Log cumulative distribution plots for the transect Brims Tr2 (a) spacing and (b) length and (c) aperture

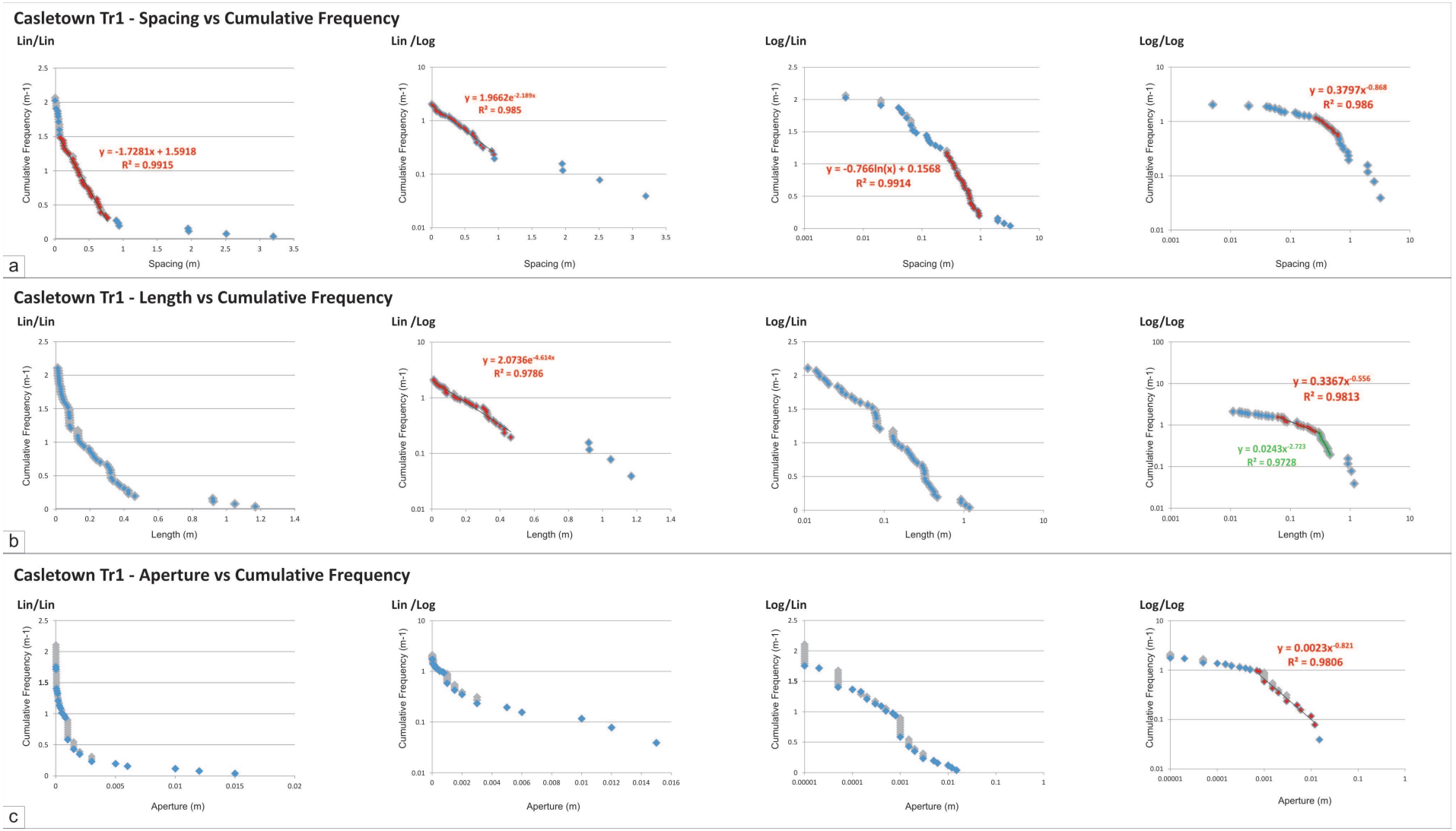

Figure D.6: Lin-Lin, Lin-Log, Log-Lin, Log-Log cumulative distribution plots for the transect Castletown Tr1 (a) spacing and (b) length and (c) aperture

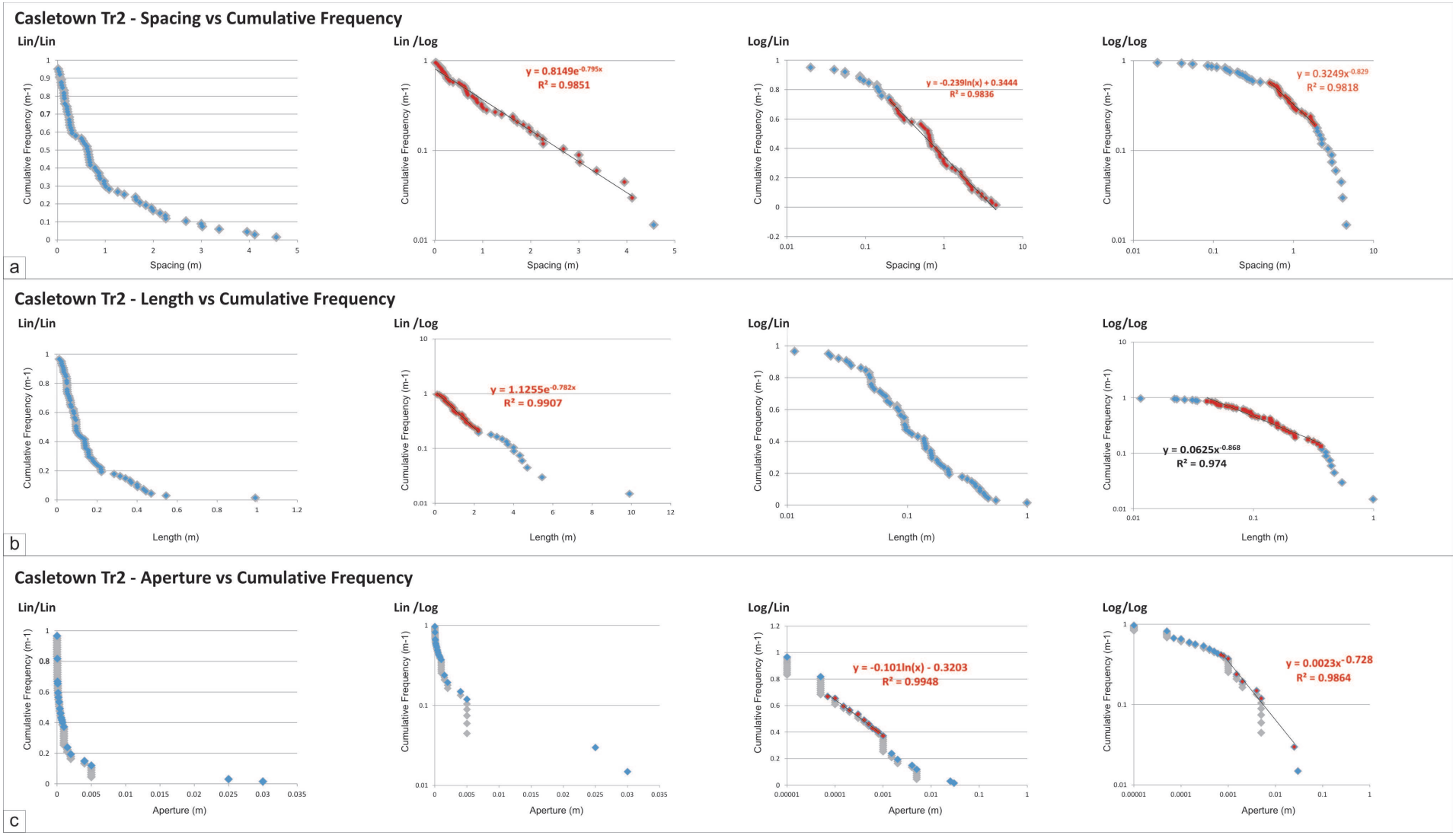

Figure D.7: Lin-Lin, Lin-Log, Log-Lin, Log-Log cumulative distribution plots for the transect Castletown Tr2 (a) spacing and (b) length and (c) aperture

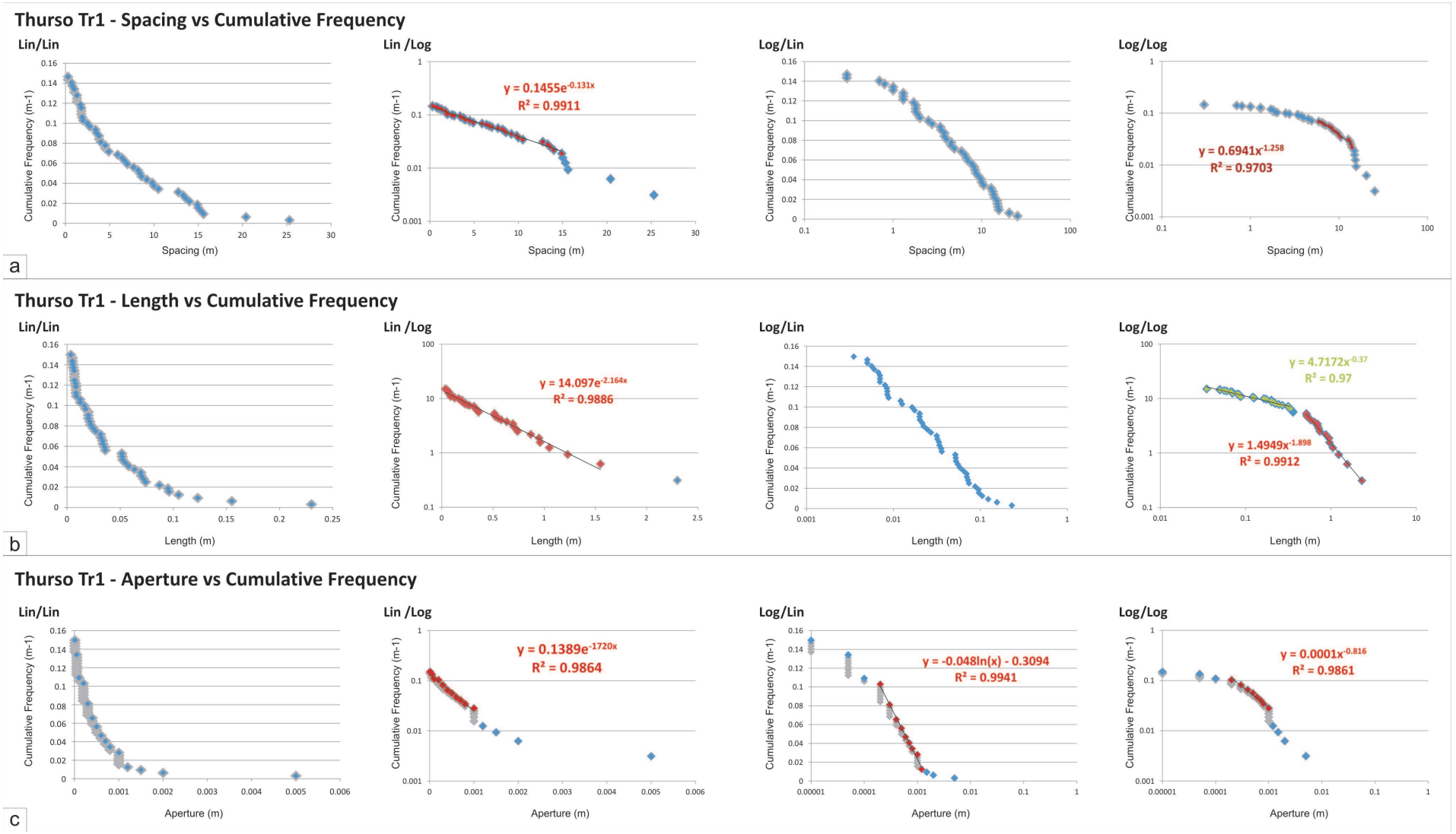

Figure D.8: Lin-Lin, Lin-Log, Log-Lin, Log-Log cumulative distribution plots for the transect Thurso Tr1 (a) spacing and (b) length and (c) aperture

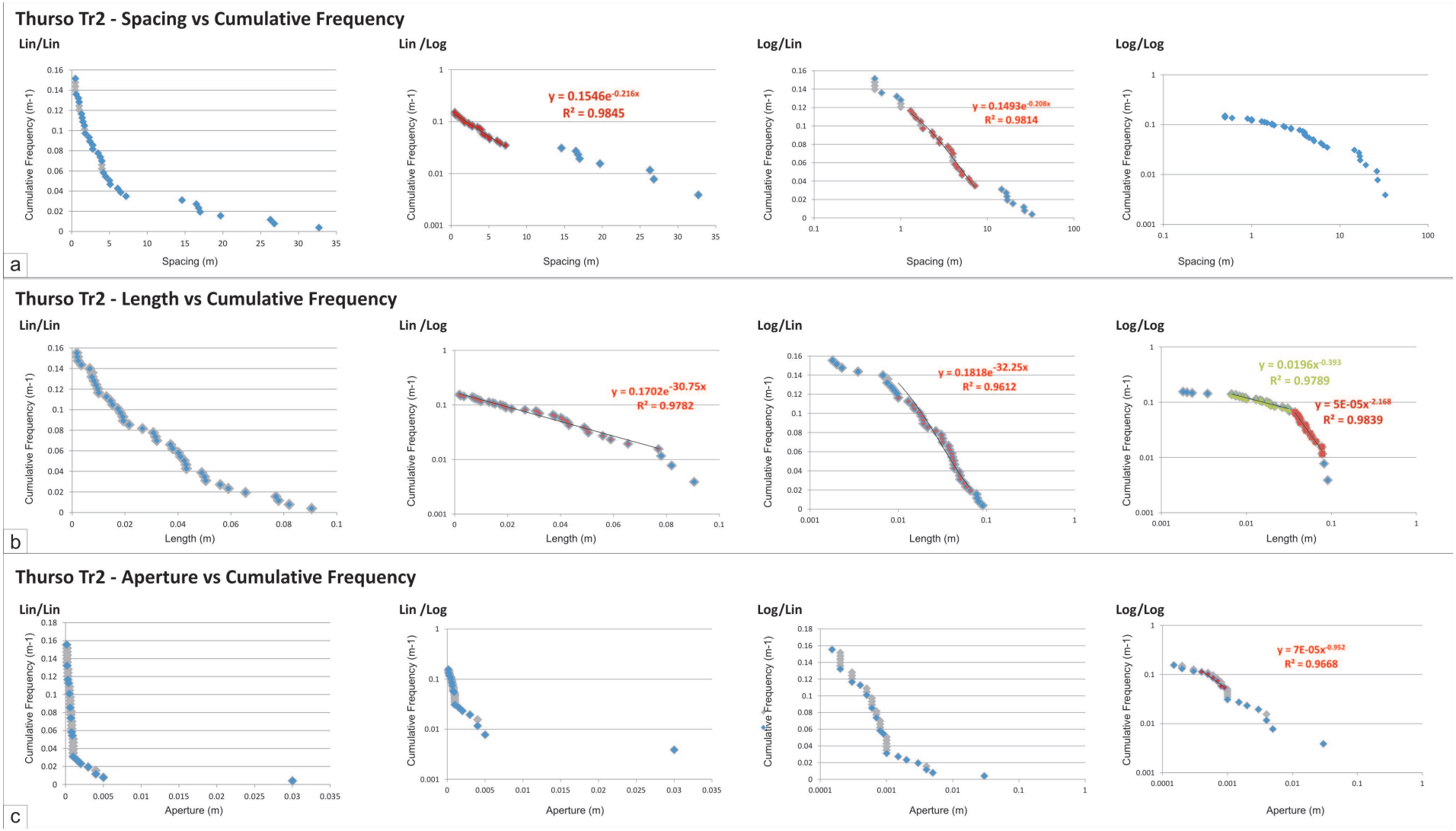

Figure D.9: Lin-Lin, Lin-Log, Log-Lin, Log-Log cumulative distribution plots for the transect Thurso Tr2 (a) spacing and (b) length and (c) aperture

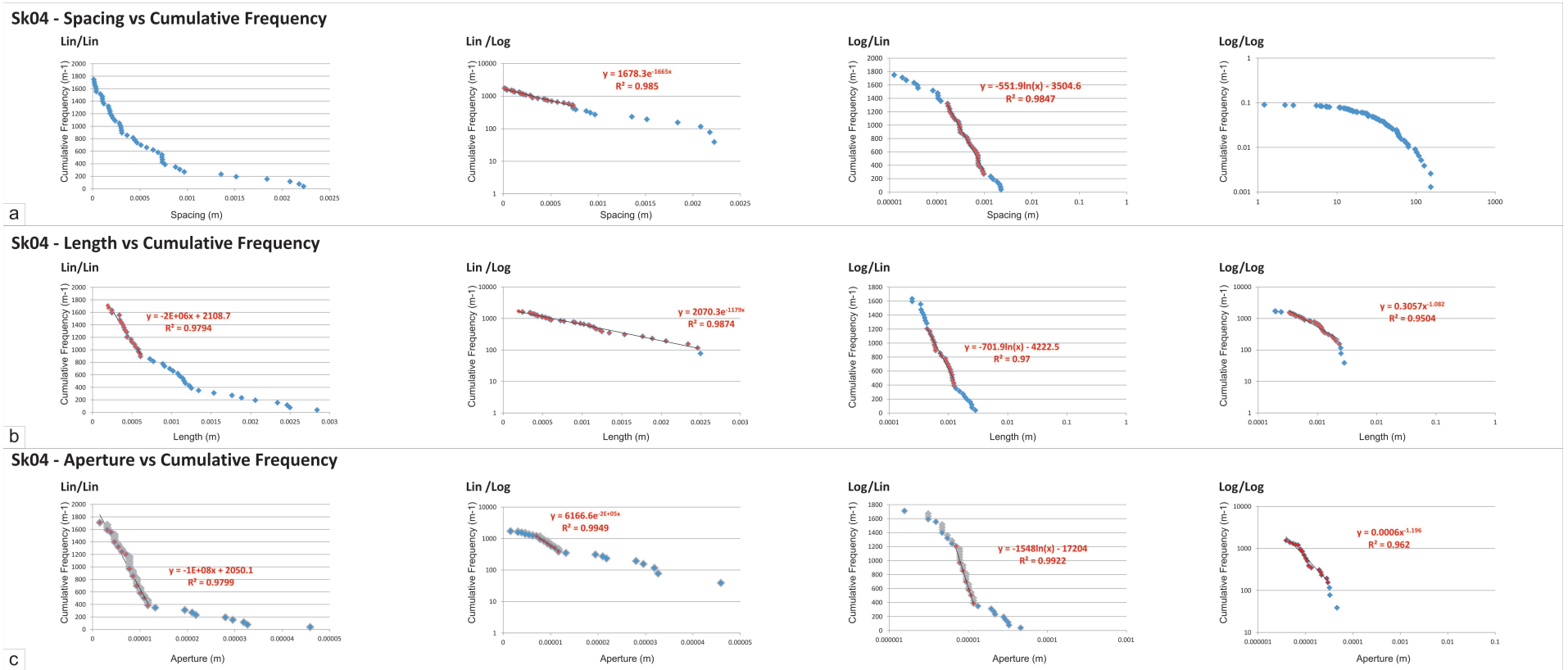

Figure D.10: Lin-Lin, Lin-Log, Log-Lin, Log-Log cumulative distribution plots for the transect Sk04 (a) spacing and (b) length and (c) aperture

Dataset Name	Attribute	Datasets Full - Simpl.	Lin/Lin R^2 - Num	Lin/Log R^2 - Num	Log/Lin R^2 - Num	Log/Log R^2 - Num
Wilson Tr1	Spacing	16 - 14	-	0.9909 -12/14	-	0.9836 - 9/14
	Length	16 - 16	-	0.9802 - 6/16	-	0.9818 - 13/16
Wilson Tr2	Spacing	11 - 11	0.9933 - 7/11	0.9925 - 9/11	0.9923 - 5/11	
	Length	11 - 8	-	0.9979 8/8	-	0.9979 4/8
Dounreay	Spacing	77 - 73	0.9849 - 41/73	0.9766 - 64/73	0.9907 - 63/73	0.9478 - 39/73
	Length	76 - 62	0.9621 - 30/62	0.9896 - 52/62	0.989 - 41/62	0.9841 - 51/62
St. John's	Spacing	70 - 68	0.9855 - 47/68	0.9923 - 65/68	0.9935 - 52/68	0.977 - 31/68
	Length	70 - 57	0.9716 - 38/57	0.9841 - 30/57	-	0.9947 - 42/57
Brims Tr1	Spacing	100 - 81	-	0.9956 - 71/81	0.9942 - 56/81	-
	Aperture	101 - 21	-	0.9752 - 11/21	0.988 - 13/21	0.99 - 17/21
	Length	101 - 87	-	0.9866 - 82/87	-	0.9896 - 38/87 & 0.9912 - 37/87
Brims Tr2	Spacing	74 - 54	-	0.9934 - 29/54	0.9917 - 44/54	0.9921 - 20/54 & 0.9857 - 27/54
	Aperture	75- 15	0.9424 - 10/16	0.99 - 11/16	0.9846 - 8/16	0.9824 - 8/16
	Length	75 - 64	0.9457 - 44/64	0.9832 - 59/64	0.9973 - 52/64	0.9824 - 26/64
Castletown Tr1	Spacing	53 - 43	0.9915 - 28/43	0.985 - 38/43	0.9834 - 24/43	0.986 - 16/43
	Aperture	54 - 20	-	-	-	0.9806 - 10/20
	Length	54 - 48	-	0.9786 - 44/48	0.9818 - 36/48	0.9813 - 21/48 & 0.9728 - 12/48
Castletown Tr2	Spacing	64 - 59	-	0.9851 - 58/59	0.9836 - 48/59	0.9818 - 26/59
	Aperture	65 - 19	-	-	0.9948 - 11/19	0.9864 - 7/19
	Length	65 - 57	-	0.9907 - 44/57	-	0.974 - 42/57
Thurso Tr1	Spacing	47 - 39	-	0.9915 - 34/39	-	0.986 - 16/39
	Aperture	48 - 15	-	0.9864 - 11/15	0.9941 9/15	0.9861 - 8/15
	Length	48 - 43	-	0.9886 - 42/43	-	0.97 - 23/43 & 0.9912 - 17/43
Thurso Tr2	Spacing	39 - 31	-	0.9845 - 23/31	0.9814 - 19/31	-
	Aperture	40 - 16	0.9779 - 10/16	-	-	0.9668 - 6/16
	Length	40 - 39	-	0.9782 - 36/39	0.9763 - 35/39	0.9789 - 17/39 & 0.9839 - 15/39
Sk04	Spacing	45 - 43	-	0.9851 - 34/45	0.9847 - 28/45	-
	Aperture	44 - 22	0.9799 - 13/22	0.9949 - 7/22	0.9922 - 7/22	0.962 - 17/22
	Length	44 - 42	0.9794 - 20/42	0.9874 - 40/42	0.97 - 22/42	0.9504 - 35/42

Table D.1: Summary of data for cumulative distribution plots of spacing, length and aperture. For each transect, the number of data of the entire and simplified populations are shown. Regression values (R^2) and range in which this value is obtained calculate for each for the Lin/Lin, Lin/Log, Log/Lin and Log/Log is also shown.

APPENDIX E

MATLAB Script - Topological Analysis of nodes

The input for the MATLAB script reported below is a .gif file (or any other format) in white backgound and with the I- Y- X- nodes represented as single pixels of different gray colours. The script recognizes the pixel as nodes and it produces density maps and circular scanlines of defined radius and position.

The .gif file map was created with the following procedure:

- Create the topology by drawing the fractures (lines) in a graphical software such as Corel Draw from any source of 2D data (aerial photo, bathymetry, outcrop photograph, etc.). An example is reported in Fig. E.1a
- Export the fractures (lines) in .DWG (AutoCAD) and import them in ArcGis.
- Convert the .DWG in a shapefile and following the procedure shown in Nixon (2013), extract fracture vertex (node) at the intersection of lines and split the lines at each vertex point.
- Associate an attribute table to the node shapefile and assign the node type (I- Y- or X-) in the attribute table. This procedure is done manually.
- Assign a colour legend to the node type. For matter of simplicity change the symbols in full colour squares and assign different colours to the different node types: light gray (I), dark gray (Y) and a black (X).
- Copy the node in CorelDraw and modify the symbols in 1px size Fig. E.1b.
- Export the figue in .gif (grayscale).

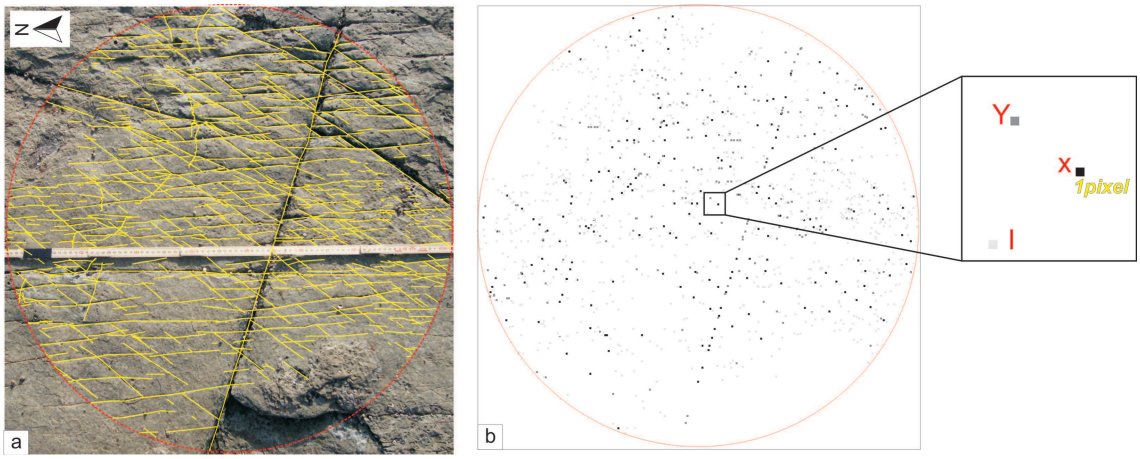

Figure E.1: (a) Example of field pavement photograph and (b) image type to import in MATLAB. Note that node points are represented as 1 pixel square of different colours (inset in Fig.b).

MATLAB SCRIPT

```
function [circ node] = connectivity_dichiarante
% connectivity_dichiarante
%
% Copyright (c) Tore Ingvald Bjoernaraa, 2016. All rights reserved.
%

show_connection_in_circle_plot = true;
plot_check = false; % Plot data points in density plots

pa = ''; % Path to GIF-files
fn = {...
    'brims_caithness.gif',1;...  % 1. Example 1
    'bathymetry_caithness.gif',1;... % 2. Example 2
    };
% format fn:
%   {filename, scaling coeff. (ratio of actual length vs. size of sample)}
ind = [1]; % Index in fn

figDensity = ['density_plot_ind_' num2str(ind)];
figCircles = ['circles_plot_ind_' num2str(ind)];

% Density plot parameter. The higher value the 'smoother' the density plot.
optW = 0.0257; % Originally logspace(-2.2,-.5,50);

% NB! Depending on ind, update:
% 1. Position and size of circles (function 'plot_circles' below)

% Script starts here:
    ****************************************************

%% Circular plot
switch ind
    case 1
        I0 = importdata(fullfile(pa,fn{ind,1}));
        I{ind} = double(flipud(I0.cdata));
        I{ind}(I{ind}==0) = 1;
        I{ind}(I{ind}==255) = 0;
        colmap{ind} = I0.colormap;
end

fh = figure('name',figCircles);
ax = [subplot(1,2,1,'parent',fh) subplot(1,2,2,'parent',fh)];
hold(ax(2),'on')
imagesc(I{ind},'parent',ax(1))
title(ax(1),['Image: ' strrep(fn{ind,1},'_','\_')])
axis(ax(1),'equal'), axis(ax(1),'tight')

% Getting the indices of each color in the image:
node = [];
```

```
un = unique(I{ind});
un(un==0) = []; % Removing background color
if length(un)>3
    disp('More than three colors in figure. Check image')
    return
end
interval = 1;
for m = 1:length(un)
    [node.row{m} node.col{m}] = ...
        find(I{ind}(1:interval:end,1:interval:end)==un(m));
end
% Plot point locations and circles:
col = {'r','g','b'}; % Node colors: {X,Y,I}
for m = 1:length(un)
    plot(node.col{m},node.row{m},['.' col{rnd(m,3)}],'parent',ax
        (2))
    axis(ax(2),'equal')
end
axis(ax(2),'equal','tight')
[circ.x circ.y circ.r] = plot_circles(ax(2),ind);
circ.no = [];
for q = 1:length(circ.x)
    circ.no{q} = [];
    m = 1;
    circ.no{q}.X = 0;
    ind0 = [];
    for n = 1:length(node.col{m})
        if ((node.col{m}(n)-circ.x(q))^2+(node.row{m}(n)-circ.y(
            q))^2-...
                circ.r^2)<0
            circ.no{q}.X = circ.no{q}.X+1;
            ind0(end+1) = n;
        end
    end
    if show_connection_in_circle_plot
        plot(node.col{m}(ind0),node.row{m}(ind0),'ro','parent',
            ax(2))
        refresh(figure(get(ax(2),'parent')))
    end
    m = 2;
    circ.no{q}.Y = 0;
    ind0 = [];
    for n = 1:length(node.col{m})
        if ((node.col{m}(n)-circ.x(q))^2+(node.row{m}(n)-circ.y(
            q))^2-...
                circ.r^2)<0
            circ.no{q}.Y = circ.no{q}.Y+1;
            ind0(end+1) = n;
        end
    end
    if show_connection_in_circle_plot
        plot(node.col{m}(ind0),node.row{m}(ind0),'go','parent',
            ax(2))
```

```
97          refresh(figure(get(ax(2),'parent')))
98      end
99      m = 3;
100     circ.no{q}.I = 0;
101     ind0 = [];
102     for n = 1:length(node.col{m})
103         if ((node.col{m}(n)-circ.x(q))^2+(node.row{m}(n)-circ.y(
                q))^2-...
104                 circ.r^2)<0
105             circ.no{q}.I = circ.no{q}.I+1;
106             ind0(end+1) = n;
107         end
108     end
109     if show_connection_in_circle_plot
110         plot(node.col{m}(ind0),node.row{m}(ind0),'bo','parent',
                ax(2))
111         refresh(figure(get(ax(2),'parent')))
112     end
113 end
114 grid(ax(2),'on'), box(ax(1),'on'), box(ax(2),'on')
115 fit_axes2(ax,[2 1 0.95 0.95])
```

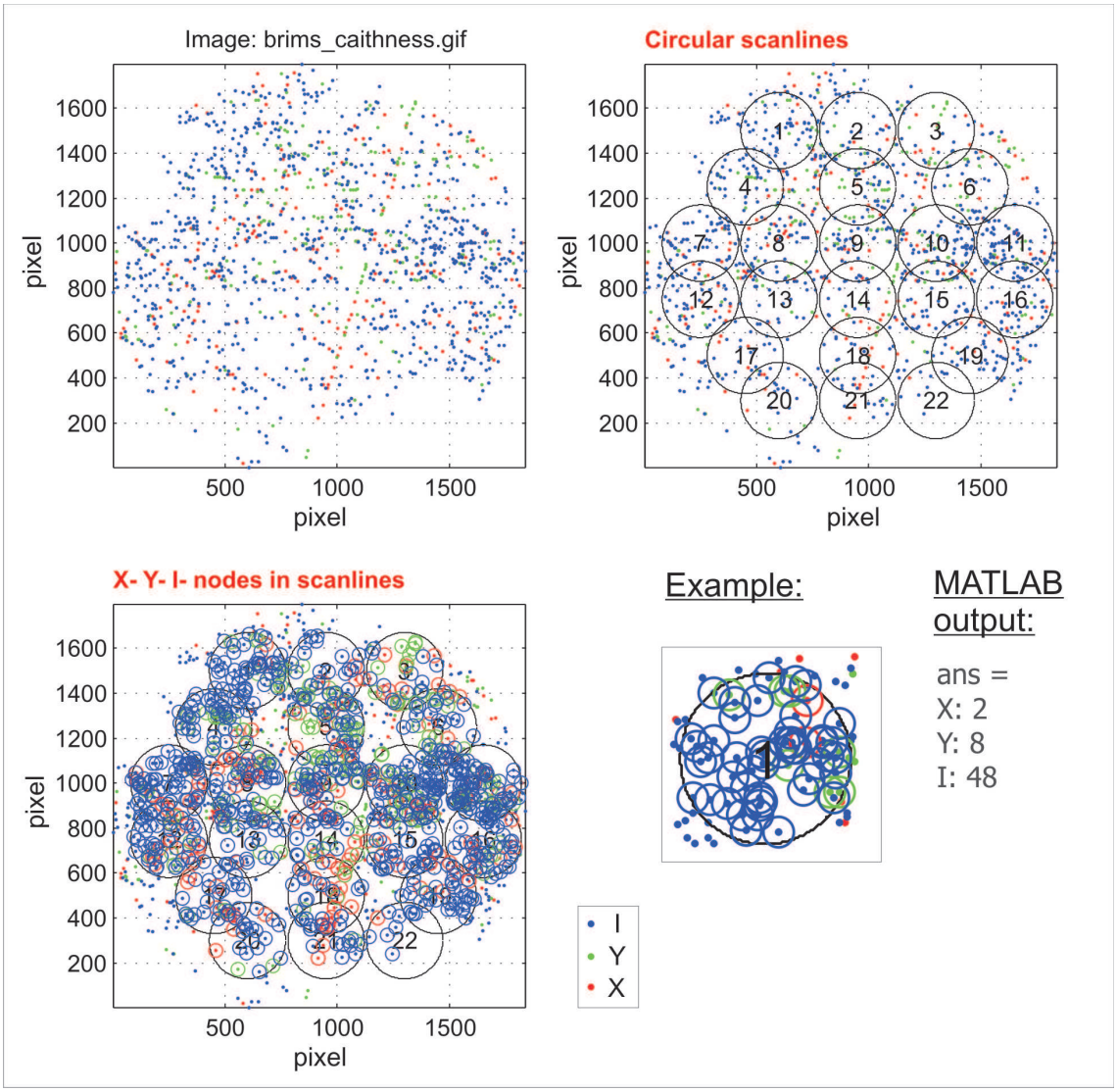

Figure E.2: Example of MATLAB image output when performing Circular Scanlines

```
%% Density plot:
node = get_node_data(node);

fh2 = figure('name',figDensity);
ax2 = [subplot(2,3,1,'parent',fh2) ...
      subplot(2,3,2,'parent',fh2) ...
      subplot(2,3,3,'parent',fh2) ...
      subplot(2,3,4,'parent',fh2) ...
      subplot(2,3,5,'parent',fh2)];
for k = 1:length(ax2)
      hold(ax2(k),'on')
      box(ax2(k),'on')
end

m = 1; % All
datarow = node.rowT;
datacol = node.colT;
try
      [optW C W X Y Z0] = density_plot([datacol datarow],ax2(m),
          optW);
```

```
20      if plot_check % show_connection_in_circle_plot
21          plot_circles(ax2(m),testId,ind,max(max(Z0)));
22      end
23  end
24  title(ax2(m),'I+Y+X')
25  refresh(figure(fh2))
26
27  m = m+1; % I
28  datarow = node.rowI;
29  datacol = node.colI;
30  try
31      [optW C W X Y Z] = density_plot([datacol datarow],ax2(m),
            optW);
32      if plot_check
33          plot3(datacol,datarow,repmat(max(max(Z0)),length(datarow
                ),1),...
34              'k.','parent',ax2(m))
35      end
36  end
37  title(ax2(m),'I')
38  refresh(figure(fh2))
39
40  m = m+1; % X
41  datarow = node.rowX;
42  datacol = node.colX;
43  try
44      [optW C W X Y Z] = density_plot([datacol datarow],ax2(m),
            optW);
45      if plot_check
46          plot3(datacol,datarow,repmat(max(max(Z0)),length(datarow
                ),1),...
47              'k.','parent',ax2(m))
48      end
49  end
50  title(ax2(m),'X')
51  refresh(figure(fh2))
52
53  m = m+1; % Y
54  datarow = node.rowY;
55  datacol = node.colY;
56  try
57      [optW C W X Y Z] = density_plot([datacol datarow],ax2(m),
            optW);
58      if plot_check
59          plot3(datacol,datarow,repmat(max(max(Z0)),length(datarow
                ),1),...
60              'k.','parent',ax2(m))
61      end
62  end
63  title(ax2(m),'Y')
64  refresh(figure(fh2))
65
66  m = m+1; % X+Y
```

```
datarow = node.rowXY;
datacol = node.colXY;
try
    [optW C W X Y Z] = density_plot2([datacol datarow],ax2(m),
        optW);
    if plot_check
        plot3(datacol,datarow,repmat(max(max(Z0)),length(datarow
            ),1),...
            'k.','parent',ax2(m))
    end
end
title(ax2(m),'X+Y')
refresh(figure(fh2))

% Formatting the axis:
M = 1;
colmap = colormap(fh2,'jet');
axis(ax2(M),'equal')
axis(ax2(M),'tight')
set(ax2(M),'xtick',[],'ytick',[])
zdata = get(findobj(ax2(M),'type','surface'),'zdata');
zratio = 100/max(max(zdata));
set(findobj(ax2(M),'type','surface'),'zdata',zdata*zratio)
limc = get(ax2(M),'clim');
limx = get(ax2(M),'xlim');
limy = get(ax2(M),'ylim');
colorbar('peer',ax2(M));
box(ax2(M),'on')
% Adjusting color scale relative to maximum density:
for M = 2:m
    zdata = get(findobj(ax2(M),'type','surface'),'zdata');
    set(findobj(ax2(M),'type','surface'),'zdata',zdata*zratio)
    axis(ax2(M),'equal')
    axis(ax2(M),'tight')
    limx2 = get(ax2(M),'xlim');
    limy2 = get(ax2(M),'ylim');
    limz2 = get(ax2(M),'zlim');
    if plot_check
        plot3([limx2(1) limx2(2) limx2(2) limx2(1) limx2(1)],...
            [limy2(1) limy2(1) limy2(2) limy2(2) limy2(1)],...
            limz2(2)*1.1*[1 1 1 1 1],...
            'w—','parent',ax2(M))
    end
    xlim(ax2(M),limx)
    ylim(ax2(M),limy)
    colorbar('peer',ax2(M));
    caxis(ax2(M),limc)
    set(ax2(M),'xtick',[],'ytick',[])
    box(ax2(M),'on')
    set(ax2(M),'color',colmap(1,:))
end
fit_axes2(ax2,[6 2 0.95 0.95])
pos = get(fh2,'position');
```

```
118 set(fh2,'position',[pos(1:2) 800 pos(4)])
119
120 function node = get_node_data(node)
121 % Getting total number of connections: X*4, Y*3, I*1:
122 node.rowT = [repmat(node.row{1},4,1); repmat(node.row{2},3,1);
    ...
123     node.row{3}];
124 node.colT = [repmat(node.col{1},4,1); repmat(node.col{2},3,1);
    ...
125     node.col{3}];
126
127 % Getting I connections: I*1:
128 node.rowI = node.row{3};
129 node.colI = node.col{3};
130
131 % Getting X connections: X*4:
132 node.rowX = repmat(node.row{1},4,1);
133 node.colX = repmat(node.col{1},4,1);
134
135 % Getting Y connections: Y*3:
136 node.rowY = repmat(node.row{2},3,1);
137 node.colY = repmat(node.col{2},3,1);
138
139 % Getting X+Y connections: X*4+Y*3:
140 node.rowXY = [repmat(node.row{1},4,1); repmat(node.row{2},3,1)];
141 node.colXY = [repmat(node.col{1},4,1); repmat(node.col{2},3,1)];
142
143 function [x y r] = plot_circles(ax,ind,z)
144 if exist('c','var')
145     delete(c)
146 end
147 x = []; y = []; r = [];
148 switch ind
149     case 1
150         % Circle, center x-position:
151         x = [600 950 1300 450 950 1450 250 600 950 1300 1650 250
                600 ...
152             950 1300 1650 450 950 1450 600 950 1300 ];
153         % Circle, center y-position:
154         y = [1500 1500 1500 1250 1250 1250 1000 1000 1000 1000
               1000 750 ...
155             750 750 750 750 500 500 500 300 300 300];
156         % Circle radius:
157         r = [170];
158     otherwise
159         x = []; % Circle, center x-position
160         y = []; % Circle, center y-position
161         r = []; % Circle radius
162 end
163 if ~exist('z'), z = 0; end
164 c = [];
165 for k = 1:length(x)
166     c(1,end+1) = circle(x(k),y(k),z,r,ax);
```

```
167     c(2,end) = text(x(k),y(k),num2str(k),'verticalalignment','
            middle',...
168         'horizontalalignment','center');
169 end
170
171 function fit_axes2(ax0,naxes)
172 x0 = 0:1/naxes(1):1-1/naxes(1);
173 x0 = x0(1:naxes(2):end);
174 y0 = 0:1/naxes(2):1-1/naxes(2);
175 w0 = 1/(naxes(1)/naxes(2));
176 h0 = 1/naxes(2);
177 dx = (1-naxes(3))/2;
178 dy = (1-naxes(4))/2;
179
180 indx0 = reshape(rnd(1:naxes(1),ceil(naxes(1)/naxes(2))),...
181     ceil(naxes(1)/naxes(2)),naxes(2));
182 indy0 = ones(ceil(naxes(1)/naxes(2)),1)*[naxes(2):-1:1];
183
184 dx = dx/size(indx0,1);
185 dy = dy/size(indx0,2);
186
187 fh = get(ax0(1),'parent');
188 colBar = ~isempty(findall(fh,'tag','Colorbar'));
189 if colBar
190     colBar0 = flipud(findall(fh,'tag','Colorbar'));
191     for k = 1:length(ax0)
192         if ~isempty(find(strcmp(get(colBar0(min(k,length(colBar0
                ))),...
193                 'location'),{'North','South','West','East'}))) %
                    Inside
194             colBar(k) = 0;
195         else
196             colBar(k) = 1;
197         end
198     end
199 else
200     colBar = zeros(1,length(ax0));
201 end
202 set(ax0,'LooseInset',[0 0 0 0])
203 refresh(figure(fh))
204 drawnow
205
206 pos1 = [];
207 out1 = [];
208 outTight1 = [];
209 for k = 1:length(ax0)
210     out1{end+1} = get(ax0(k),'outerposition');
211     outTight1{end+1} = get(ax0(k),'tightInset');
212     pos1{end+1} = get(ax0(k),'position');
213 end
214
215 outTight0   = cell2mat(outTight1(:));
216 outTight0_1 = max(outTight0(:,1));
```

```
outTight0_2 = max(outTight0(:,2));
outTight0_3 = max(outTight0(:,3));
outTight0_4 = max(outTight0(:,4));
out0        = cell2mat(out1(:));
out0_3      = max(out0(:,3));
pos0        = cell2mat(pos1(:));
pos0_2      = max(pos0(:,2));
pos0_3      = min(pos0(:,3));

newPos1 = [];
for k = 1:length(ax0)
    newPos1{end+1}      = x0(indx0(k))+dx + outTight0_1;
    newPos1{end}(end+1) = y0(indy0(k))+dy + outTight0_2;
    if colBar(k)
        newPos1{end}(end+1) = w0-2*dx-outTight0_1-outTight0_3
            -...
             (pos0_3-outTight0_3);
    else
        newPos1{end}(end+1) = w0-2*dx-outTight0_1-outTight0_3;
    end
    newPos1{end}(end+1) = h0-2*dy-outTight0_2-outTight0_4;
end
for k = 1:length(ax0)
    set(ax0(k),'position',newPos1{k})
end
refresh(figure(fh))

function new_lim = new_lim(new_lim,ntick,step,new_lim0)
if length(new_lim)>ntick
    new_lim = check_lim(new_lim,step,new_lim0);
    while length(new_lim)>2*ntick
        step = step*2;
        if min(new_lim0)<0 && max(new_lim0)>0 % Include zero:
            new_lim = [fliplr(0:-step:new_lim(1)) step:step:
                new_lim(end)];
        else
            new_lim = floor(new_lim(1)):step:ceil(new_lim(end));
        end
        new_lim = check_lim(new_lim,step,new_lim0);
    end
else
    new_lim = check_lim(new_lim,step,new_lim0);
    while length(new_lim)<ntick
        step = step/2;
        if min(new_lim0)<0 && max(new_lim0)>0 % Include zero:
            new_lim = [fliplr(0:-step:new_lim(1)) step:step:
                new_lim(end)];
        else
            new_lim = floor(new_lim(1)):step:ceil(new_lim(end));
        end
        new_lim = check_lim(new_lim,step,new_lim0);
    end
end
```

```
267
268 function new_lim = check_lim(new_lim,step,new_lim0)
269 try
270     while new_lim(2)<min(new_lim0)
271         new_lim(1) = [];
272     end
273 end
274 try
275     while new_lim(end-1)>max(new_lim0)
276         new_lim(end) = [];
277     end
278 end
279 try
280     while new_lim(1)>min(new_lim0)
281         new_lim = [new_lim(1)-step new_lim];
282     end
283 end
284 try
285     while new_lim(end)<max(new_lim0)
286         new_lim = [new_lim new_lim(end)+step];
287     end
288 end
289
290 function [optW C W X Y Z] = density_plot2(x0,ax,W)
291 %   [optW C W X Y Z] = density_plot2(x0,ax,W)
292 %
293 % This function calls a code SSKERNEL2D developed by Hideaki
    Shimazaki
294 % (http://2000.jukuin.keio.ac.jp/shimazaki)
295 %
296 % Input:
297 %   x0 - double, {default data}, 2D point-data, mx2 matrix
298 %   ax - double, optional, {new axes} handle to axes to plot in
299 %    W - vector, optional, {logspace(-2,-1.6,2)}, bandwidths to
    be
300 %        searched. Original range is {logspace(-2.2,-.5,50)}. It
    seems that
301 %        the narrower the range the less smoothing, but the
    range should be
302 %        optimized for every use.
303 %
304 % Output:
305 %   optW - double, optimal bandwidth
306 %      C - Bandwith
307 %      W - Bandwidth
308 %      X - double, griddata, x-values
309 %      Y - double, griddata, y-values
310 %      Z - double, griddata, density-values
311 %
312 [optW C W X Y Z] = sskernel2d2(x0,ax,W);
313
314 function [optW C W X Y Z] = sskernel2d2(x0,ax,W)
315 %   [optW C W X Y Z] = sskernel2d2(x0,ax,W)
```

```
%
% Copyright (c) 2010, Hideaki Shimazaki All rights reserved.
% http://2000.jukuin.keio.ac.jp/shimazaki
% See also: http://toyoizumilab.brain.riken.jp/hideaki/res/kernel.html
%
x = x0;
dimension = '2d';
gn = 100; % # of grid points

% %%%%%%%%%%%%%%%%%%%%%%%%%%%%%%%%%%%%%%%%%%%%%%%%%%%%%%%%%%%%%%%%%%%%%%%%%%%%
% Parameters Settings
Dx = (max(x(:,1))-min(x(:,1)));
Dy = (max(x(:,2))-min(x(:,2)));
x(:,1) = (x(:,1) - min(x(:,1)))/Dx;
x(:,2) = (x(:,2) - min(x(:,2)))/Dy;

N_total = length(x(:,1));   % Total number of samples.

% %%%%%%%%%%%%%%%%%%%%%%%%%%%%%%%%%%%%%%%%%%%%%%%%%%%%%%%%%%%%%%%%%%%%%%%%%%%%
% Compute a Cost Function
tau = triu( ones(N_total,1)*x(:,1)' - x(:,1)*ones(1,N_total), 1);
idx = triu( ones(N_total,N_total), 1);
TAU1 = tau(logical(idx)) .^2;

tau = triu( ones(N_total,1)*x(:,2)' - x(:,2)*ones(1,N_total), 1);
TAU2 = tau(logical(idx)) .^2;

TAU = TAU1+TAU2;

C = zeros(1,length(W));

switch dimension
    case '2d'
        for k = 1: length(W)
            w = W(k);
            C(k) = N_total/w/w + 2/w/w*sum(sum(exp(-TAU/4/w/w) - ...
                4*exp(-TAU/2/w/w) )); %2d
        end
        C = C/4/pi; %2d
    case '1d'
        for k = 1: length(W)
            w = W(k);
            C(k) = N_total/w + 2/w*sum(sum(2*exp(-TAU/4/w/w) - ...
                2*sqrt(2)*exp(-TAU/2/w/w) )); %1d
```

```
            end
            C = C/2/sqrt(pi); %1d
end

%
    %%%%%%%%%%%%%%%%%%%%%%%%%%%%%%%%%%%%%%%%%%%%%%%%%%%%%%%%%%%%%%%%%%%%%%%%%%%%%%%%%%%%%%%%%%%%%%%%%%%%%%%%%%%%%

% Selection of Optimal Bandwidth
[optC,nC] = min(C);
optW = W(nC);

%
    %%%%%%%%%%%%%%%%%%%%%%%%%%%%%%%%%%%%%%%%%%%%%%%%%%%%%%%%%%%%%%%%%%%%%%%%%%%%%%%%%%%%%%%%%%%%%%%%%%%%%%%%%%%%%

x_grid = linspace(0,1,gn);
y_grid = linspace(0,1,gn);
Z = zeros(gn,gn); X = Z; Y = Z;

gauss2d = @(x,w) 1/(2*pi*w*w) * exp(-sum(x.^2,2)/2/w/w);

for i = 1: length(x_grid)
    for j = 1: length(y_grid)
        d = ones(N_total,1)*[x_grid(i) y_grid(j)] - x;
        Z(i,j) = mean( gauss2d(d,optW) );

        X(i,j) = x_grid(i);
        Y(i,j) = y_grid(j);
    end
end

X = X*Dx+min(x0(:,1));
Y = Y*Dy+min(x0(:,2));
Z = Z*N_total/gn;

surf(X,Y,Z,'parent',ax);
view(ax,2), shading(ax,'flat'); lighting(ax,'phong')
```

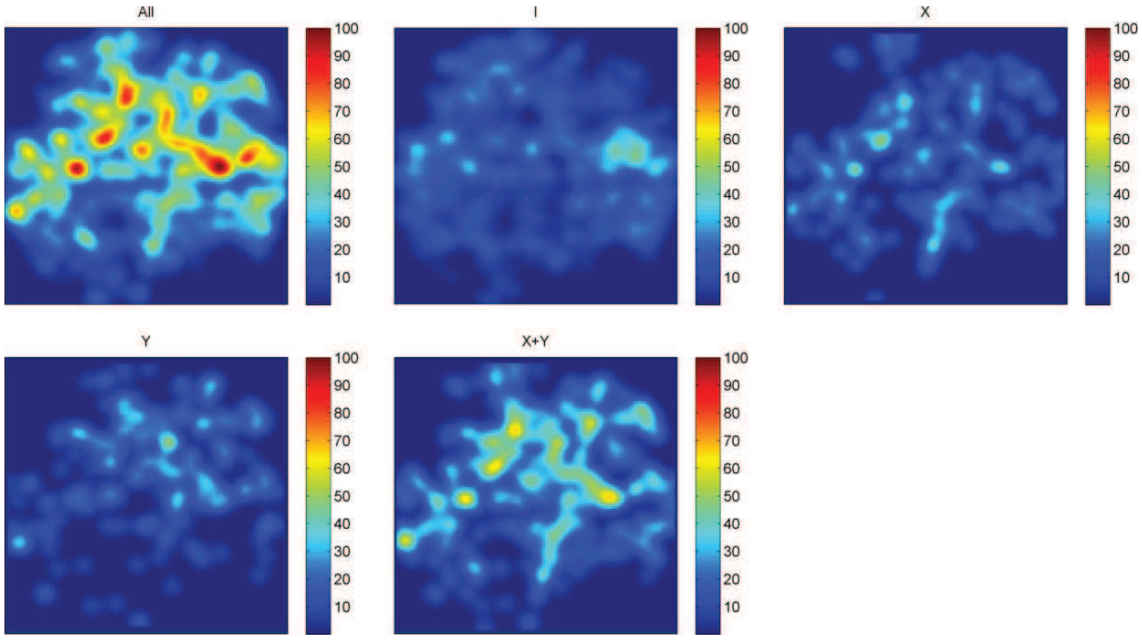

Figure E.3: Example of density maps output

Bibliography

NIXON, C. W. (2013). Analysis of fault networks and conjugate systems. Ph.D. thesis, University of Southampton.

APPENDIX F

Detailed Core log13z - Clair

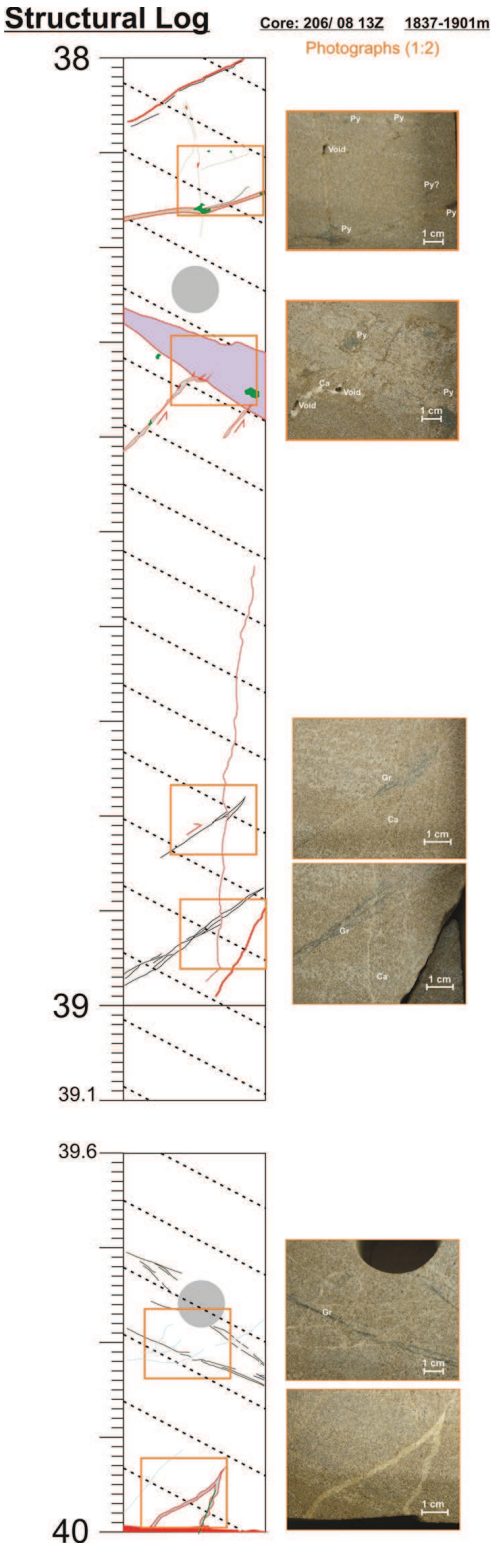

Description	Structural Information	
Thin fracture nucleated on granulation seams 5 mm thick veins trend orthogonal to the core cutting. It is associated with "degraded" pyrite mineralization. Vuggy thin (1-2 mm) veins trend orthogonal to the layering and they are associated with "degraded" pyrite mineralization.	Fractures: 29° & 10° dip Veins = 85°, 75°, 76°, 18° & 66° dip Granulation seams: 25°, 41° & 18°	 N = 2 N = 5 N = 3
3 cm thick cemented area with white calcite trends parallel to bedding. "Degraded" pyrite is also present in this area. Two small vuggy veins trending orthogonal to the bedding, occur (see bottom left in the photo). The longer is about 3mm thick. Apparent normal displacement is about 3-4 mm.	Fractures: 48° & 31° dip	 N = 2
A vertical vuggy fracture with calcite (about 1 mm thick) displaces granulation seams. Its length is about 70 cm and has an irregular shape. Anastomosed granulation seams show apparent reverse displacement. A later carbonate cemented vein displaces the granulation seams.	Fractures: 59°, 83° to 87° dip Granulation seams: 33°, 32°, 34°, 33° dip	 N = 3 N = 4
Anastomosed granulation seams trend sub-parallel to bedding. These are predated by carbonate veins. Thin carbonate veins trend sub/orthogonal to the layering (from bottom left to upper right). They have irregular, curved shape. Two "conjugate" carbonate veins and a thin (1-2 mm) vein are observed trending orthogonal to the layering (from bottom left to upper right).	Fractures: 29°, 60°, 67° dip Veins: 44°, 24°, 20°, 48°, 51°, 51°, 26 °, 68° dip Granulation seams: 22°, 39°, 23°, 38°, 48° dip	 N = 7 N = 3 N = 4

Structural Log

Core: 206/ 08 13Z 1837-1901m

Photographs (1:2)

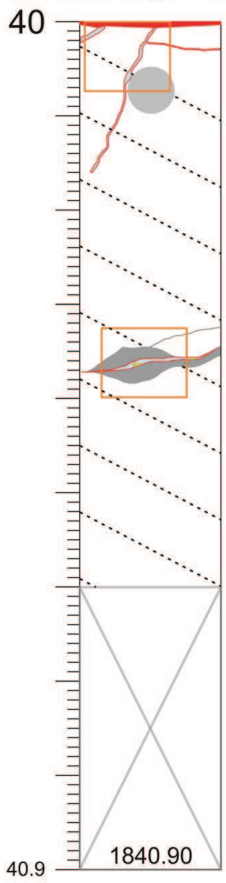

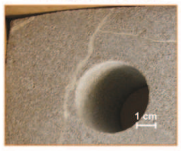

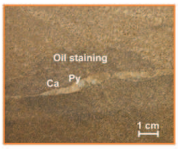

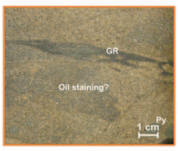

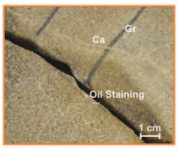

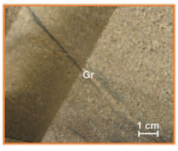

Thin-section 1841.37 (2/6/2)
"Indipendent Petrographic Services"

Description	Structural Information	
Two curved carbonate veins (see previous core cutting) trend sub-orthogonal to the layering.	Fractures: 30°, 62° & 5° dip	 N = 3
Sigmoidal calcite vein with golden rounded pyrite "clasts" in the central part and at the edges. The thickness of calcite vein is about 5 mm in the centre. Black oil staining is observed around this vein. It has an elliptic shape.	Fractures: 32°, 20° & 0° dip Oil trail: 14° dip	 N = 3 N = 1
Calcite vein (1mm thick) associated with bitumen. Granulation seams trend horizontally to the core cutting. They show ribbon shape and they are associated with pyrite and oil staining (?). Rounded "clasts" of weathered pyrite also occur.	Granulation seams: 0°, 17°, 7°, 37°, 75° dip	 N = 5
Two fractures trend parallel to bedding; one of them is open, the other is sealed by carbonate cement. Granulation seams have trend orthogonal to the layering from the open fracture in direction upper right. Oil staining is mainly observed at the top of the open fracture.	Fractures: 20°, 39°, 17°, 29° dip Granulation seams: 50° & 54° dip	 N = 2 N = 4
Granulation seams running upper left to bottom right.	Granulation seams: 50°, 44° & 40° dip	 N = 3

Structural Log

Core: 206/ 08 13Z 1837-1901m

Photographs (1:2)

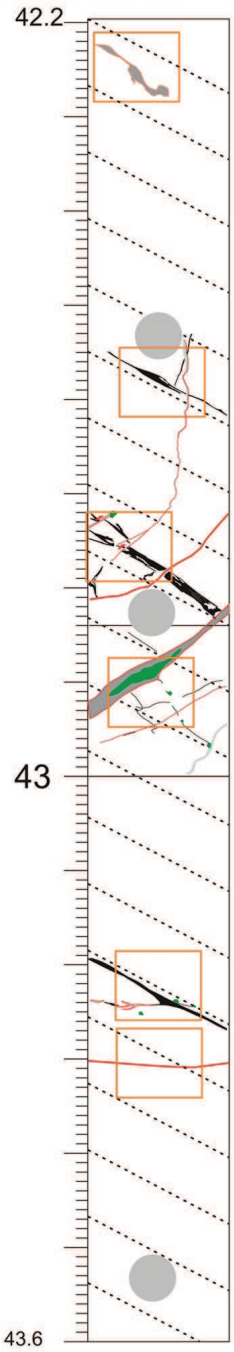

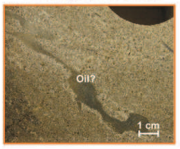

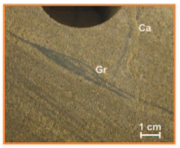

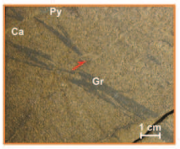

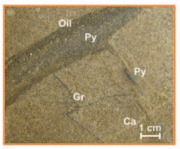

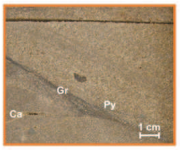

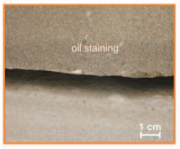

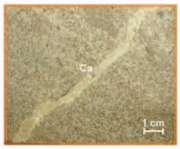

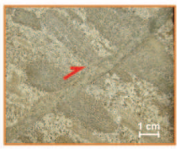

Description	Structural Information	
1-2mm thick vein runs parallel to the cutting and shows an irregular shape. This vein displaces granulation seams in 3 points (5 mm apparent reverse offset). Granulation seams trend parallel to the layering and they show a anastomosed shape. Gouge with oil staining and pyrite occur orthogonal to the layering. Thin granulation seams with irregular shape trend from top left to bottom right. Small clasts (<1mm) of degraded pyrite are associated with one of them.	Granulation seams: 27°, 31°, 39°, 21°, 19°, 4°, 7°, 6° dip Fractures: 84°, 87°, 50°, 36°, 24°, 30°, 50°, 35°, 20°, 7°, 27°, 40°, 70°, 27°, 33°, 30°	 N = 16 N = 8
Granulation seam trends parallel to layering. It is partially reactivated and associated with calcite and small clasts of degraded pyrite. A fracture orthogonal to the core represent a barrier to oil.	Fractures: 1°, 5°, 6° dip Granulation seams: 1°, 30° dip	 N = 3 N = 2
1 cm thick carbonate vein with irregular shape trends orthogonally to the layering.	Fractures: 44	 N = 1
1 cm thick carbonate vein with irregular shape trend orthogonally to the layering and it shows 1 cm of apparent reverse displacement	Fractures: 77°, 37° dip	 N = 2

Structural Log

Core: 206/ 08 13Z 1837-1901m

Photographs (1:2)

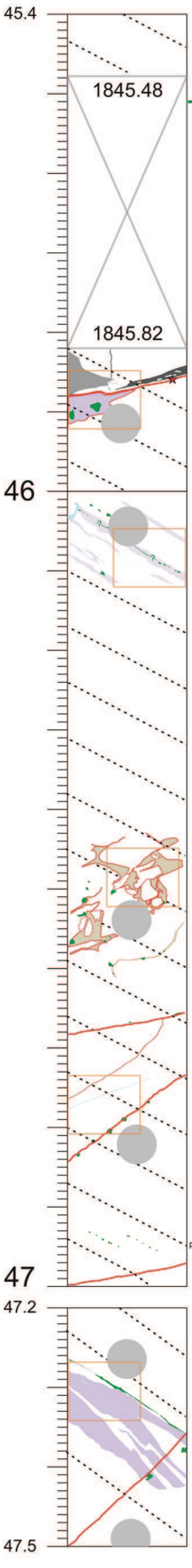

Thin-section 1845.51 (2/7/1)
"Indipendent Petrographic Services"

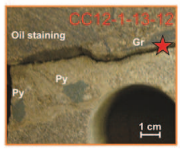

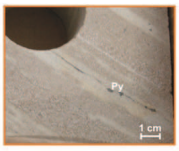

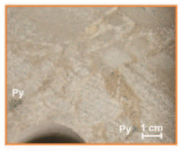

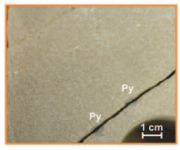

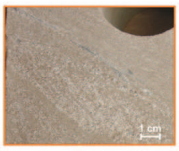

Description	Structural Information	
Subhorizontal fracture reactivated a granulation seams observed at the top right Oil staining is observed in the upper left. A small region made of cemented sandstones with rounded clasts of degraded pyrite occurs under the fracture.	Fractures: 11°, 7°, 13° dip Granulation seams: 88°, 16°, 9°, 89° dip	 N = 3 N = 4
Alternated regions of darker and lighter bands occur (different cement ?). In the lighter regions a thin fracture with degraded pyrite occur.		
Complex brecciated region underlined by the different cement. Small pyrite have been observed associated mainly with the cemented areas.	Fractures: 12°, 24°, 16°, 36°, 27°, 22° dip	 N = 6
Four fractures trrend top right to bottom left and show the presence of pyrite (golden on the fresh surface). 1mm thin carbonate vein trends bottom left to upper right	Fractures: 9°, 9°, 38° dip	 N = 3
Region with sedimentary carbonate cement. At the top of this region has been observed a thin elongate region with green degraded pyrite. Fracture trends bottom left to top right	Fractures: 42°, 45°, 64° dip	 N = 3

Structural Log

Core: 206/ 08 13Z 1837-1901m

Photographs (1:2)

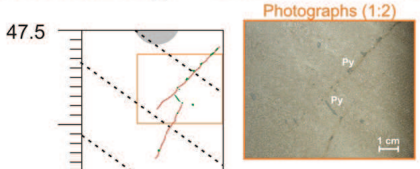

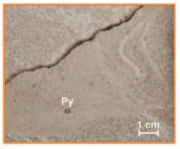

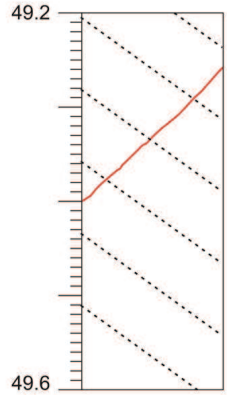

Description	Structural Information	
Two thin fractures are associated with carbonate cement and "degraded" pyrite		
Fracture orthogonal to the core cutting.	Fractures: 7° dip	 N = 1
Fracture associated with finer sandstone which show some soft sediment deformations. The contact at the bottom of this area creates an angle of 30° with the layering, while the contact at the top is marked by a fracture at 60° to bedding.	Fractures: 31, 16, 34° dip	 N = 3
Fracture trending orthogonal to the layering	Fractures: 42° dip	 N = 1

Structural Log

Core: 206/ 08 13Z 1837-1901m

Photographs (1:2)

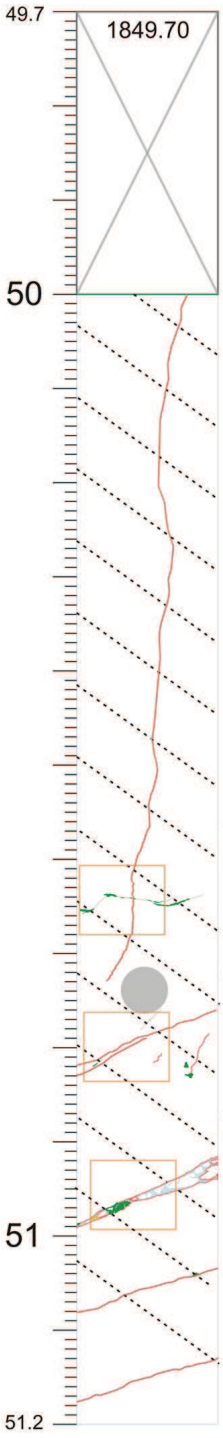

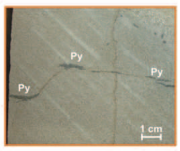

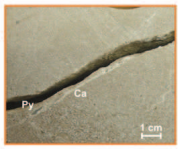

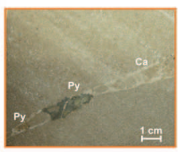

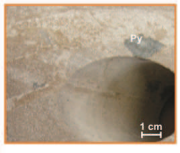

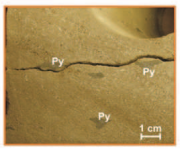

Description	Structural Information	
	Fractures: 65, 84, 60, 86, 87° dip	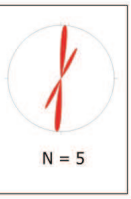 N = 5
A vertical and partially cemented fracture is more than 1m long. Thin fracture orthogonal to the core cutting with "S shape" shows pyrite mineralization at the fracture bends. Four parallel carbonate veins occur. They are 1 to 3 mm thick. One of them is open and associated with carbonate infil. Pyrite occurs associated with a calcite filled fractures.	Fractures: 45, 20, 29, 67, 23, 15, 15, 16° dip	 N = 8
Large cemented regions with pyrite	Fractures: 10°, 14°, 25°, 5°, 5°, 15°, 75°, 90°, 23° dip	 N = 8
Fracture trending subhorizontal to the core cutting. Small pyrite (<5mm) is observed along the fracture and parallel to bedding	Fractures: 7° dip	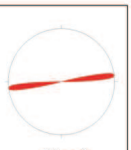 N = 1

Structural Log

Core: 206/ 08 13Z 1837-1901m

Photographs (1:2)

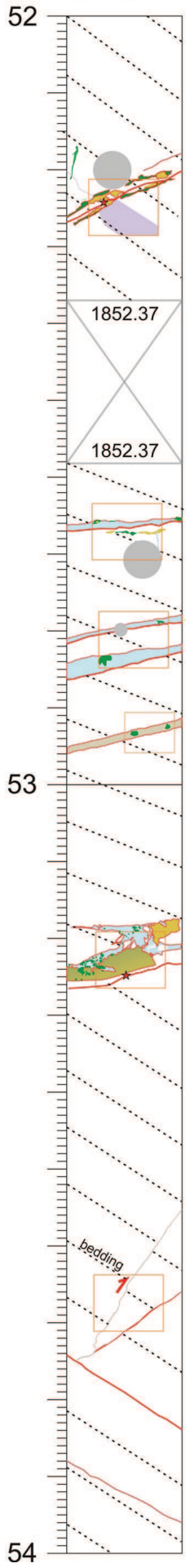

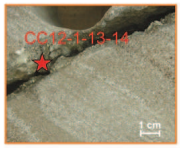

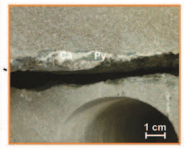

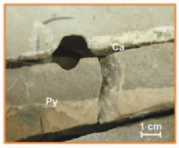

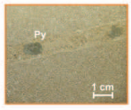

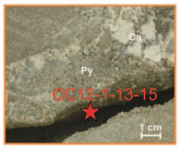

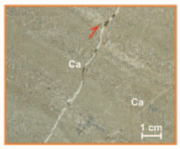

Description	Structural Information	
Fracture oriented at 45° to the bedding with fresh golden pyrite and calcite (sampled).	Fractures: 29°, 20°, 9°, 31° dip	 N = 4
Fracture with 5mm thick carbonate mineralization and golden pyrite sub-horizontal to the core cutting A 2mm thin vein trends vertically to join the fracture. Parallel to these fractures, a region with altered calcite cement occurs. It is fractured at its bottom edge where golden pyrite occurs. 6mm of darker sandstones (different cement ?) has the same trend of previous fractures. Two degraded and rounded clasts of pyrite are also present there.	Fractures: 5°, 5°, 17°, 15°, 15°, 15° dip	 N = 6
Breccia with golden, fresh pyrite, degraded pyrite and carbonate cement	Fractures: 4°, 8°, 18°, 5°, 10° dip	 N = 5
Two fractures orthogonal to the core cutting occur. They are carbonate filled terminates on a parallel bedding fracture. One of these fractures shows apparent reverse offset. Two fractures sub-parallel to bedding occur.	Fractures: 54°, 35°, 34°, 28° dip	 N = 4

Structural Log

Core: 206/ 08 13Z 1837-1901m

Photographs (1:2)

54

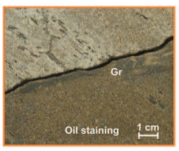

Curved fracture oriented at low angle to the layering

Fracture parallel to bedding

Fracture at a low angle to the bedding. It represents a good conduit for fluid along the fracture and a barrier across the fracture. Oil occur along the fracture and at the bottom.

Fractures: 6°, 19°, 32°, 18° dip

N = 4

55

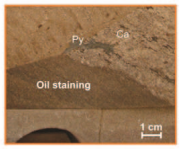

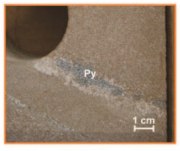

Cemented stratigraphic layers (lighter) associated with degraded elongate clasts of pyrite.

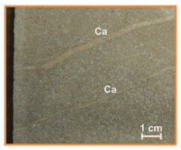

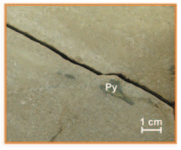

Fractures with carbonate mineralization occur. Thickness is about 0.5 mm.
Small clasts of degraded pyrite are not associated with fractures or veining.

Fracture parallel bedding occurs. Elongate clasts of pyrite have been observed below it.

Fractures: 5°, 17°, 17°, 37° dip

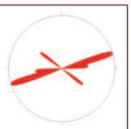

N = 4

Thin-section 1856.96 (3/4/2)
"Indipendent Petrographic Services"

56

Structural Log

Core: 206/ 08 13Z 1837-1901m

Photographs (1:2)

Description	Structural Information	
The fracture in direction bottom left to upper right are partially associated with carbonate mineralization (2mm thin). Another fracture is parallel to the bedding and terminated on the previous one. Degraded pyrite is observed at the intersection between the two fractures.	Fractures: 19°, 38°, 24°, 15°, 19°, 15°, 7°, 5°, 7° dip	N = 9
Carbonate filled fractures normally displace the layers	Fractures: 29, 32, 17, 20, 42, 75, 63° dip	N = 6
Granulation seams orthogonal to the bedding and showing reverse displacement.	Fractures: 49, 31, 38, 24° dip	N = 4
2 fractures sub-orthogonal to the layering.	Fractures: 45°, 38° dip	N = 2

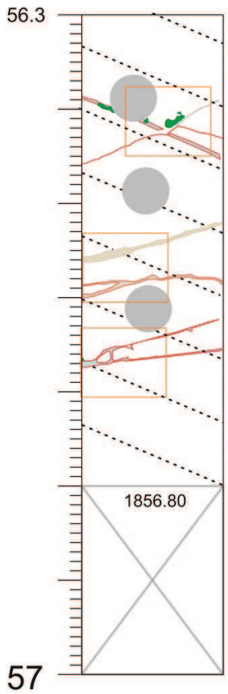

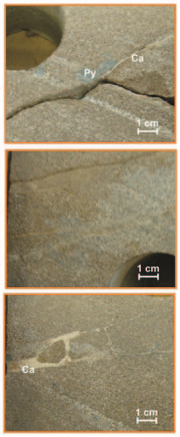

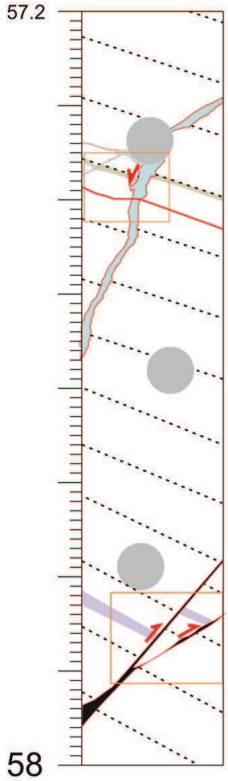

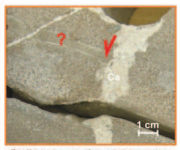

Sedimentary carbonate cement -> Carbonate veins

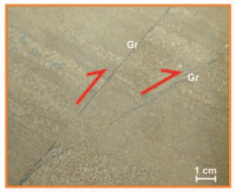

Sedimentary carbonate cement -> Bitumen

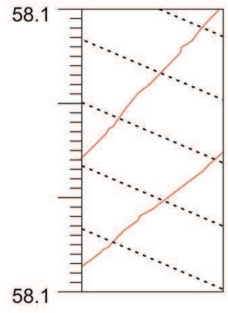

Structural Log

Core: 206/ 08 13Z 1837-1901m

Photographs (1:2)

Description	Structural Information
	Fractures: 45°, 38° dip

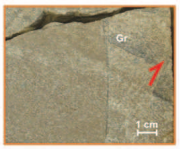

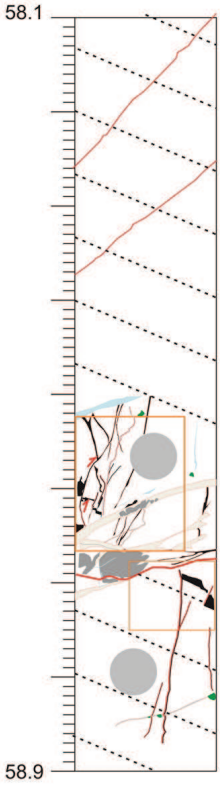

	Fractures: 76, 53, 77, 61, 73, 77, 80, 75, 81, 65, 74, 68, 76, 70, 68, 58, 22, 22, 17, 32, 81, 12, 12, 16, 24, 28, 86, 66, 82, 24, 74, 85° dip

Deformed sandstones contrast due probably to calcite cement and grainsize. The oil trail is cutted by these veins.	Fractures: 26, 9, 17, 17, 25, 70, 83, 5, 11, 11, 30, 65, 45, 47, 24, 54° dip

oil -> calcite -> "degraded" carbonate veins

	Fractures: 18°, 88° dip

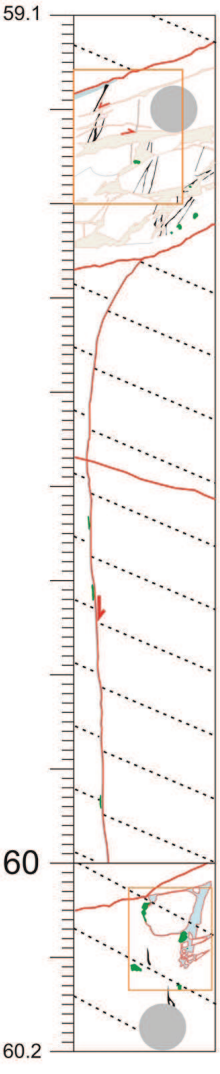

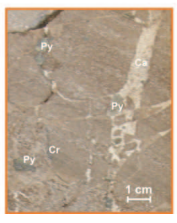

	Fractures: 10°, 24°, 44°, 7°, 7°, 8°, 17°, 37°, 11°, 72°, 80° dip

Structural Log

Core: 206/ 08 13Z 1837-1901m

Photographs (1:2)

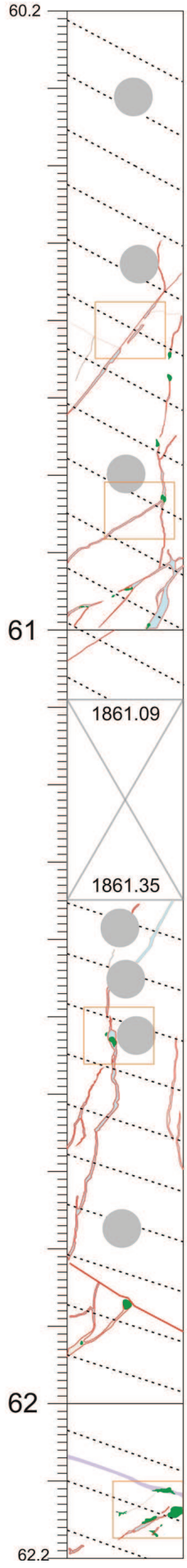

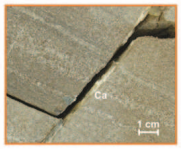

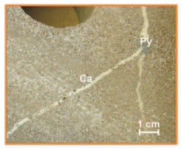

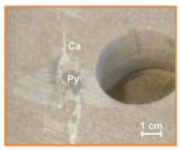

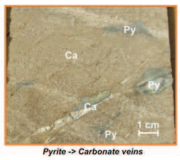

Pyrite -> Carbonate veins

Description	Structural Information	
Carbonate vein (2mm thick) oriented orthogonal to the layering and showing tensile behaviour. Thin (< 0.5 cm) carbonate veins associated with pyrite	Fractures: 50, 24, 61, 2, 76, 81, 81, 90, 29, 45, 83, 29, 45, 83, 29, 50, 64, 48, 54, 34° dip	 N = 17
4mm thick vein with apparent reverse displacement (?) It is associated with weatered pyrite areas.	Fractures: 66, 61, 85, 64, 82, 81, 88, 52, 75, 85, 33, 38, 15° dip	 N = 13
	Fractures: 27°, 40°, 31°, 30°, 30°, 44° dip	 N = 6

Structural Log

Core: 206/ 08 13Z 1837-1901m

Photographs (1:2)

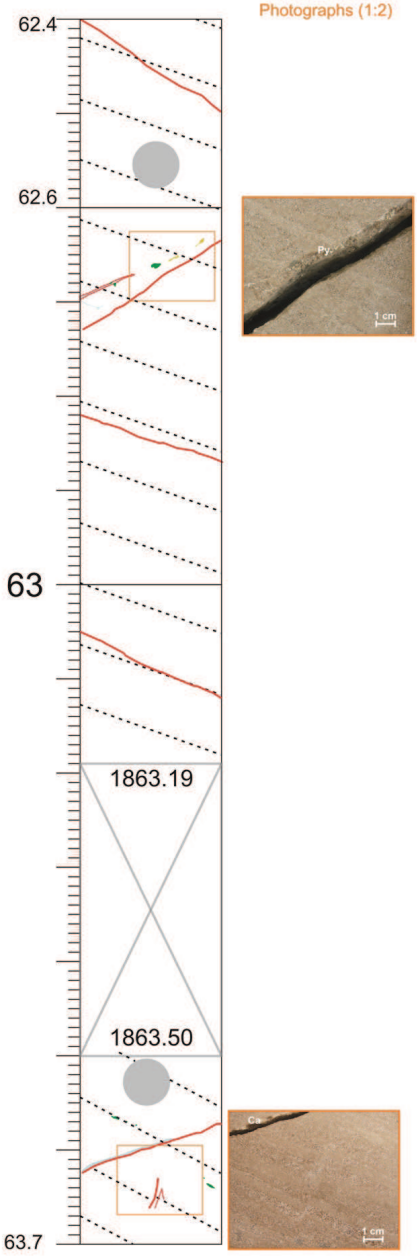

Description	Structural Information
	Fractures: 32° dip N = 1
	Fractures: 23°, 33° dip N = 2
	Fractures: 14° dip N = 1
	Fractures: 22° dip N = 1
	Fractures: 17°, 61°, 82° dip N = 3
	Fractures: 10° dip N = 1
	Fractures: 12° dip N = 1

Structural Log

Core: 206/ 08 13Z 1837-1901m

Photographs (1:2)

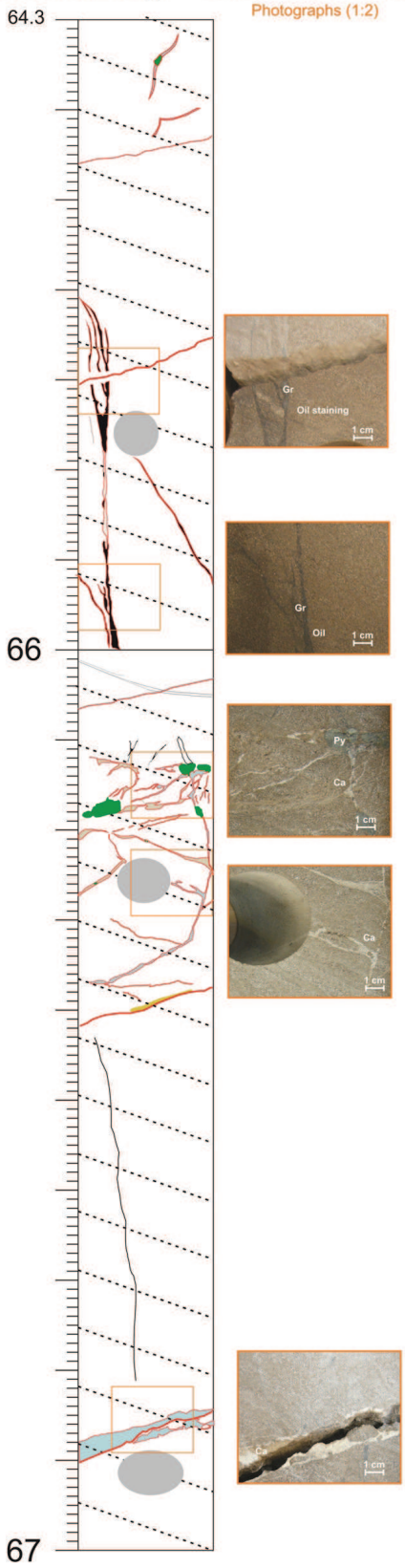

Description	Structural Information	
	Fractures: 10°, 67°, 26°, 5°, 83°, 33°, 64° dip	 N = 7
Fracture cutting granulation seams and showing oil staining at its bottom (footwall)	Fractures: 17, 62, 78, 9, 9, 76, 57, 79	 N = 8
Calcite along fracture (similar trend of 51-52) with some sand clasts (breccia). Thin vein (top) (with 3-4mmclasts of pyrite) has the same trend of previous to subvertical.	Fractures: 11, 11, 10, 7, 16, 40, 80, 80, 78, 13, 17, 25, 57, 47, 29, 75, 30, 13, 24, 12, 17, 17° dip Oil trails: 20, 8, 51, 65, 85, 88, 90,	 N = 7 N = 21
Large fracture with breccia and with thick (>1cm) carbonate mineralization	Fractures: 20°, 30°, 10°, 14°, 12° dip	 N = 5

Structural Log

Core: 206/ 08 13Z 1837-1901m
Photographs (1:2)

Description	Structural Information
Granulation seams parallel to the layering (top) and also orthogonal to the core cutting. A fracture with carbonate infil displaces the latter. Pyrite is associated with carbonate mineralization.	Fractures: 25, 25, 20, 26, 83, 81, 12, 14, 25 Oil trail: 29, 24, 72, 65, 75, 85, 59, 66, 69, 73, 80, 80, 78, 67, 68° dip

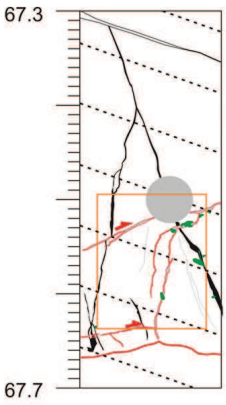

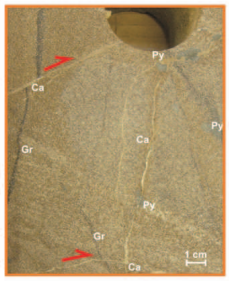

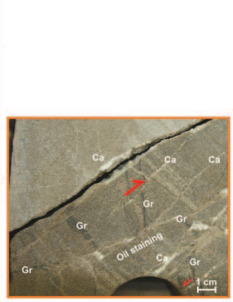

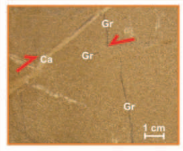

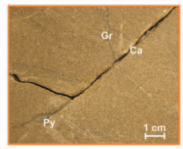

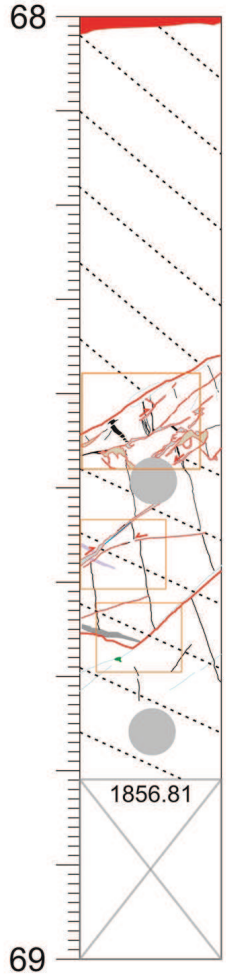

★ CC12-1-13-05

Fractures: 2° dip

Description	Structural Information
Crosscutting relationship showing granulation seams repeatedly cut by mainly tensile carbonate veins.	Fractures: 32°, 45°, 45°, 30°, 39°, 30°, 41°, 46°, 35°, 44°, 39°, 30°, 42°, 22° dip Oil trails: 35, 58, 58, 98, 11, 80, 85, 88, 82, 81, 37, 69, 77, 77, 38, 17, 81, 71, 53, 53, 88, 72 Veins: 6, 28, 45, 41, 33, 37, 22

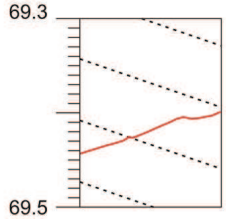

Fractures: 10°, 23° dip

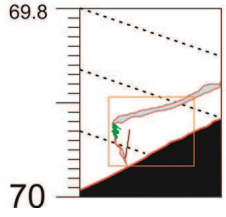

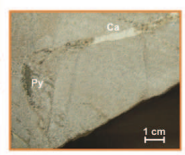

Fractures: 13°, 22°, 70°, 81°, 29°, 23°, 24° dip

Structural Log

Core: 206/ 08 13Z 1837-1901m

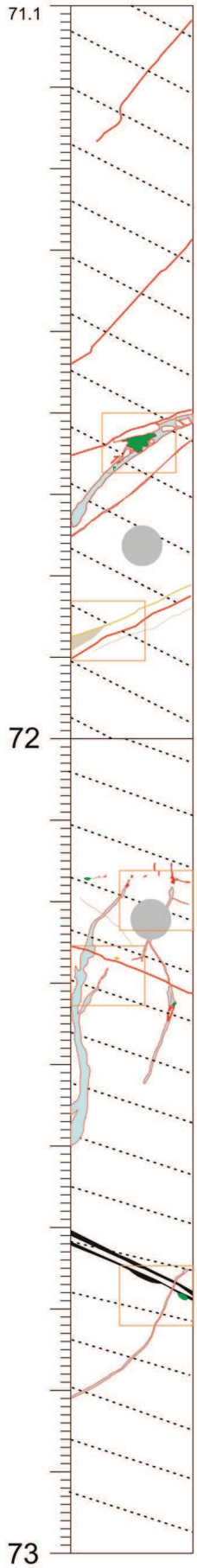

Photographs (1:2)

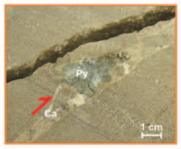

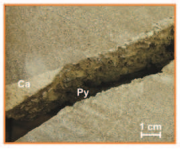

Photographs (1:2)

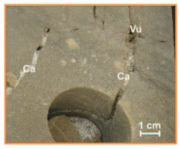

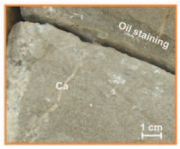

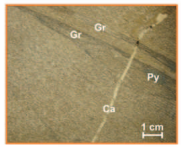

Description	Structural Information	
	Fractures: 52°, 42°, 89° dip	 N = 3
	Fractures: 47°, 30° dip	 N = 2
	Fractures: 30°, 19°, 17°, 33°, 18°, 15°, 37°, 41° dip	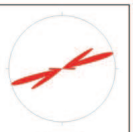 N = 8
	Fractures: 32°, 19°, 25°, 35° dip	 N = 4
	Fractures: 14°, 87°, 64°, 74°, 57°, 9°, 44°, 70°, 19°, 44°, 33°, 54°, 73°, 82°, 70°, 36°, 63°, 19° dip	 N = 18
Granulation seams cut by tensile vein	Fractures: 64°, 36°, 30°, 44° dip Oil trail: 26° ,22° ,27° dip	 N = 3 N = 4

Structural Log

Core: 206/ 08 13Z 1837-1901m

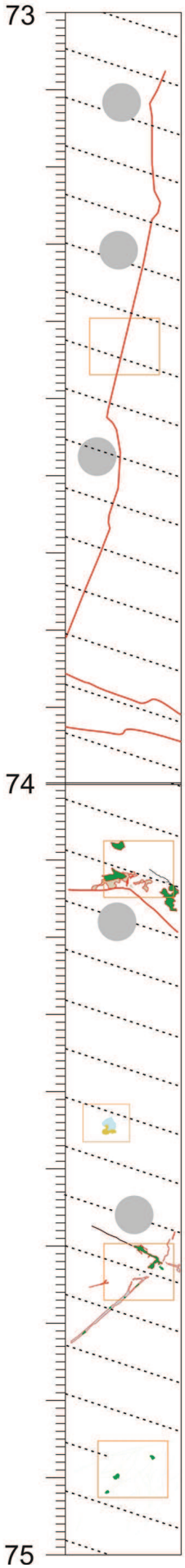

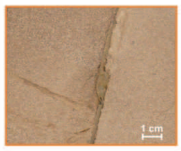

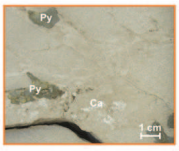

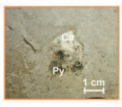

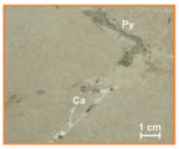

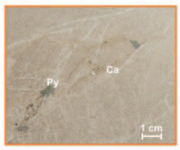

Description	Structural Information	
Fracture orthogonal to the layering which cuts the core for about 80cm	Fractures: 66°, 89°, 78°, 68°, 72°, 88°, 41° dip	 N = 7
Curved fractures sub-parallel to the layering	Fractures: 21°, 34°, 17°, 7°, 21°, 53° dip	 N = 6
	Fractures: 1°, 5°, 42°, 65°, 18° & 9° dip	 N = 6
Carbonate mineralization occurring along a fracture orthogonal to the layering and pyrite in a fracture sub-parallel to the layering.	Fractures: 27°, 41°, 15°, 71°, 61°, 64°, 44°, 36° dip	 N = 8
	Fractures: 24°, 13°, 12°, 57°, 44°, 46°, 77°, 43°, 44°, 71°, 88°, 67°, 34°, 41°, 66°, 34°, 59°, 43°, 65°, 49°, 79°, 58°, 89° dip	N = 23

Structural Log

Core: 206/ 08 13Z 1837-1901m

Photographs (1:2)

Description	Structural Information
Fracture with pyrite (< 1cm thick) and calcite infil. Minor fracture terminate on it.	Fractures: 21°, 49°, 18°, 64°, 85°, 76°, 89° dip
Fracture with thin carbonate mineralization	Fractures: 36° dip
Fracture with pyrite infil (< 0.8 cm thick)	Fractures: 25° & 13° dip
	Fractures: 20°, 31°, 21°, 13° dip
Carbonate veins oriented parallel and orthogonal to the layering	Fractures: 54°, 35°, 36°, 69°, 72°, 25°, 28°, 25°, 25°, 19° dip

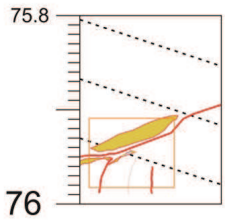

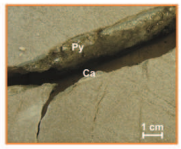

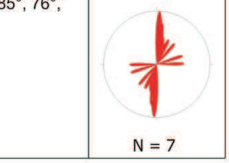

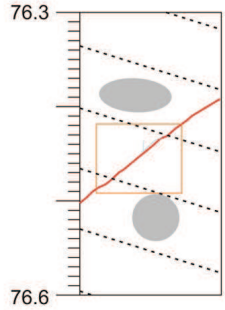

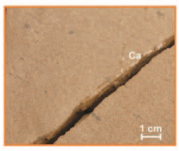

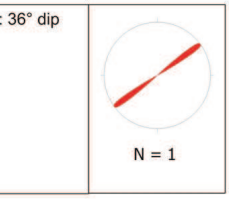

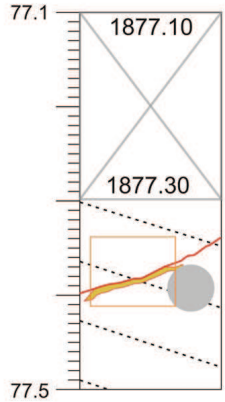

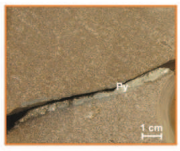

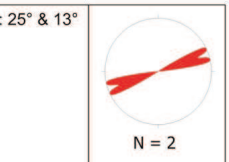

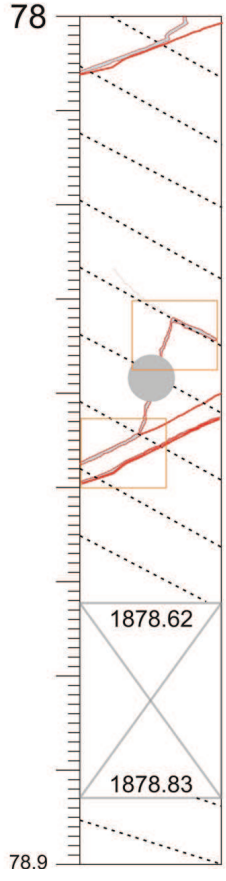

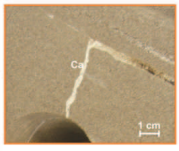

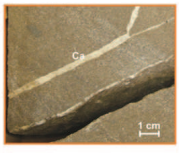

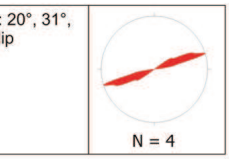

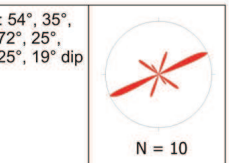

Structural Log

Core: 206/ 08 13Z 1837-1901m

Photographs (1:2)

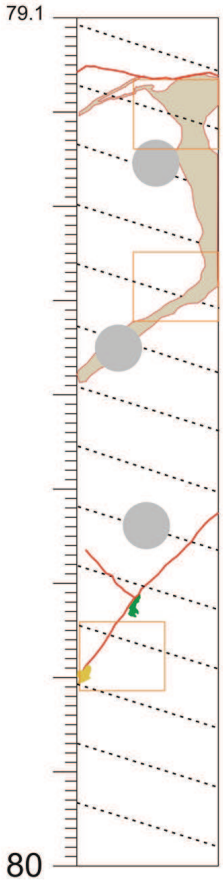

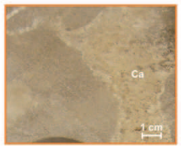

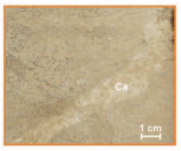

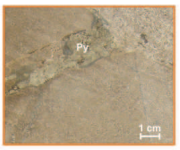

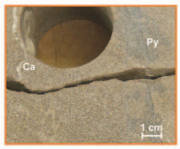

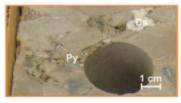

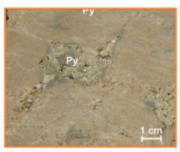

Description	Structural Information	
	Fractures: 32°, 13°, 8°, 22°, 28°, 17°, 34°, 76° dip	 N = 8
Fault orthogonal to the layering associated with pyrite mineralization	Fractures: 46°, 44°, 54° dip	 N = 3
Pyrite at the contact between	Fractures: 10°, 8° & 27° dip Granulation seams: 88°, 85°, 79°, 76°, 82° dip Veins: 23°, 58°, 66°, 12°, 85°, 83°, 83°, 69°, 74°,73° dip	 N = 3 N = 5 N = 11
Pyrite mainly localized at the intersection between fractures orthogonal to the layering and carbonate cemented fractures parallel to the layering	Fractures 1: 19, 7, 15, 23, 17, 1, 36, 35, 38, 9, 22, 67, 45, 57, 56, 57, 30 Fractures 2: 15, 44, 20, 25, 32, 62, 37, 15, 21 Fractures 3: 29, 6, 6, 57, 34, 29, 23, 18, 10, 78, 94, 58, 58, 34, 18, 61	 N = 17  N = 9  N = 16

Structural Log

Core: 206/ 08 13Z 1837-1901m

Photographs (1:2)

Description	Structural Information
Fault breccia made of clasts of host rocks, pyrite and calcite.	Fractures: 38°, 16°, 26°, 76°, 36°, 6°, 52°, 17°, 35°, 17° & 5° dip Granulation seams: 24°, 55°, 58°, 19°, 41°, 15° dip

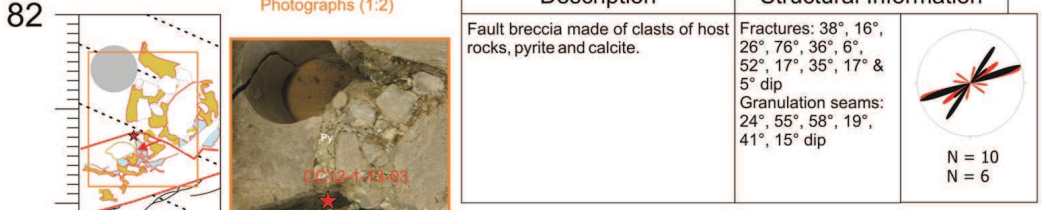

82

82.3

82.7

1882.73

→ *Thin-section 1882.92 (4/3/1)*
"Indipendent Petrographic Services"

83

Fractures: 28° dip

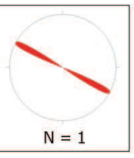

83.4

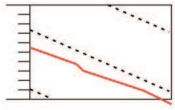

83.5

83.8

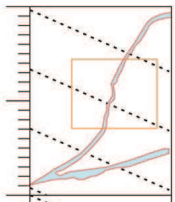

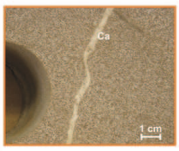

Fractures: 19°, 61°, 78°, 31°, 7°, 19° dip

84

1884.07

→ *Thin-section 1884.12 (4/4/2)*
"Indipendent Petrographic Services"

→ *Thin-section 1884.30 (4/4/3)*
"Indipendent Petrographic Services"

1884.35

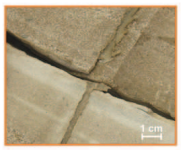

Fractures: 57°, 57°, 35° & 68° dip

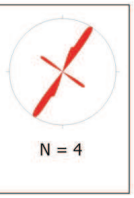

Fractures: 53°, 45°, 69°, 57° dip

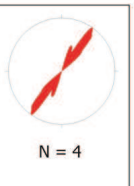

84.9

Structural Log

Core: 206/ 08 13Z 1837-1901m

Photographs (1:2)

Description	Structural Information
	Fractures: 69°, 47°, 56°, 63° dip

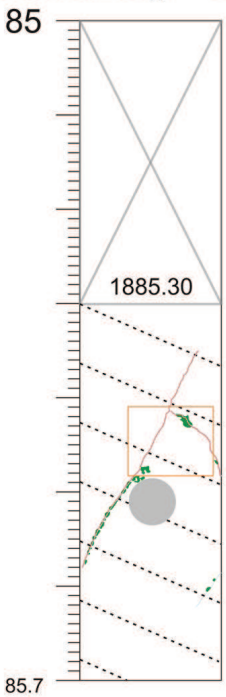

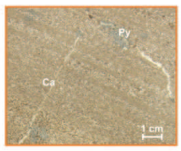

Description	Structural Information
Carbonate-infilled fractures (+ pyrite) orthogonal to the layering and with apparent reverse displacement.	Fractures: 87°, 86°, 51°, 51°, 49°, 85°, 55°, 52°, 52° dip

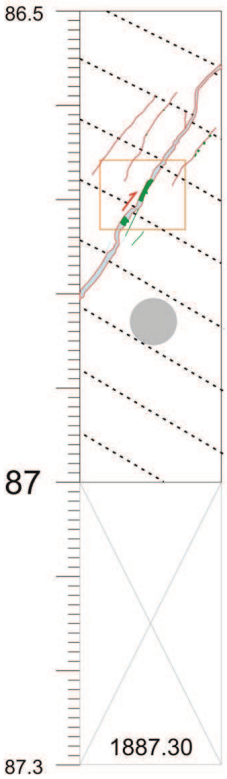

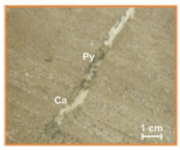

Description	Structural Information
Carbonate-infilled fractures (+ pyrite) orthogonal to the layering.	Fractures: 53°, 53°, 70° dip

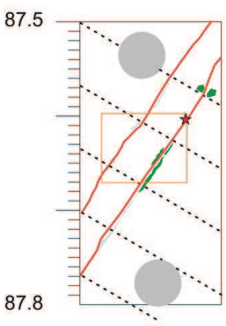

CC12-1-13-06

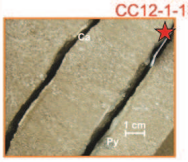

Structural Log

Core: 206/ 08 13Z 1837-1901m

Photographs (1:2)

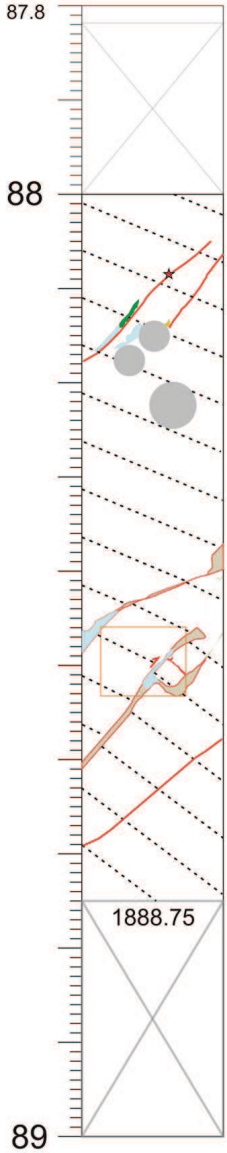

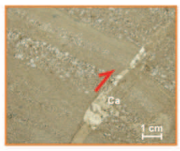

Description	Structural Information	
Carbonate-infilled fractures (+ gold pyrite) orthogonal to the layering.	Fractures: 42°, 53° & 40° dip	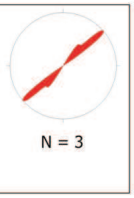 N = 3
Carbonate-infilled fractures orthogonal to the layering and with apparent reverse displacement.	Fractures: 39°, 53°, 42°, 40°, 50°, 51°, 21° dip	 N = 7
	Fractures:° dip	 N = 1
	Fractures: 87°, 83°, 57°, 42°, 58° dip	 N = 5

Structural Log

Core: 206/ 08 13Z 1837-1901m

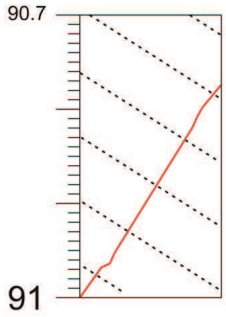

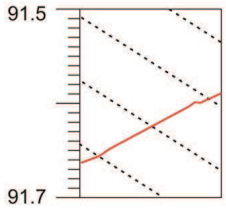

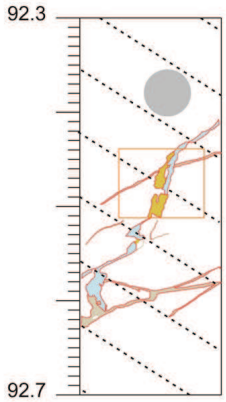

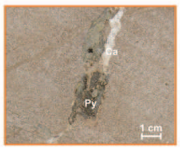

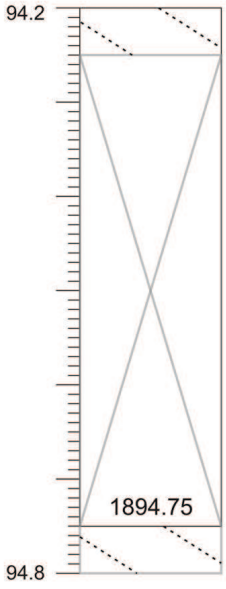

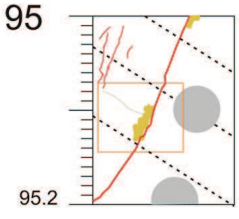

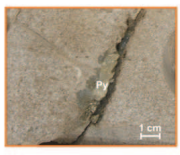

Description	Structural Information	
	Fractures: 58° dip	 N = 1
	Fractures: 27° dip	 N = 1
Carbonate-infilled fractures (+ pyrite) orthogonal to the layering.	Fractures: 31°, 31°, 74°, 18°, 47°, 66°, 19°, 42°, 72°, 21°, 13°, 8°, 33°, 25°, 25° dip	 N = 15
Fractures with gold pyrite mineralization orthogonal to the layering.	Fractures: 68°, 68°, 82° & 51° dip Veins: 36° & 52° dip	 N = 2 N = 4

Structural Log

Core: 206/ 08 13Z 1837-1901m

Photographs (1:2)

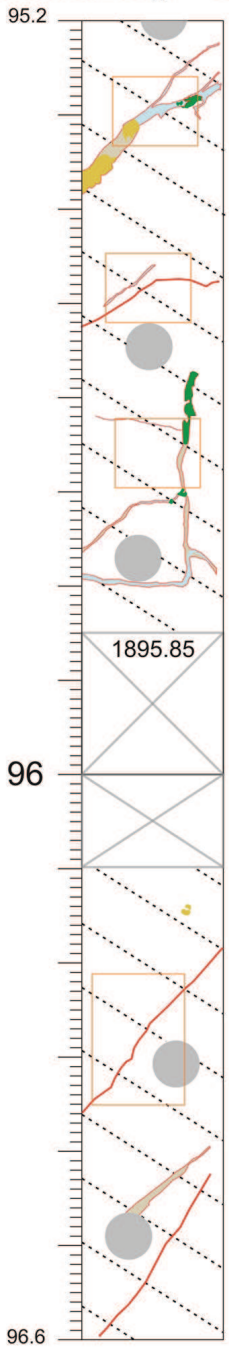

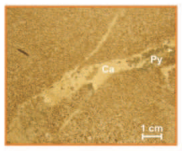

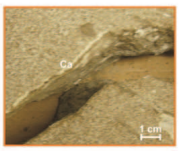

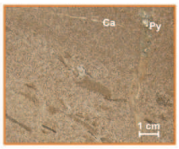

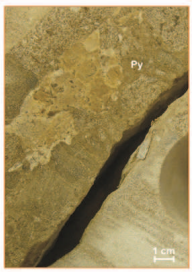

Description	Structural Information	
Carbonate-infilled fractures (+ pyrite) orthogonal to the layering.	Fractures: 50°, 36°, 56°, 38°, 14°, 46°, 66°, 23° dip	N = 8
	Fractures: 35°, 38°, 2°, 22°, 31° & 6° dip	N = 6
	Fractures: 21°, 85°, 67°, 100°, 87°, 52°, 42°, 1° & 3° dip	N = 9
	Fractures: 44°, 57°, 57°, 48°, 38°, 45° dip	N = 6
	Fractures: 22°, 35°, 19°, 10°, 41° & 72° dip	N = 6

Structural Log

Core: 206/ 08 13Z 1837-1901m

Photographs (1:2)

98

99

1900

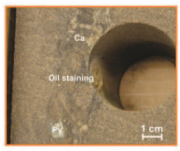

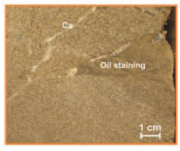

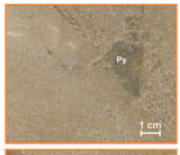

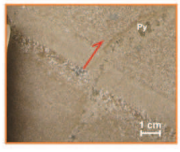

Description	Structural Information
	Fractures: 45°to 56° dip  N = 2
	Granulation seams: 34° dip  N = 1
	Fractures: 77°, 26°, 0°, 19°, 10°, 38, 32°, 21°, 9°, 32° dip Veins: 22° dip  N = 10 N = 1
	Fractures: 24° dip  N = 1
	Fractures: 20°, 24°, 42°, 29°, 71°, 5°, 5°, 13° dip  N = 8
	Fractures: 30°, 47°, 30°, 36°, 73°, 62°, 80°, 20° dip  N = 8

Structural Log

Core: 206/ 08 13Z 1837-1901m

Photographs (1:2)

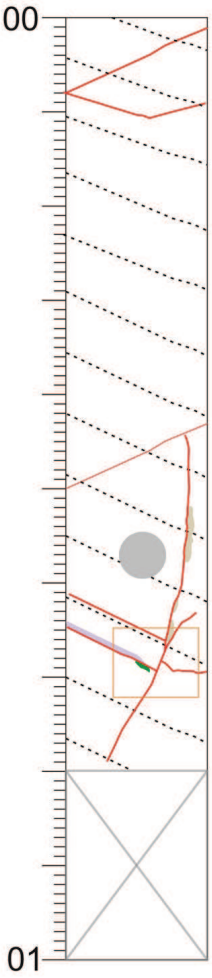

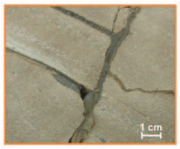

Description	Structural Information
	Fractures: 23°, 27° & 14° dip  N = 3
	Fractures: 24°, 88°, 73°, 57°, 64°, 26°, 60°, 37° dip  N = 8

Legend

- Gap
- Fault / Fracture
- Bedding
- Granulation seams
- Carbonate Vein
- "Degraded" Carbonate Veins
- Void
- Sedimentary Carbonate Calcite
- Oil Staining
- Pyrite
- "Degraded" Pyrite
- Sample core
- Sample for geochemical dating

Fractures

N = 592

Granulation seams

N = 94

Veins

N = 56